THERMODYNAMICS AND SOLUBILITY MODELING IN HYDROFLUOROALKANE SYSTEMS

by

William L. Hoye

A dissertation Submitted to the Faculty of the

DEPARTMENT OF PHARMACEUTICAL SCIENCE

In Partial Fulfillment of the Requirements

For the Degree of

DOCTOR OF PHILOSOPHY

In the Graduate College

THE UNIVERSITY OF ARIZONA

2008

FINAL EXAMINING COMMITTEE APPROVAL FORM

THE UNIVERSITY OF ARIZONA
GRADUATE COLLEGE

As members of the Dissertation Committee, we certify that we have read the dissertation prepared by William Hoye

Entitled Thermodynamics and Solubility Modeling in Hydrofluoroalkane Systems

And recommend that it be accepted as fulfilling the dissertation requirement for the Degree of Doctor of Philosophy

_____Date: 5/8/08
Dr. Paul Myrdal

_____Date: 5/8/08
Dr. Samuel Yalkowsky

_____Date: 5/8/08
Dr. Michael Mayersohn

Final approval and acceptance of this dissertation is contingent upon the candidate's submission of the final copies of the dissertation to the Graduate College.
I hereby certify that I have read this dissertation prepared under my direction and recommend that it be accepted as fulfilling the dissertation requirement.

Dr. Paul Myrdal _____Date: 5/8/08
Dissertation Director

STATEMENT BY AUTHOR

SIGNED: William Leslie Hoye

ACKNOWLEDGMENTS

I would like to thank all of my family for their encouragement and support. I would especially like to thank my parents. This degree was made possible through their many sacrifices. I would also like to thank my brother Steve for his friendship and support throughout my life.

To my wife Julie, thank you for everything. We are a team and I wouldn't be able to do any of this without you.

To my advisor Dr Myrdal, thank you. I truly appreciate the opportunity you have given me and can not thank you enough for all the time and effort you have invested in me.

DEDICATION

For my parents, Mark and Judy

TABLE OF CONTENTS

Page

TABLE OF CONTENTS – *Continued*

TABLE OF CONTENTS – *Continued*

LIST OF FIGURES

LIST OF FIGURES – *Continued*

LIST OF FIGURES – *Continued*

LIST OF FIGURES – *Continued*

LIST OF FIGURES – *Continued*

LIST OF TABLES

LIST OF TABLES – *Continued*

LIST OF TABLES – *Continued*

ABSTRACT

The phase-out of chlorofluorocarbons (CFCs) has resulted in an expanding new area of research in alternative ozone friendly propellants, for example hydrofluoroalkanes (HFAs). The HFA solvent system is unique in that many CFC soluble compounds behave differently in the HFA alternatives, such as HFA-134a and HFA-227. The reason for the difference in solubility is not fully recognized. This work investigates the solubility of 22 compounds in HFA-227 with the addition of ethanol as a cosolvent. The physical properties of both solute and solvent were investigated in order to determine the effects on solubility. The solubilities of 5 compounds in HFA-134a were also investigated. A thermodynamic approach was utilized in order to look at the enthalpic and entropic effects on solubility in the propellant. Due to the high vapor pressure of propellants, a liquid model was utilized, owing to its ease of use in characterizing solubility. The correlation between the liquid model 2H,3H-decafluoropentane (DFP) and the propellants HFA-134a and HFA-227 was examined.

The solubilities in HFA-227 with ethanol ranged from 0.001 to 3.282 %w/w, where the solubilities always increase when ethanol was added. The experimental solubilities were compared to calculated values obtained from ideal solubility and regular solution theory models. A clear correlation with the ideal solubility (melting point) combined with an intercept term and two physical properties was noted. A regression approach was also used to predict the activity coefficient in HFA-227 with 0 – 20% ethanol. These equations were combined with the extended ideal solubility equation, creating a useful

predictive equation with AAE values ranging from 0.32 to 0.36, or factor errors of 2.09 to 2.29. The equations shown in this work are useful for the prediction of solute solubility in HFA-227/ethanol mixtures.

Results in the liquid model DFP with 0 – 20% ethanol show that a regression equation results in a useful predictive equation for the solubilities in both HFA-134/ethanol and HFA-227/ethanol systems, where the AAE values ranged from 0.3 to 0.56, or factor errors of 2.0 to 3.6.

The solubilities of a series of chlorobenzene compounds along with a group of hydrogen donating and/or accepting compounds was examined in HFA-134a. The entropic effects appear to be the limiting factor in the solubility of these compounds. The compounds capable of hydrogen accepting and donating exhibited negative enthalpy of mixing values when placed in HFA-134a, a stark contrast to the values obtained for the chlorobenzenes. This suggests HFA-134a is able to strongly interact with solutes capable of donating or accepting hydrogen.

CHAPTER 1

INTRODUCTION

Ayurvedic medicine described the first inhalation therapy, consisting of smoking the leaves of the belladonna plant to treat diseases of the respiratory tract, over 4000 years ago.[1] Since that time, numerous methods for delivering medication to the airways and lungs have been developed. Currently, the most popular of these methods is the pressurized metered dose inhaler (pMDI). Over 800 million pulmonary drug delivery devices are used annually with pMDIs accounting for 80% of prescribed aerosols.[2] pMDIs use a liquefied propellant in order to aerosolize medication for inhalation and delivery to the targeted region of the airways or lungs. Inhalation drug delivery is an attractive route of administration for respiratory ailments because the drug is delivered directly to the site of action where it can have a local and immediate effect. The pMDI is used to treat a variety of diseases, most common being asthma and chronic obstructive pulmonary disease (COPD). While traditionally used for the treatment of respiratory ailments, inhalation drug delivery has recently gained attention for its ability to deliver drugs systemically.

Chlorofluorocarbons (CFCs) have been the customary propellants used in pMDIs. However, the impending phasing out of CFC propellants for medicinal use has lead to the research and development of alternatives. While some manufacturers are using new

forms of drug delivery, such as dry-powder inhalers, others have developed pMDIs with propellants that are less deleterious to the environment. These new MDI products contain the hydrofluoroalkane (HFA) propellants 134a and 227 in place of the traditional CFCs. While these HFAs are easier on the environment, they also present a number of new challenges to formulators. The biggest of these challenges is a change in solubility of traditionally used excipients and active pharmaceutical ingredients (APIs). Due to the change in solubility, a way to understand or predict solubility in HFAs could potentially save considerable time and money for aerosol formulators. The prediction of solubility would be an invaluable tool when designing solution and suspension MDI formulations. Without knowing what factors govern solubility, it is difficult to make informed decisions.

A logical starting point for aerosol research would be the application of theories successful at predicting solubility in other media. Hoye *et al*.[3] examined two of these theories, ideal solubility and regular solution theory (RST), in HFA-134a. While no strong correlation to solubility was found for either of these theories, they are worth re-examining when studying solubility in HFA-227. The effect of temperature on solubility is another method that can be useful in helping to understand solubility. It allows for a thermodynamic evaluation of the solubility process.

This work explores solubility in HFA-227 and HFA-227/ethanol and correlates the solute's solubilities to physico-chemical properties. This work also examines the thermodynamics of solubility in HFA-134a. Finally, the solubilities in HFA-134a and

HFA-227 are correlated to a potential liquid model propellant, 2H, 3H-decafluoropentane (DFP). An improved understanding of solubility in the HFA propellants would expedite the identification of candidates for solution or suspension pMDI formulations.

I. Pulmonary Drug Delivery

Drug delivery to the lungs is an attractive route of administration. When used to treat respiratory ailments, like asthma and COPD, it allows drug to be delivered directly to the site of action where it can have a local and immediate effect. This route also allows medications to bypass the traditional "first-pass effect" that a medication taken orally may undergo. While enzymatic degradation still takes place in the lungs, it does so to a lesser extent compared to the oral route. This allows smaller doses to result in higher tissue concentrations at the targeted regions of the airways as compared to medications dosed systemically. Exposing the body to a lesser amount of API also minimizes the incidence of unwanted side effects.

Inhalation drug delivery is a viable route of administration for systemic drug delivery. The lung has a huge surface area capable of absorption, approximately 75 m^2, and can be accessed by noninvasive means. The recent FDA approval of Exubera, an inhaled insulin, is a validation of this route for systemic delivery. A disadvantage of pulmonary drug delivery is the physiology of the airways themselves. They are specifically designed to filter out particulate matter from inspired air. In order for an aerosol to be considered

respirable and capable of reaching the lung, the particles must possess a mass median aerodynamic diameter (MMAD) of less than 5 microns. The particle size window for medications intended for systemic use is even smaller, with any particle over 3 microns not capable of reaching the terminal bronchi or alveoli. When considering the compromised airways of diseased patients, it is easy to see how difficult it can be for formulators to deliver a sufficient quantity of medication to elicit a therapeutic response.

II. HFA Propellants

Chlorofluorocarbon (CFC) propellants were first discovered in the 1890s and were originally used for spraying insecticides and as a refrigerant. They were also widely used as foam blowing agents, industrial solvents, and cleaning agents. In 1956, George Maison and Irvin Porush, of Riker Laboratories, developed the first pMDI for delivery of asthma medications. They developed two inhalers, Medihaler Iso and Medihaler Epi, containing the APIs isoproteranol and epinephrine, respectively. The formulations for these pMDIs consisted of CFC 12, and CFC 114 and ethanol. This, along with their favorable physical properties, allowed CFCs to become the propellants of choice for pMDIs over the next 50 years.

The first observation that CFC propellants were not decomposing but were actually accumulating in the atmosphere came in 1971.[4] In 1974, Molina and Rowland explained the mechanism of this phenomenon and the effect it was having on the ozone layer. This

work would ultimately earn them a Nobel Prize in chemistry. In 1978, the Environmental Protection Agency and the FDA prohibited the use of CFCs in all aerosol products with the exception of pMDIs. The Montreal Protocol, ratified in 1987, called for the ban of ozone depleting substances with the exception of "essential-use" ozone depleting substances such as pMDIs. The FDA has since stipulated that CFC pMDIs will be prohibited after 2008. In anticipation of this ban the pharmaceutical industry formed a coalition to search for replacement propellants. The result of this effort was the selection of HFA-134a as an alternative propellant. Since that time, HFA-227 has also emerged as a viable alternative. The structures of HFA-134 and 227 can be seen in Figure 1.1.

Figure 1.1 Molecular structures of the propellant 1, 1, 1, 2-Tetrafluoroethane (HFA-134a) (left) and 1,1,1,2,3,3,3-heptafluoropropane (HFA-227) (right).

The names of the propellants are the result of the Halocarbon Numbering System employed by The American Society of Heating, Refrigerating, and Air Conditioning Engineers. In this system, the first number represents the number of carbon atoms minus one. The second number represents the number of hydrogen atoms plus one. The third number equals the number of fluorine atoms. Any remaining atoms are assumed to be chlorine atoms. If the first number is zero, it is omitted. When there are two or more

carbon atoms present, isomers that may have identical halocarbon numbers are possible. To differentiate these isomers a lower case letter is added based on the difference in the sum of the atomic masses of the carbon substituents.

While no method for predicting solubility in CFCs had been developed, a working understanding was achieved after over half a century of use. Although a familiarity of excipient solubilities in the different CFC blends has aided in the formulation of pMDIs, this is not the case with new HFA propellants. Formulators are forced to start from scratch due to completely different solute, surfactant, and cosolvent solubilities in HFAs. The reformulation of existing products and the formulation of future ones have presented scientists with an opportunity to improve on a drug delivery method mostly unchanged since its inception.

The basic differences in physico-chemical properties among the propellants can be seen in Table 1.1. The densities of the CFC and HFA propellants are fairly similar, but differences in the boiling point and vapor pressure are substantial. Desired densities are essential for uniform dose delivery and stability of suspension formulations. Compared to CFC propellants, the increased vapor pressure of the HFA propellants provides a more complete atomization of the formulation when the pMDI is actuated, resulting in a smaller and more penetrable drug particle. HFA-134a is the more polar of the two propellants with a logP of 1.05 compared to 2.05 for HFA-227. The dipole moment for HFA-134a and HFA-227 are 2.06 and 0.93 Debye, respectively. These differences in

polarity and dipole moment may play a large role in solvent-solvent, solute-solvent interactions, and ultimately solute solubility.

Propellant	Density (g/mL)	BP (°C)	VP Psig -20 °C
CFC-11 (CCl_3F)	1.49	24	-1.8
CFC-12 (CCl_2F_2)	1.33	-30	67.6
CFC-114 ($C_2Cl_2F_4$)	1.47	4	11.9
HFA-134a (CF_3CH_2F)	1.22	-27	81
HFA-227 (CF_3CHFCF_3)	1.41	-17	73

Table 1.1 Physical properties of chlorofluorocarbon (CFC) and hydrofluoroalkane (HFA) propellants.

III. Solubility in HFA-134a and HFA-227

The knowledge of a solute's solubility is essential when developing a solution or suspension formulation. The ability to understand or predict solubility in HFA propellants would be a valuable tool for candidate selection in pMDI formulations. When trying to understand solubility in any medium a logical starting point is the ideal crystalline solubility. The ideal solubility of a crystalline solute is dependent on fusion properties alone and does not consider the influence of solvents. A solubility value at or near the ideal crystalline solubility would imply that the solvent, HFA propellant in this case, was behaving as a near ideal solvent. Deviations from ideality are attributed to the activity coefficient. This coefficient is the result of interactions between the solute and solvent. An explanation for deviations from ideality in non-aqueous systems is provided by Scatchard and Hildebrand's regular solution theory.[5,6] Previous work by Hoye *et al.*[3] examined the ability of these theoretical models to predict solubility in HFA-134a. The investigators found that neither ideal solubility nor RST accurately predicted solubility, where both models over-predicted the solubility in HFA-134a.

Physico-chemical properties play a large role in solubility. Much like the use of melting point and partition coefficient (logP) in aqueous solubility,[7] the discovery of an easily obtained or estimated physicochemical property that can be related or correlated to the solubility in HFA propellants would be of great value to formulators. Dickinson *et al.*[8] were the first to attempt to correlate physical properties to solubility in HFAs. They

evaluated the predictive ability of Fedors' solubility parameter and logP values with regard to solubility. No direct relationship between solubility and Fedors' solubility parameter was found. In contrast, a somewhat linear relationship was observed between solubility and logP, with solubility in both HFA-134a and HFA-227 increasing as logP decreased. Hoye *et al*.[4] examined a more thorough exploration of the relationship between physicochemical properties and solubility in HFA-134a. They found that none of the 12 parameters considered, including logP and Fedors' solubility parameter, had a practical relationship when utilized individually with the exception of the crystal term (melting point – 25°C). Of the regressions containing multiple parameters, melting point paired with either logP or molar volume resulted in promising correlations.

The purpose of this work was to relate the observed solubility, obtained for a number of compounds in HFA-227, to the ideal crystalline solubility or regular solution theory (RST). Solubility was also regressed against a number of physicochemical properties in an attempt to better understand their contribution to miscibility in HFA-227. All predictions were judged with respect to the observed values obtained experimentally.

IV. The Effect of Ethanol on Solubility in HFA-227

Cosolvents are an invaluable tool for the enhancement of aqueous solubility. They are capable of increasing the solubility of non-polar solutes by several orders of magnitude in an aqueous system. Cosolvents are typically organic molecules that are liquid at room

temperature and capable of interacting with both polar and non-polar molecules. The presence of a hydrogen bond donor and/or acceptor group on the molecule in combination with a limited number of carbons, allows for these interactions. Through these interactions, cosolvents disturb the highly organized structure of water allowing solutes that would normally be squeezed out to gain increased miscibility. Another explanation is that they alter the polarity of the solvent, causing the polarity to shift towards that of the solute. In addition to greatly increasing solubility, cosolvents have the benefit of being relatively inexpensive and having well defined toxicity profiles.

While the role of cosolvents in the aqueous medium is well understood, the same cannot be said for HFA propellants. The biggest hurdle to understanding how excipients interact with HFA propellants is a lack of understanding of how the propellant molecules interact with themselves. While there has been much speculation, little is known about the solvent-solvent interactions within the HFA propellants. It is unclear whether dipole-dipole interactions or hydrogen bonding occurs between the HFA molecules. For this reason it is hard to predict the effect that cosolvents will have on solubility. Hoye *et al.*[4] examined the effect of ethanol on solubility in HFA-134a. The solubility of all compounds tested increased with the use of cosolvent but the magnitude of this increase was extremely variable. There was also no observed relationship between logP and the increase in solubility due to the cosolvent.

The effect of cosolvent concentration on pMDI performance is a complex issue that needs to be considered. While a cosolvent may increase solute solubility, it also decreases volatility of the propellant. By doing so, it decreases the vapor pressure of the formulation and increases the evaporation rate of the particles. Gupta *et al*.[9] examined the effect of ethanol concentration on product performance in HFA-134a pMDIs and found that the 'maximum respirable mass,' defined as the product of the drug solubility multiplied by the respirable fraction at a given ethanol concentration, increased up to 10% ethanol and then plateaued. A range of 0 to 20% w/w ethanol content was used in this work based on those findings.

V. Solubility in the Liquid Model 2H, 3H-Decafluoropentane (DFP)

The volatile nature of HFA-134a and HFA-227 makes solubility determination in these liquid propellants a challenging task. A closed and pressurized system is required to maintain these propellants as a liquid. An inline direct injection HPLC method for solubility determination in pMDIs has been developed to overcome this. Currently, the utility of this new method extends to solution based pMDIs only. The existence of a liquid model capable of predicting solubility in one or both of these HFA propellants would greatly aid investigations in better understanding interactions governing solubility. Dickinson *et al*.[8] was the first to investigate the use of model liquids to predict solubility in HFA propellants. A linear relationship was found between the solubilities in 1H-perfluorohexane and the solubilities in both HFA propellants. Both Rogueda[10] and

Ridder[11] investigated the use of 2H,3H-decafluoropentane (DFP) for the prediction of surfactant solubility in the HFA propellants. The physical properties of DFP were determined by Rogueda and found to be comparable to HFA-227 and similar to HFA-134a. The approximate surfactant solubilities of Brij and POE-PPO block copolymers in the HFA propellants were determined by visual assessment. Ridder found that DFP was a better model for solubility in HFA-134 while Rogueda's results suggested a better model for HFA-227. This work compared the solubility of 13 solid solutes in DFP with their solubilities in the HFA propellants.

CHAPTER 2

THEORETICAL BACKGROUND

The solubility of a crystalline solute is dependent upon its crystal structure and molecular structure. The crystal structure is used to predict ideal solubility, while the molecular structure is responsible for the deviations from ideality, also know as the activity coefficient. By combining these two terms the solubility of a crystalline solid in a solvent is determined as described by the following equation:

$$\log X = \log X_i^c - \log \gamma \qquad (2.1)$$

where X is mole fraction solubility, X_i^c is the ideal crystalline solubility and γ is the activity coefficient.

I. Ideal Solubility

Before a molecule from a crystalline solute can mix with a solvent, the energetics of the solute's crystal lattice must be overcome. The greater the change in free energy required for the molecule to dissociate from the crystal lattice, the less soluble the solute will be. The ideal solubility of a crystalline solute is governed by the molar free energy of melting

required to create a super cooled liquid at a specified temperature obtained by the following equation:

$$\log X_i^c = -\frac{\Delta S_m}{2.303R}\left(\frac{T_m - T}{T}\right) + \frac{\Delta Cp}{2.303R}\left(\frac{T_m - T}{T}\right) - \frac{\Delta Cp}{2.303R}\log\left(\frac{T_m}{T}\right) \qquad (2.2)$$

Where X_i^c is the ideal crystalline solubility in mole fraction units, ΔS_m is the entropy of melting, T_m is melting point of the solute in degrees Kelvin, T is the temperature of interest in degrees Kelvin, R is the universal gas constant (8.314 J/molK), and ΔCp is the heat capacity change of melting. This equation can be further simplified by making one of two assumptions. The first assumption, known as the van't Hoff expression, states that the value for ΔCp is equal to or close to zero. The second assumption, the Hildebrand expression, assumes that the value of ΔCp is equal to ΔS_m. The elimination of the heat capacity term by the van't Hoff expression allows Equation 2.2 to be approximated by Equation 2.3:

$$\log X_i^c = -\frac{\Delta S_m}{2.303R}\left(\frac{T_m - T}{T}\right) \qquad (2.3)$$

When the second assumption is used, ΔCp is equal to ΔS_m, Equation 2.2 reduces to:

$$\log X_i^c = -\frac{\Delta S_m}{2.303R}\log\left(\frac{T_m}{T}\right) \qquad (2.4)$$

If the experimental entropy of fusion is not known, Walden's Rule can be applied. Walden's Rule states that for rigid organic compounds, ΔS_m can be considered a constant at 56.5 *J/(K•mole).*[12] If the experimental temperature of interest is room temperature (T = 298 K) and Walden's Rule is applied, then Equation 2.4 can be simplified to Equation 2.5:

$$\log X_2^{ideal} = -0.01(T_m - 298) = -0.01(MP - 25) \qquad (2.5)$$

where, *MP* is the melting point in degrees Celsius.[7] If the solute's melting point is less than the temperature of interest, it exists as a liquid and the crystal term does not limit solubility. It is important to note that the ideal solubility for a crystalline solute is solvent independent. This is easily seen in Equation 2.5 whose only variable is the melting point of the solute. For the purpose of this study all assumptions will be examined.

II. Activity Coefficient: Regular Solution Theory (RST)

The activity coefficient is used to describe a compound's deviation from ideality. This deviation is attributed to a less than ideal mixing of the solute and solvent due to differences in molecular structure. A compound's activity coefficient can be calculated when the experimental and ideal solubility are known by a simple rearrangement of Equation 2.1 to give Equation 2.6:

$$\log \gamma = \log X_i^c - \log X \tag{2.6}$$

When the solubility is unknown, a popular method to describe a non-aqueous and non-ideal solution is the regular solution theory (RST). The RST is a method for calculating the activity coefficient of real solutions by describing the enthalpic effects according to Scatchard-Hildebrand[5,6] and is defined by Equation 2.7:

$$\log \gamma_2^{RST} = \frac{V_2 \Phi_1}{2.303RT}(\delta_1 - \delta_2)^2 \tag{2.7}$$

where, V_2 is the molar volume, Φ_1 is the volume fraction, and δ is the solubility parameter. The solvent is noted by the subscript 1, and solute by 2. The volume fraction of the solvent can be eliminated by assigning it a value of one ($\Phi_1 \approx 1.0$) when limited solute solubility is assumed. The solubility parameter, δ, also known as the cohesive energy density, was calculated by Equation 2.8.

$$\delta = \sqrt{\frac{\Delta H_v}{V_m} - \frac{RT}{V_m}} = \sqrt{\frac{\Delta E_v}{\Delta V_m}} \tag{2.8}$$

where ΔE_v is the change in enthalpy of vaporization, and ΔV_m is the change in molar volume. The energy of vaporization and molar volume are additive and were calculated

by a group contribution method proposed by Fedors for solid solutes.[13] The solubility parameter for HFA-134a and HFA-227 are 6.8 $(cal/cm^3)^{0.5}$ and 5.4 $(cal/cm^3)^{0.5}$ respectively, according to SolvayFluor, Germany.[14]

The introduction of the solubility parameter for the solute and solvent not only takes the size and nature of the molecules into consideration, but also accounts for the strength of solute-solute and solvent-solvent intermolecular forces. A solution will behave as an ideal solution when the solubility parameters of the solute and solvent are similar. In other work, the RST was used to establish semi-empirical correlations in the supercritical fluid carbon dioxide, which yielded good agreement with experimental data.[15,16]

The expression for a real solution of a solid solute (i.e., solubility, log X_2^{RST}) can be obtained by combining Equation 2.3 (ideal solubility) and Equation 2.7 (RST):

$$\log X_2^{RST} = -\frac{\Delta S_m}{2.303R}\left(\frac{T_m - T}{T}\right) - \frac{V_2}{2.303RT}(\delta_1 - \delta_2)^2 \qquad (2.9)$$

III. Thermodynamics of Solubility

The solubility of any crystalline solute in a solvent is determined by the energetics of the process. The change in the Gibbs free energy of solution is what governs solubility. The less energy required to go from a crystalline solute to a solution, the more favorable the process and the higher the solubility of the solute in that solvent. The change in Gibbs free energy of any solution is equal to Equation 2.10:

$$\Delta G_{solution} = \Delta H_{solution} - T\Delta S_{solution} \tag{2.10}$$

Where *ΔG* is the change in Gibbs free energy of the solution, *ΔH* is the change in enthalpy of solution, *T* is the temperature in degrees Kelvin, and *ΔS* is the entropy of solution. The free energy change for the dissolution of the crystalline solid is composed of 2 steps, (1) the melting of the crystalline solid and formation of a hypothetical super-cooled liquid, (2) the mixing of the super-cooled liquid's molecules with the molecules of the solvent. Figure 2.1 illustrates the step-wise dissolution processes of going from a solid solute to a solution. From Figure 2.1 it is clear that while the overall thermodynamic properties of a solution (*ΔG, ΔH, ΔS*) govern solubility, they are also composed of the melting and mixing properties. The free energy change for the melting and mixing of the solute are determined by their respective enthalpy and entropy values. The overall free energy change of the solution is given by Equation 2.10 but also by Equation 2.11. This summation of values holds true for the enthalpy and entropy as well.

$$\Delta G_{Solution} = \Delta G_{melting} + \Delta G_{Mixing} \tag{2.11}$$

The Change in Gibbs free energy for a solution can be calculated by Equation 2.12:

$$\Delta G_{Solution} = -RT \ln X_2 \tag{2.12}$$

In which R is the universal gas constant, T is the temperature in degrees Kelvin, and X_2 is the solute mole fraction solubility. When looking at a relatively small temperature range it can often be assumed that the enthalpy of solution is a constant. Integration of the van't Hoff equation produces Equation 2.13:

$$\ln X_2 = \frac{-\Delta H_s}{RT} + constant \tag{2.13}$$

This equation allows the calculation of the enthalpy of solution with solubility values at varied temperatures. When the mole fraction solubility of a compound is plotted against the reciprocal of the temperature, the slope of the line gives the enthalpy of solution. With both the ΔG_s and ΔH_s values known, it is then possible to calculate entropy's contribution to the solution's free energy change at a defined temperature by a simple rearrangement of Equation 10 to form Equation 2.14:

$$-T\Delta S_s = \Delta H_s - \Delta G_s \tag{2.14}$$

ΔG_{melt} is the change in energy required to break down the crystal structure of the solute and form a super-cooled liquid. This step is analogous to ideal solubility described previously. The fusion or melting properties of the compounds can be obtained experimentally through the use of a differential scanning calorimeter (DSC). Integration

of the DSC thermogram peak gives the enthalpy of fusion. The entropy of fusion is then calculated by Equation 2.15:

$$\Delta S_{melt} = \frac{\Delta H_{melt}}{T_m} \tag{2.15}$$

This equation assumes that, at the melting point, ΔG_{melt} is equal to zero and thus the enthalpic and entropic contributions are equivalent. The ΔG_{melt} at temperatures other than the melting point are not equal to zero and can be obtained by Equation 2.16:

$$\Delta G_{melt} = \Delta S_{melt}(T_m - T) \tag{2.16}$$

In an ideal solution there is no change in the volume, free energy, enthalpy, and entropy when mixing the super-cooled liquid solute with the solvent. Since this is only true when a compound is mixed with itself, these deviations must be accounted for in all real solutions. The overall solution parameters are composed of a summation of the melting and mixing properties. With the melting and overall solution thermodynamic parameters known, the mixing parameters are obtained by equations 2.17, 2.18, and 2.19.

$$\Delta G_{mix} = \Delta G_{solution} - \Delta G_{melt} \tag{2.17}$$

$$\Delta H_{mix} = \Delta H_{solution} - \Delta H_{melt} \tag{2.18}$$

$$\Delta S_{mix} = \Delta S_{solution} - \Delta S_{melt} \tag{2.19}$$

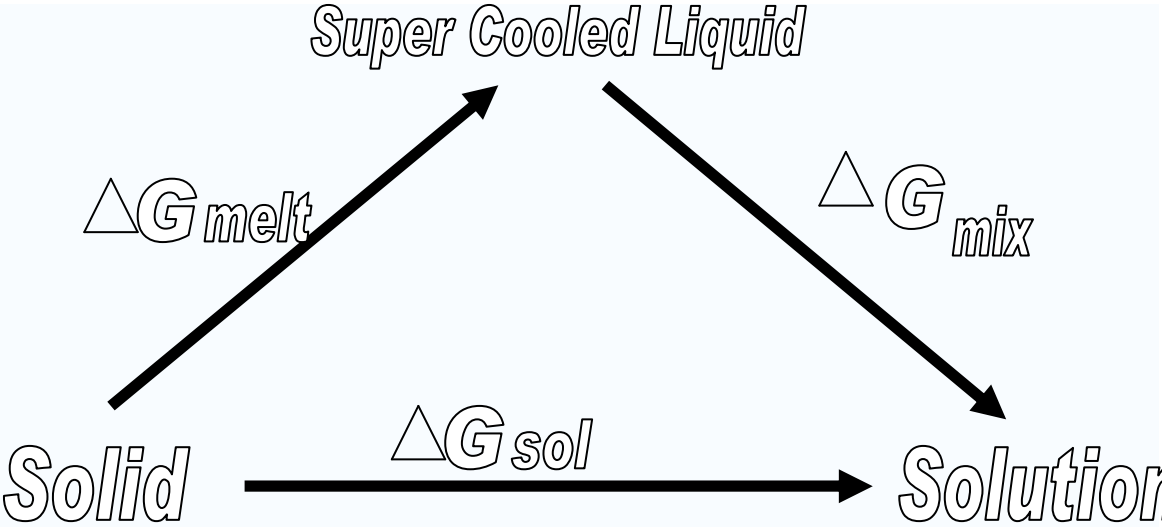

Figure 2.1: The step-wise dissolution processes of going from a solid solute to a solution defined thermodynamic.

CHAPTER 3

EXPERIMENTAL

I. Materials

Thirteen compounds having diverse physicochemical properties (log P values ranging from -0.13 to 9.85) were selected for the HFA-227 solubility investigation and purchased from Sigma-Aldrich (St. Louis, MO), LKT Laboratories (St. Paul, MN), Melford Laboratories (Suffolk, UK) and Byron Chemical Co. (Long Island, NY) as shown in Table 3.1. The propellant 1,1,1,2,3,3,3-heptafluoropropane (HFA-227) was purchased from Honeywell (Morristown, NJ).

These same thirteen compounds were selected for the HFA-227/cosolvent solubility study. The ethanol (200 proof) was purchased from AAPER Alcohol and Chemical Co. (Shelbyville, KY). These compounds were also selected for solubility tests in 2H,3H-decafluoropentane (DFP) obtained from Apollo Scientific LTD (Cheshire, UK).

A series of five chlorobenzene compounds were selected for a solubility investigation in HFA-134a at three different temperatures. The compounds were obtained from Sigma-Aldrich and can be seen in Table 3.1. The propellant 1,1,1,2-tetrafluoroethane (Genetron 134a) was purchased from Honeywell (Morristown, NJ).

II. Methods

A. Solute Solubility

For all the HFA-134a and HFA-227 formulations prepared, solid solute was directly weighed into safety-coated pressure resistant glass pMDI vials. For the HFA-227 formulations used in the cosolvent study, ethanol was weighed directly into the vials containing the solid solute. After the addition of the solute, and when necessary, ethanol, each vial was immediately crimped with a continuous valve (3M Drug Delivery Systems, St. Paul, MN) using a small scale bottle crimper (Model # 3000B, Aerotech laboratory equipment company, Maryland, NY). HFA-134a or HFA-227 was pressure filled into these vials using a pressure burette (series 3SB Pressure Filler; Aerotech Laboratory Equipment Company). Solubility samples were equilibrated for at least 48 hours before analysis. For determination of solute solubility in HFA-227, the standard pMDI solubility technique, first used by Dalby *et al.,*[17] was employed. A donor vial containing excess solid solute in the propellant and a second empty receiving vial whose weight is prerecorded are both crimped with continuous spray valves. Both vials have an adapter which allows them to connect to an air tight filter, with the donor vial mounted on top. The receiving vial is traditionally kept in dry ice in order to keep it cold and provide the driving force for the transfer of formulation. Once the formulation is transferred, the receiving vial is chilled and decrimped. The formulation is allowed to evaporate and a set quantity of diluent is added. These diluted samples are then analyzed via HPLC. For the determination of solute solubility in HFA-134a, a direct on-line solubility technique

was used.[18,19,20] Filtered formulation was injected directly into the injector port of a manual injector coupled to an HPLC for analysis at the proper wavelength. When the formulation in the original vials were determined to be too concentrated for accurate quantitation the formulation was diluted by the same process used in the traditional pMDI solubility technique.

For the determination of solute solubility in DFP, solute and cosolvent were placed in 4 ml glass vials and sealed with a cap. The samples were equilibrated for at least 24 hours before analysis at ambient laboratory conditions (25˚C). Autosampler and direct inject methods were utilized, since DFP is a liquid at room temperature. The excess solute was filtered and placed in autosampler HPLC vials or injected directly onto an HPLC column. For the determination of solute solubility in water, excess solute was placed in scintillation vials and sealed with a cap. The samples were equilibrated for 24 hours at 4°C, 25°C, and 48°C. The high temperature samples were heated in a VWR oven and the low temperature samples were equilibrated in a Haier refrigerator. The solutions were then filtered into HPLC vials and analyzed for content. The samples kept at 48°C were filtered and 1 ml aliquots were taken from the filtered solution by volumetric pipettes and placed in 5 ml volumetric flasks for dilution in order to prevent precipitation. The flasks were diluted with acetonitrile and injected onto the HPLC.

B. Equipment

The following instruments were used to obtain the physical properties and solubilities of the solutes used in this study.

Differential Scanning Calorimeter (DSC)

A Q1000 DSC (TA Instruments) was used to determine the melting point and enthalpy of fusion for the compounds used. A known quantity of solute was placed in aluminum crucibles and sealed. An empty crucible was used as a reference. The area under the curve was used to determine the enthalpy of fusion for the test compounds. Once the enthalpy of fusion is known, the entropy of fusion can be calculated by the following equation:

$$\Delta S_m = \frac{\Delta H_m}{T_m} \tag{3.1}$$

High Performance Liquid Chromatography (HPLC)

The HPLC instrumentation comprised a Waters 2695 Separations module (Waters, Milford, MA) coupled with a Waters 2487 dual wavelength absorbance detector or a Waters 996 Photodiode Array Detector. The Waters 2695 Separations module was connected with a Rheodyne model 7725 manual sample injector (Rheodyne, L.P., Rohnert Park, CA) (Figure 3.1). The sample loop overflow tubing of the manual injector was interfaced with a pressure regulator (Amtek U.S. Gauge Division, Sellersville, PA) and an adjustable backpressure regulator (Alltech Associates Inc., Deerfield, IL). The

excess sample waste was collected in a waste bottle (note that it is advisable to keep the waste container in a containment system).

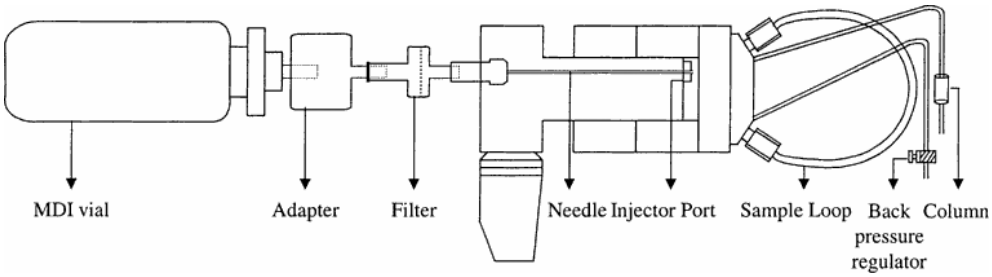

Figure 3.1. Schematic diagram of direct inject on-line HPLC system.

The analytical columns used consisted of a 150 × 4.6 mm, 5 μm Apollo C18 column and a 150 × 4.6 mm, 5 μm Apollo Silica column (for Albuterol). The wavelengths used for ultraviolet detection were determined for each compound with the photodiode array detector (PDA). Quantitation was accomplished by the peak area from a five point standard curve. The sample loop delivers formulation based on volume, so a density correction was required for analysis of the different standards and formulations. Based on the density correction, the formulation mass dispensed from the sample loop was calculated.

A list of the compounds used for the solubility evaluation along with their physico-chemical properties is presented in Table 3.1.

Compound	Molecular Weight (g/mol)	logP	Melting Point (°C)
Caffeine [1,4,5]	194.19	-0.13	238
Hexachlorobenzene [1,6]	284.78	4.89	232
Anthracene [1,4,5]	178.23	4.68	218
4-aminophenol [3,4]	109.13	-0.29	189
Albuterol [2,4,5]	239.31	0.02	185
Naphthoic acid [1,4,5]	172.18	3.13	158
Dehydrocholesterol [1,4,5]	314.46	9.80	149
Biphenylacetic acid [3,4]	212.25	3.25	147
Cholesterol [1,4,5]	386.65	9.85	146
1,2,4,5-tetrachlorobenzene [1,6]	215.89	4.23	140
Naphthylacetic acid [1,4,5]	186.21	2.74	130
Benzoic Acid [1,4,5]	122.12	1.89	122
Naphthol [1,4,5]	144.17	2.71	122
Phenanthrene [1,4,5]	178.23	4.68	100
Pentachlorobenzene [1,6]	250.34	4.60	86
Naphthalene [1,4,5]	128.17	3.45	81
Methoxynaphthalene [1,4,5]	158.20	3.36	72
Perfluorononanoic acid [3,4]	464.08	8.64	70
9H-Hexadecafluorononanoic acid [3,4]	446.09	7.60	67
4-Bromophenol [3,4]	173.01	2.50	65
1,3,5-Trichlorobenzene [1,6]	181.45	4.04	64
1,2,3-Trichlorobenzene [1,6]	181.45	3.77	54
Nitronaphthalene [1,4,5]	173.17	3.18	55
4-Chlorophenol [3,4]	128.56	2.43	43
Phenol [3,4]	94.11	1.48	41
4-Methylphenol [3,4]	108.14	1.94	33
Dodecan-1-ol [3,4]	186.34	5.13	26

[1]Sigma-Aldrich (St. Louis, MO)
[2]Byron Chemical Co. (Long Island, NY)
[3]Dickinson *et al.*[9]
[4]HFA-227 study
[5]HFA-227/ethanol & DFP/ethanol study
[6]HFA-134a study

Table 3.1 Physicochemical properties for all compounds used in this work.

C. Multiple Linear Regression

A program for Multiple Linear Regression (MLR) was used to develop and evaluate mathematical correlations with solubility in HFA-227. The physico-chemical properties that were considered in this work included melting point, logP (Scifinder Scholar 2006), molar volume[14], entropy of melting, ΔS_m (Equation 3.1), molecular weight, number of OH groups, number of COOH groups, sum of H-accepting groups (i.e. C=O, OH, N, NH), sum of H-donating groups (i.e. COOH, OH, NH, NH_2) and Hydrogen Bond Number (HBN). HBN is defined by Equation 3.2 as,

$$HBN = \frac{\sqrt{OH + COOH} + 0.33\sqrt{NH_2}}{MW} \qquad (3.2)$$

where, OH, COOH, and NH_2 represent the number of alcohols, carboxylic acids, or primary amines, respectively, and MW is the molecular weight of the compound.[21] The HBN is a parameter designed to weight hydrogen bonding relative to the solutes size.

D. Average Absolute Error

The average absolute error (AAE) was used to determine the predictive accuracy of the methods and is calculated by Equation 3.3:

$$AAE = \frac{\sum |observed - predicted|}{N} \tag{3.3}$$

where *observed* and *predicted* are the observed and predicted log solubilities, respectively, and *N* is the number of solubility data points. The AAE is the summation of the absolute value of each deviation. An AAE of 0.40 represents an average deviation of a predicted value from the experimental value by a factor of 2.5.

CHAPTER 4

RESULTS AND DISCUSSION

I. Solubility in HFA-227 and HFA-227 with Ethanol

The solubilities of 13 solutes were determined in HFA-227 with 0 – 20% w/w ethanol using previously published methods. The solubility values of nine compounds in HFA-227 were obtained from Dickinson *et al.*,[9] where the compounds were all solid solutes. The melting points of the experimental solutes ranged from 55 to 238°C, and the logP values ranged from -0.13 to 9.85. All 22 solutes had measurable solubilities in HFA-227, which ranged from 0.001 to 3.282% w/w. Interestingly, the addition of ethanol resulted in an increase in solubility for each compound tested. Compounds such as naphthalene and methoxynaphthalene had the highest solubilities in HFA-227 with no ethanol, 0.485 and 0.402% w/w, respectively. However, compounds such as naphthoic acid and albuterol had the lowest solubilites, both at 0.001% w/w. Compounds such as naphthol and benzoic acid had the highest solubilities in HFA-227 with 20% w/w ethanol, 3.282 and 3.171% w/w respectively. The % w/w solubilities were plotted against the fraction ethanol as shown in Figures 4.1 and 4.2, where the solutes are grouped by similar solubility values.

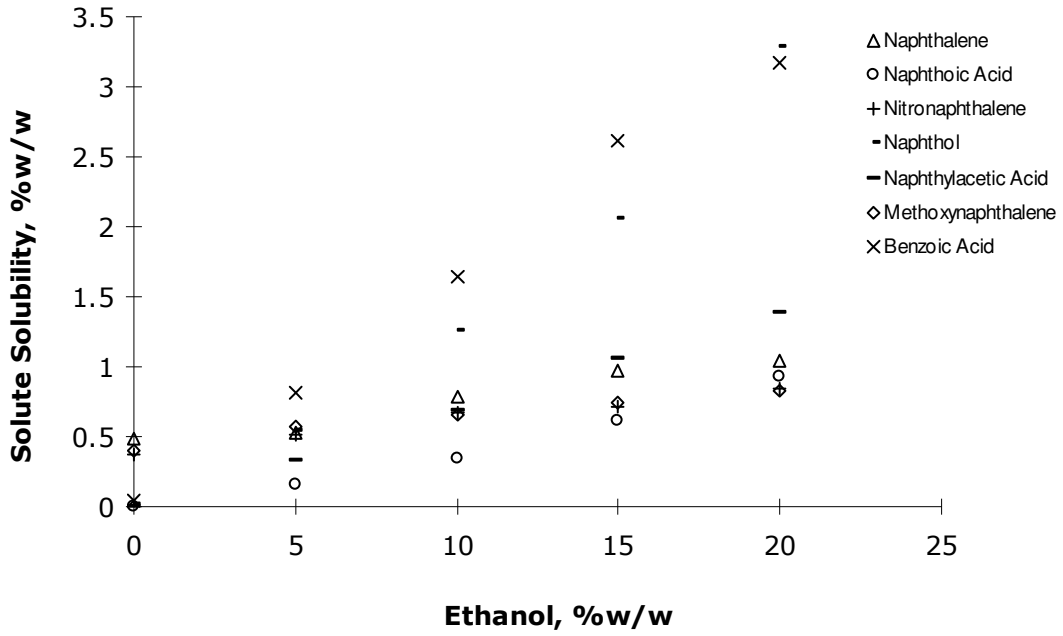

Figure 4.1. Solute solubility (% w/w) in HFA-227 plotted against the fraction ethanol (0 – 20% w/w) for those solutes with high solubilities.

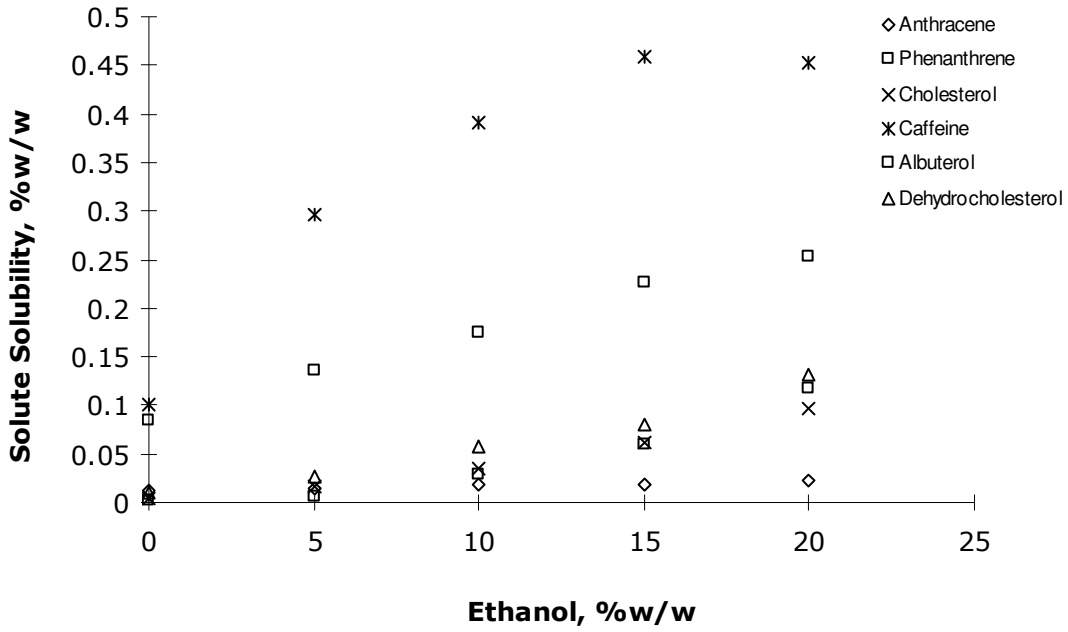

Figure 4.2. Solute solubility (% w/w) in HFA-227 plotted against the fraction ethanol (0 – 20% w/w) for those solutes with lower solubilities.

II. Ideal Solubility

The solubility of a solid in an ideal solution is dependent on temperature, melting point of the solid, and the molar heat of fusion. Calculation of the ideal solubility of a crystalline solute in a liquid solvent requires knowledge of the difference in the molar heat capacity, ΔCp, at constant pressure of the solid, and the supercooled liquid form of the solute. Since this parameter is not usually known, two assumptions have been used to simplify the expression. The first is that the molar entropy of melting, ΔS_m, is an estimate of ΔCp (Equation 2.4). The alternate assumption is that ΔCp can be considered equal to 0 (Equation 2.3). Reports claiming the superiority for each assumption have been reported in the literature. Figure 4.3 shows the relationship between the calculated solubility and the ideal solubility according to Equation 2.4, which assumes, $\Delta Cp = \Delta S_m$, for the 22 experimental solutes. The ideal solubility over-predicted the experimental log mole fraction solubilities for all compounds with an AAE of 2.30, or an error factor of 199.53. A slightly different result is seen with Equation 2.3, where, $\Delta Cp = 0$, as seen in Figure 4.4. The data points are slightly closer to the line of unity, and the AAE is 2.15, an error factor of 141.25. For both assumptions, ΔS_m values were obtained from DSC for the 13 compounds tested with the presence of ethanol. Reported ΔS_m values for the majority of compounds from Dickinson *et al.*[9] were obtained. Walden's Rule[12] was applied, ΔS_m = 56.5 J/molK, for 9H-hexadecafluorononanoic acid and perfluorononanoic acid whose reported ΔS_m values could not be found.

For simplification and ease of use, the assumption that ΔS_m is constant was applied to the ideal solubility equation, therefore, resulting in Equation 2.5. Figure 4.5 shows the relationship between the calculated solubility, log X_2^{ideal}, and the experimental log mole fraction solubility, log X_2^{obs}, where the AAE is 2.19, an error factor of 154.88. Since Equation 2.3 (Cp=0) results in the lowest AAE for this data set, it will be used to calculate the ideal solubility in HFA-227 through out the rest of this work.

On average, the ideal solubility over-predicts the experimental solubility in HFA-227 by a factor of 141.25. However, there appears to be a correlation between the experimental log mole fraction solubility, log X_2^{obs}, and a solute's melting point. Figure 4.6 shows the relationship, which compares both ideal solubility, log X_2^{ideal} (broken line) and experimental solubility, log X_2^{obs} (solid line) as a function of the crystal term (MP – 25) from the ideal solubility equation. The experimental solubility values parallel those of the ideal solubilities, where the experimental solubilities have a slope of -0.02 and an intercept of -1.60.

The deviation between each ideal solubility and experimental solubility data point in Figure 4.6 represents the activity coefficient, γ_2, for each individual solute, where the average value is -1.60. In other words, the solubility in HFA-227 deviates from ideal solubility by an average log value of -1.60.

Using the equation determined in Figure 4.6, it is possible to develop a new empirical equation for the solubility in HFA-227 according to Equation 4.1

$$\log X_2^{calc} = -0.0167(\text{MP} - 25) - 1.604 \qquad (4.1)$$

Figure 4.7 shows the relationship between Equation 4.1 and the experimental log mole fraction solubility, $\log X_2^{obs}$, where the AAE is 0.90, or an average factor error of 7.94. The intercept value -1.60 is only an average activity coefficient for the 22 compounds and may not be sufficient for a larger collection of structurally different solutes.

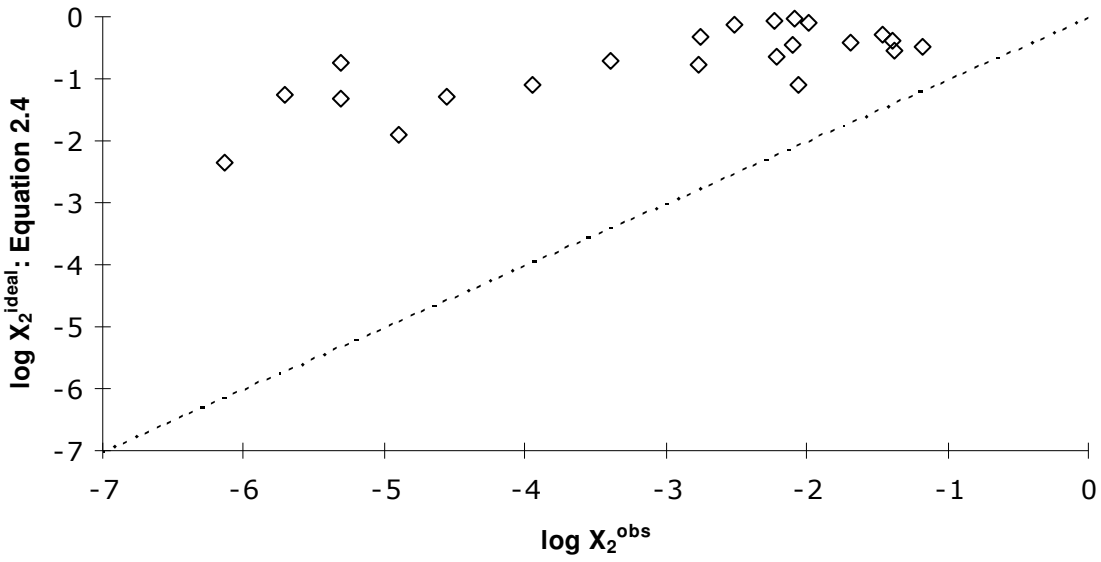

Figure 4.3. Calculated log mole fraction solubility, log X_2^{ideal}, according to Equation 2.4 ($Cp = S_m$) plotted against the experimental log mole fraction solubility, log X_2^{obs}. The broken line illustrates the line of unity.

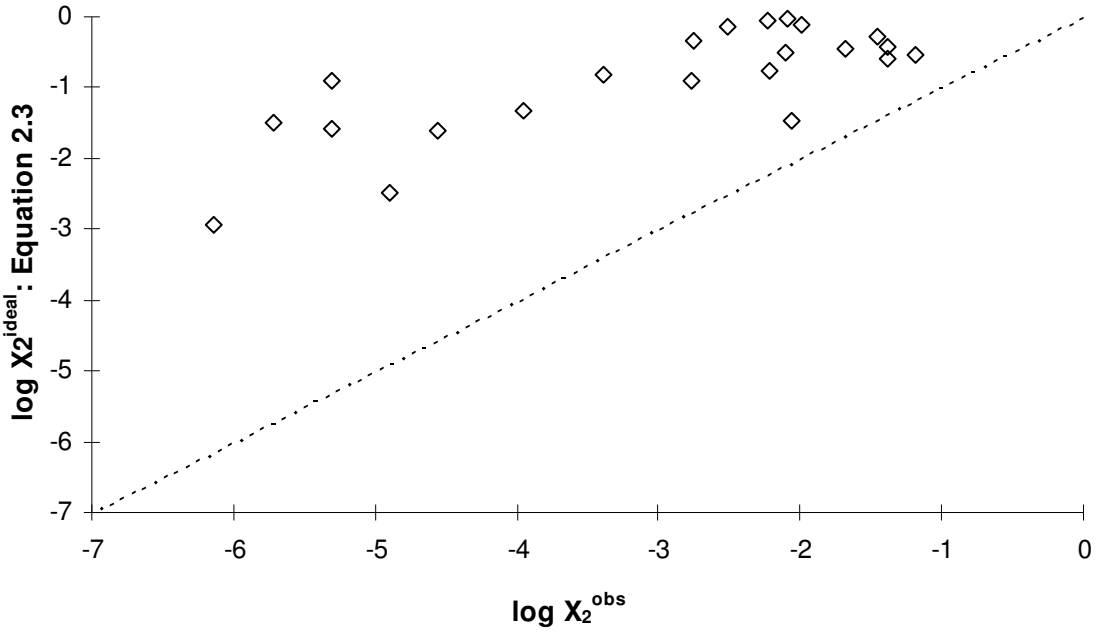

Figure 4.4. Calculated log mole fraction solubility, log X_2^{ideal}, according to Equation 2.3 ($\Delta Cp = 0$) plotted against the experimental log mole fraction solubility, log X_2^{obs}. The broken line illustrates the line of unity.

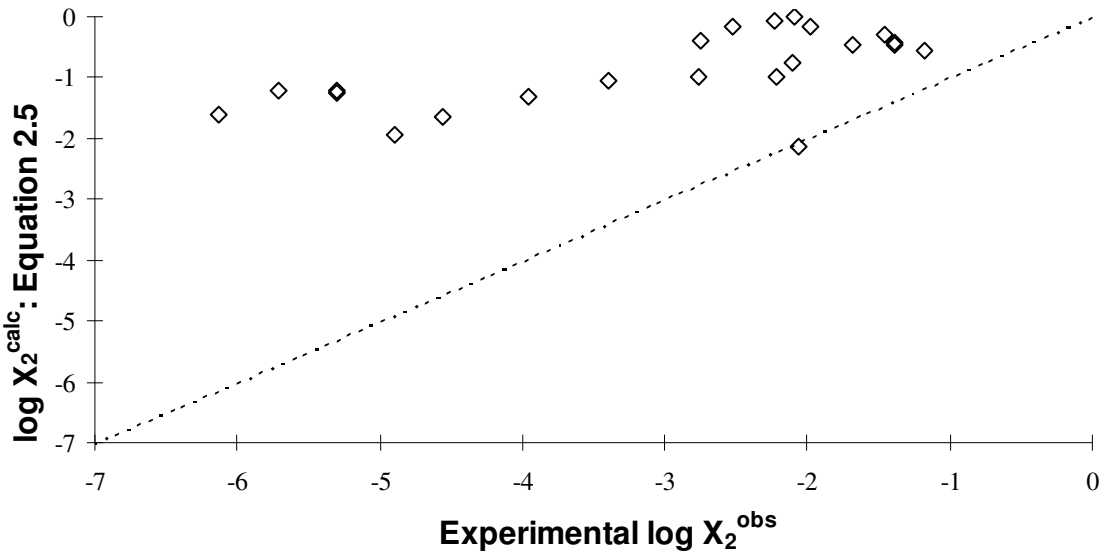

Figure 4.5. Calculated log mole fraction solubility, log X_2^{ideal}, according to Equation 2.5 plotted against the experimental log mole fraction solubility, log X_2^{obs}. The broken line illustrates the line of unity.

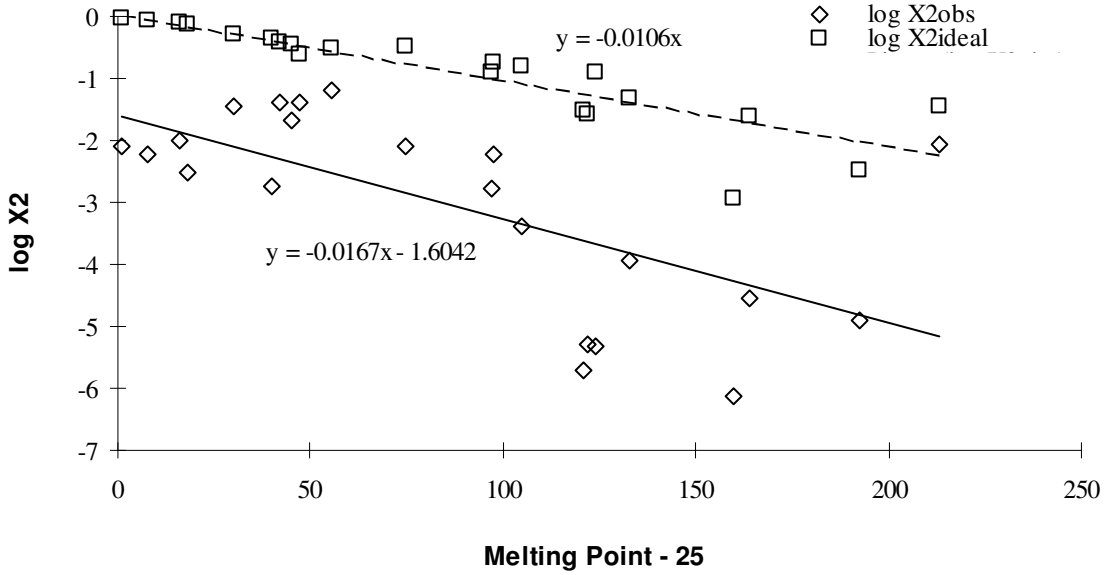

Figure 4.6. Calculated ideal solubility (Equation 2.3) (broken line) and experimental solubility, log X_2^{obs} (solid line) plotted against Melting Point – 25 (°C).

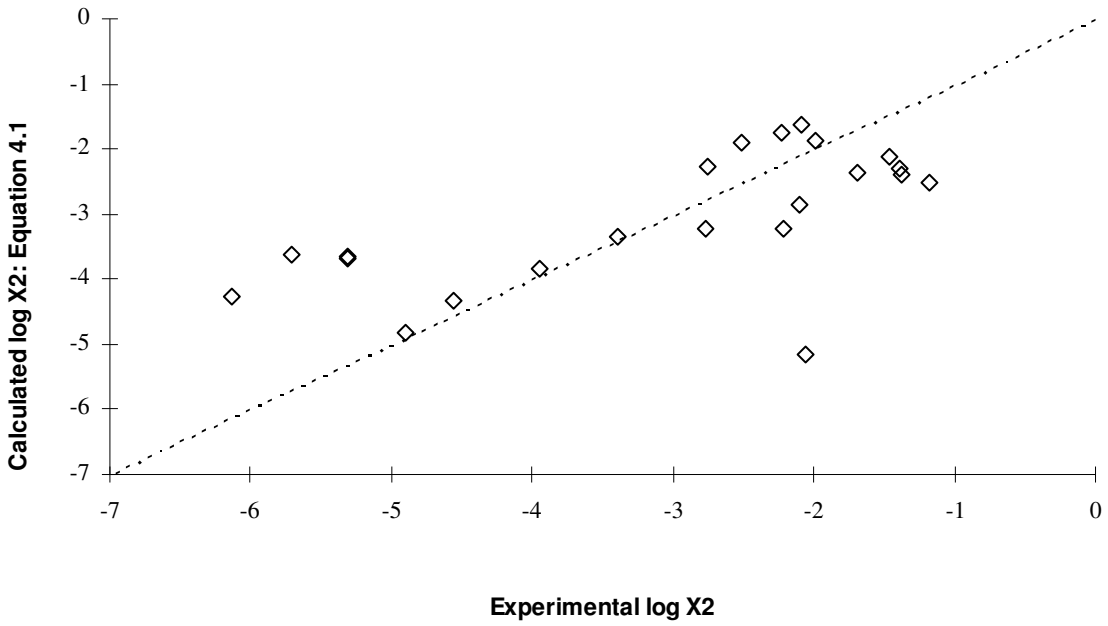

Figure 4.7. Calculated solubility, log X_2^{calc}, plotted against experimental solubility, log X_2^{obs}, for Equation 4.1. The broken line illustrates the line of unity.

III. Ideal Solubility: HFA-227 with Ethanol

The ideal solubility model (Equation 2.3) was also applied to 13 compounds in HFA-227 with 0, 5, 10, 15 and 20 %w/w ethanol. Figure 4.8 shows the relationship between the ideal solubility, $\log X_2^{ideal}$, and the experimental solubility, $\log X_2^{obs}$, for 0 and 20% ethanol, where the AAE values are 2.12 and 1.12, respectively. At 0% ethanol, the ideal solubility over-predicts the experimental solubility for almost all the compounds. As the ethanol concentration increases, the data points shift to the right, towards, and in some cases past the line of unity (broken line). At 20% ethanol, eleven of the thirteen compounds are over predicted. The predictive error decreases when 5% ethanol is added to HFA-227, 1.44, compared to that at 0% ethanol, 2.12. This is also seen in Figure 4.9 with 5, 10, and 15% ethanol, where the AAE values are 1.44, 1.24 and 1.17, respectively. These results point to the idea that the ideal solubility model does not accurately describe the log mole fraction solubility, $\log X_2^{obs}$, in HFA-227 for this data set. Also, the error between the ideal solubility model and the observed values decreased with an increase in ethanol concentration.

Figure 4.10 shows a shift to the right of the data points towards the line of unity (ideality) when ethanol is added for five sample compounds, where the ideal solubility is plotted against the experimental values for 0 – 20% w/w ethanol in HFA-227. For all five compounds, the ideal solubility does not change as the ethanol concentration increases, due to the model being solvent-independent.

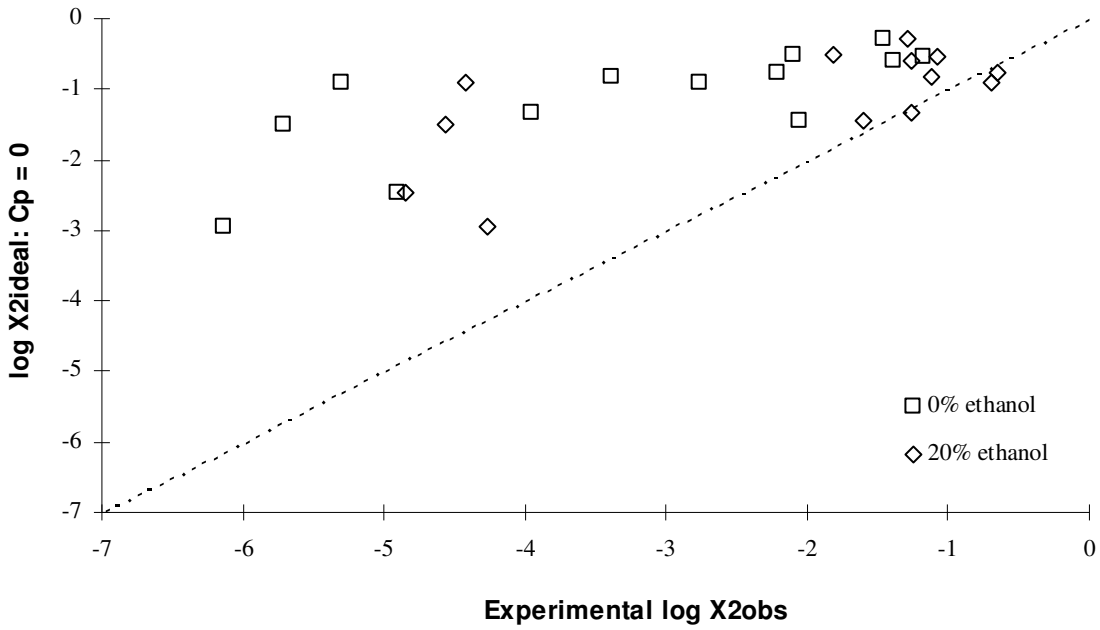

Figure 4.8. Calculated ideal solubility, log X_2^{ideal} (Equation 2.3), plotted against the experimental log mole fraction solubility, log X_2^{obs}, in HFA-227 with 0 and 20% ethanol. The broken line illustrates the line of unity.

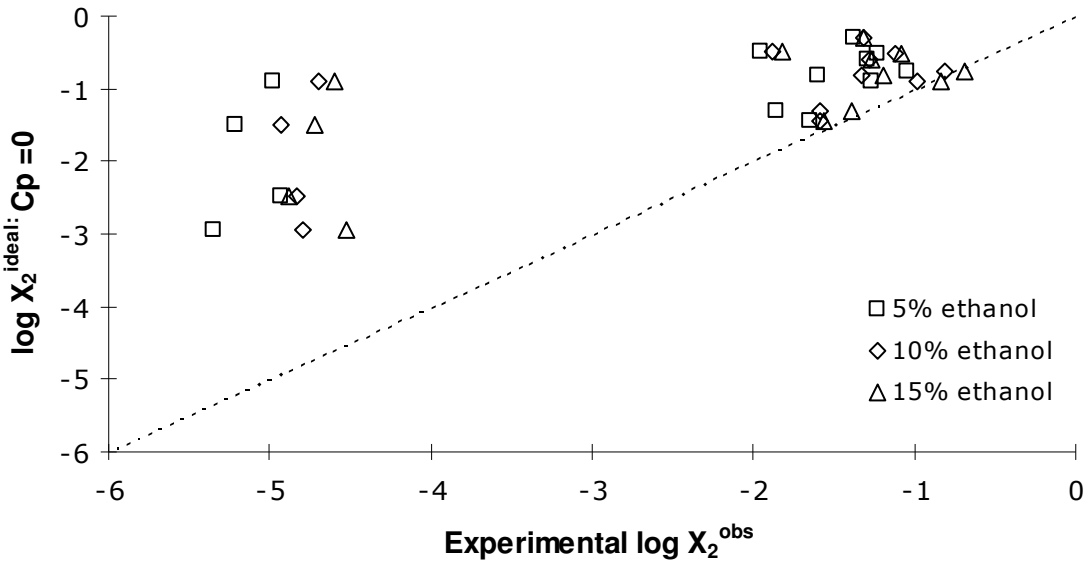

Figure 4.9. Calculated ideal solubility, log X_2^{ideal} (Equation 2.3), plotted against the experimental log mole fraction solubility, log X_2^{obs}, in HFA-227 with 5, 10 and 15% ethanol. The broken line illustrates the line of unity.

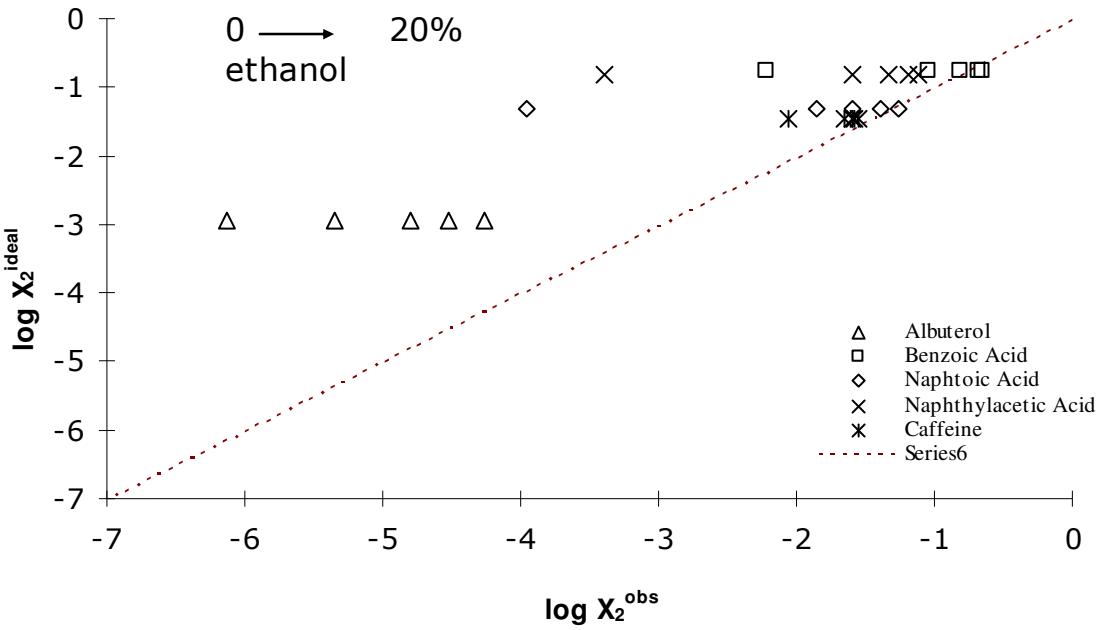

Figure 4.10. Calculated ideal solubility, log X_2^{ideal} (Equation 2.3) plotted against the experimental log mole fraction solubility, log X_2^{obs}, of 5 experimental solutes in HFA-227 with 0 – 20% ethanol. The broken line illustrates the line of unity.

IV. Regular Solution Theory (RST): HFA-227

The regular solution theory (RST) model for a binary mixture requires two parameters, the interaction solubility parameter of the solvent, δ_1, and the interaction solubility parameter of the solute, δ_2. Equation 2.7 calculates the activity coefficient, log γ_2^{RST}, utilizing the RST model, which accounts for the enthalpic interactions between the solute and solvent. The experimental log γ_2^{obs} was obtained by subtracting the experimental solubility, log X_2^{obs}, from the ideal solubility, log X_2^{ideal} (Equation 2.3) according to Equation 2.6,

$$\log \gamma_2^{obs} = \log X_2^{ideal} - \log X_2^{obs} \qquad (2.6)$$

The solubility parameter for HFA-227 has been reported to be 5.40 $(cal/cm^3)^{0.5}$. Figure 4.11 shows the relationship between the calculated activity coefficient, log γ_2^{RST}, and the experimental activity coefficient, γ_2^{obs}, where the AAE is 2.48. It appears that the RST over-predicts the activity coefficient in HFA-227 for the majority of compounds. Only three of the compounds, cholesterol, dehydrocholesterol, and perfluorononanoic acid, have activity coefficients under-predicted by the RST. These three compounds are the largest and most non-polar of the molecules examined. It is apparent that the RST model does not accurately describe the log γ_2^{obs} in HFA-227 for this data set. This error may be due to the fact that HFA-227 has one C-H group capable of hydrogen bonding, and it is known that the RST does not accurately predict systems that have hydrogen bonding properties.

The RST activity coefficient, $\log \gamma_2^{RST}$, can be combined with the ideal solubility model in order to better predict the solubility in HFA-227 as shown in Equation 4.2:

$$\log X_2^{RST} = \log X_2^{ideal} - \frac{V_2}{2.303RT}(5.4 - \delta_2)^2 \qquad (4.2)$$

Applying the RST model activity coefficient did not adequately explain the experimental solubility in HFA-227, as seen by Figure 4.12. The data points appear to move farther away from the line of unity, where the AAE is 3.06 as apposed to an AAE of 2.15 with ideal solubility alone.

The solubility parameter is a calculated value based on the total Van der Waals force derived from the cohesive energy density of the solvent, HFA-227. In an attempt to improve the RST model, a new activity coefficient was proposed. Using the experimental activity coefficient, $\log \gamma_2^{obs}$, the solubility parameter in HFA-227 was back calculated from the RST model to determine the best solubility parameter to describe the 22 compounds. The value was calculated to be 16.09 $(cal/cm^3)^{0.5}$ (RSD = 20.33 %) according to Equation 4.3, similar to that of HFA-134a, which was found to be 21.5 $(cal/cm^3)^{0.5}$ (Figure 4.13).

$$\log \gamma_2^{RST} = -\frac{V_2}{2.303RT}(16.09 - \delta_2)^2 \qquad (4.3)$$

$$\log X_2^{RST} = \log X_2^{ideal} - \frac{V_2}{2.303RT}(16.09 - \delta_2)^2 \qquad (4.4)$$

As seen with the back calculated solubility parameter in HFA-134a, the new parameter in HFA-227 improved the error of the activity coefficient prediction utilizing the RST model, where the AAE decreased to 1.59, as opposed to 2.48 using the theoretical value of 5.40 $(cal/cm^3)^{0.5}$. The data points appear to be more scattered about the line of unity (Figure 4.14) for log mole fraction solubility, $\log X_2^{RST}$, indicating that the RST model does not adequately describe the deviation from ideality in HFA-227.

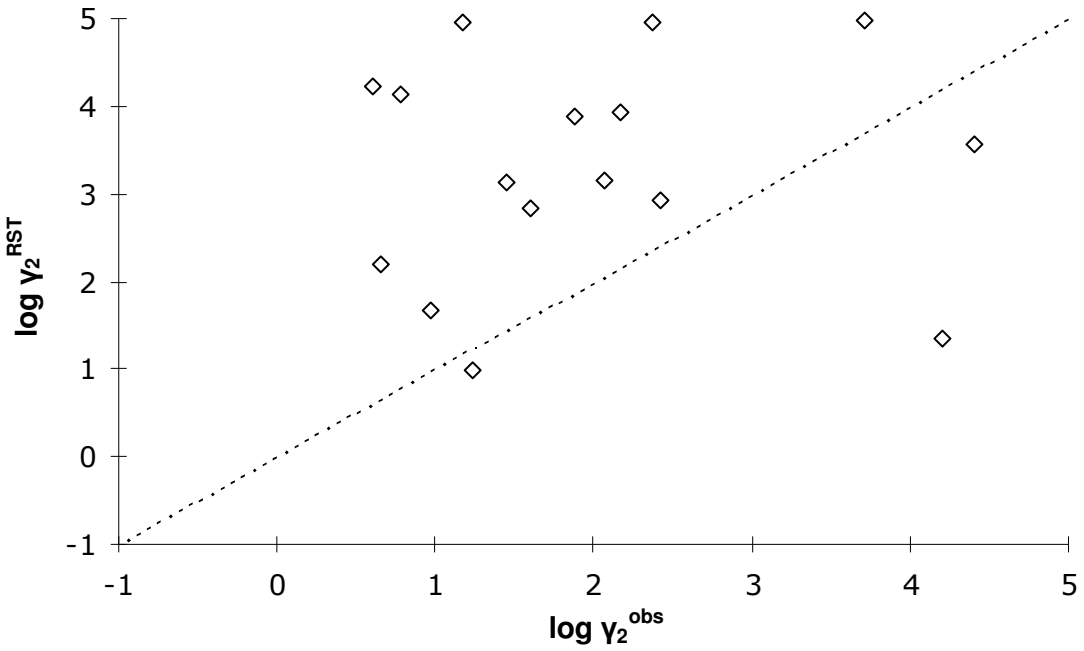

Figure 4.11. Calculated regular solution theory (RST) activity coefficient, log γ_2^{RST}, (Equation 2.7) plotted against the experimental activity coefficient, log γ_2^{obs} (Equation 2.6) in HFA-227. The broken line illustrates the line of unity.

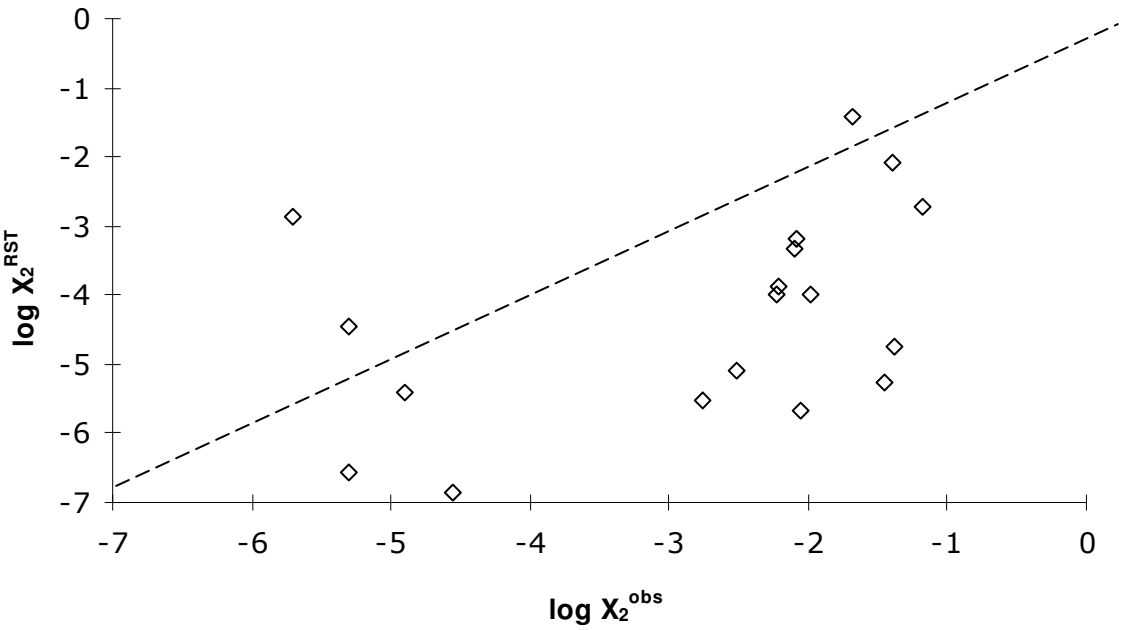

Figure 4.12. Calculated ideal solubility with RST, log X_2^{RST}, (Equation 4.2) plotted against the experimental log mole fraction solubility in HFA-227. The broken line illustrates the line of unity.

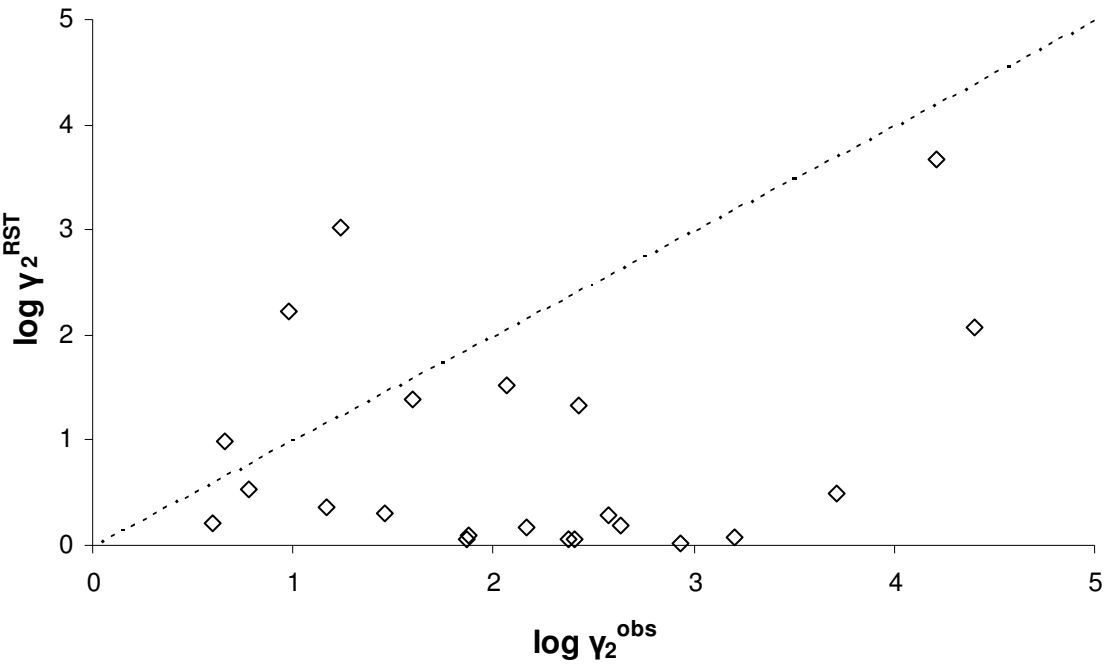

Figure 4.13. Calculated activity coefficient, log γ_2^{RST}, (Equation 4.3) plotted against the experimental activity coefficient, log γ_2^{obs}. The broken line illustrates the line of unity.

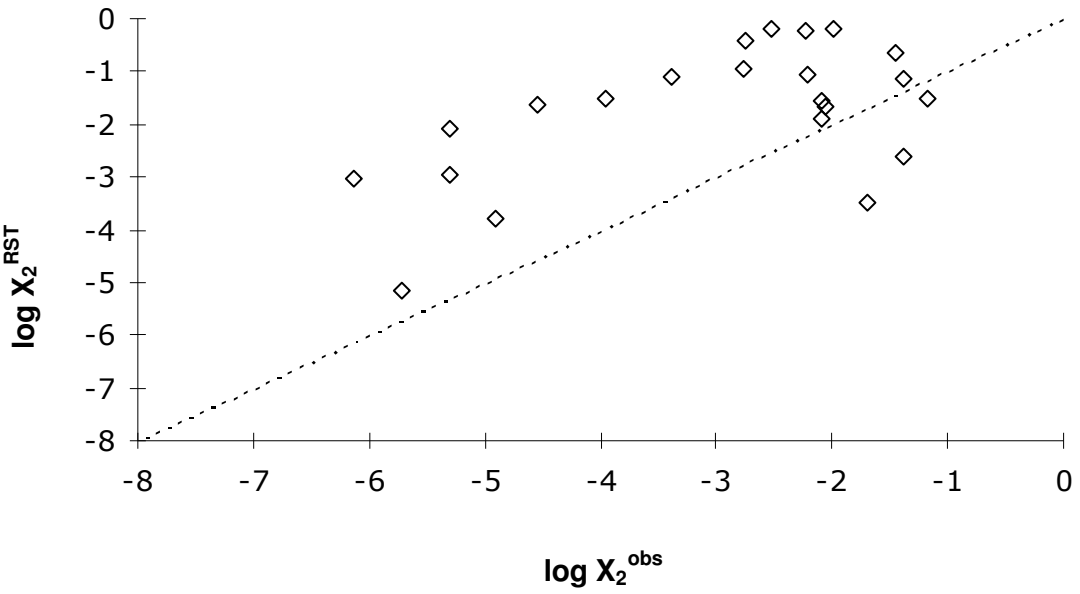

Figure 4.14. Calculated solubility, log X_2^{RST}, (Equation 4.4) plotted against the experimental log mole fraction solubility, log X_2^{obs}. The broken line illustrates the line of unity.

V. Regular Solution Theory (RST): HFA-227 with Ethanol

In order to account for the presence of ethanol, a new calculated solubility parameter was applied to the RST model, which accounts for the different ethanol concentrations according to Equation 4.5:

$$SP = (\%\ \text{ethanol})*SP^{\text{ethanol}} + (\%\ \text{HFA-227})*SP^{\text{HFA}} \qquad (4.5)$$

The solubility parameter for ethanol was calculated to be 12.58 $(cal/cm^3)^{0.5}$ according to Fedors.

The RST model under-predicted the experimental activity coefficient, log γ_2^{obs}, for two of the 13 compounds investigated in this study at 0% ethanol, and 4 of the 13 compounds at 20% ethanol in HFA-227. When 20% ethanol was added to the HFA-227 solution, the activity coefficient values shifted slightly to the left, as seen in Figure 4.15, where the AAE is 1.90 in HFA-227 with 20% ethanol compared to 3.12 at 0% ethanol. The RST model under-predicted the experimental activity coefficient in HFA-227 with 20% ethanol for some of the compounds that were over-predicted at 0% ethanol, such as phenanthrene and anthracene. Figure 4.16 shows that at 5, 10 and 15% ethanol concentrations in HFA-227, more compounds shift towards the line of unity compared to those values at 0% ethanol when the RST was applied. The AAE values for 5, 10, and 15% ethanol in HFA-227 are 2.79, 2.47 and 2.18, respectively.

The RST model for activity coefficient was combined with ideal solubility to solve for the log mole fraction of a ‘real’ solution as seen in Figure 4.17 and 4.18. When ideal solubility is combined with the RST model, the solubility in HFA-227 with 0 – 20% w/w ethanol is more accurately predicted compared to the ideal solubility equation alone.

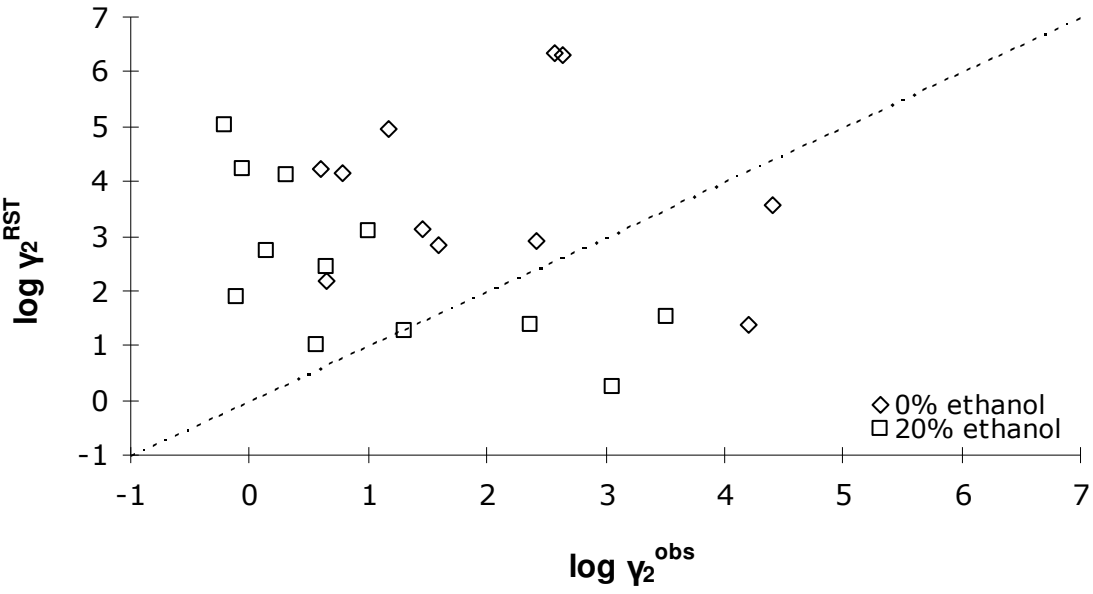

Figure 4.15. Calculated RST activity coefficient, log γ_2^{RST}, (Equation 4.3) plotted against the experimental log activity coefficient, log γ_2^{obs}, in HFA-227 with 0 and 20% ethanol. The broken line illustrates the line of unity.

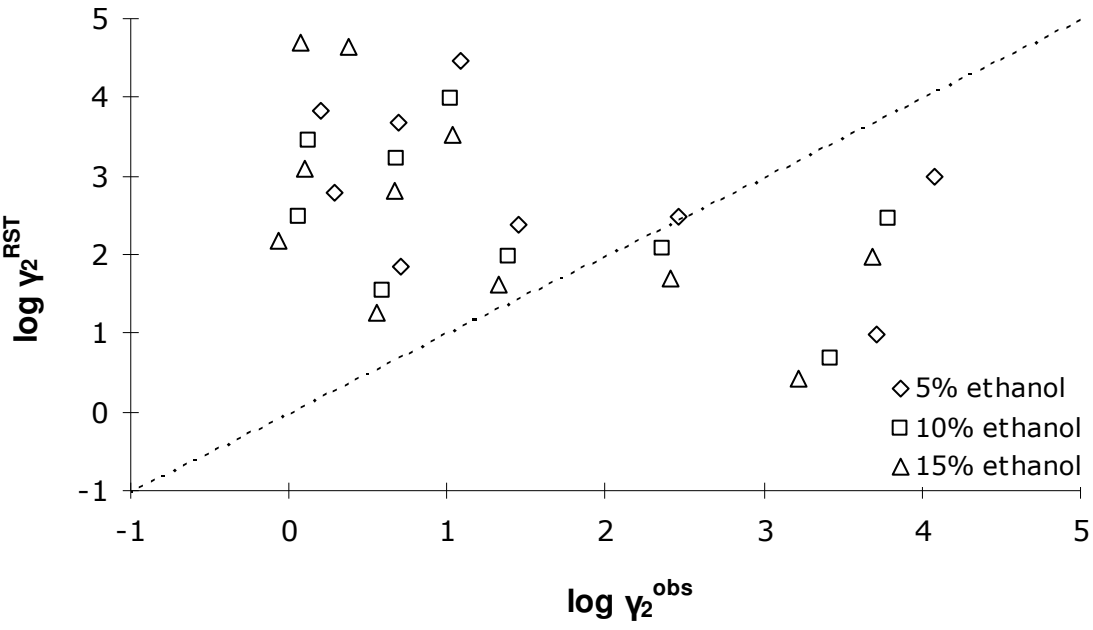

Figure 4.16. Calculated RST activity coefficient, log γ_2^{RST}, (Equation 4.3) plotted against the experimental log activity coefficient, log γ_2^{obs}, in HFA-227 with 5, 10 and 15% w/w ethanol. The broken line illustrates the line of unity.

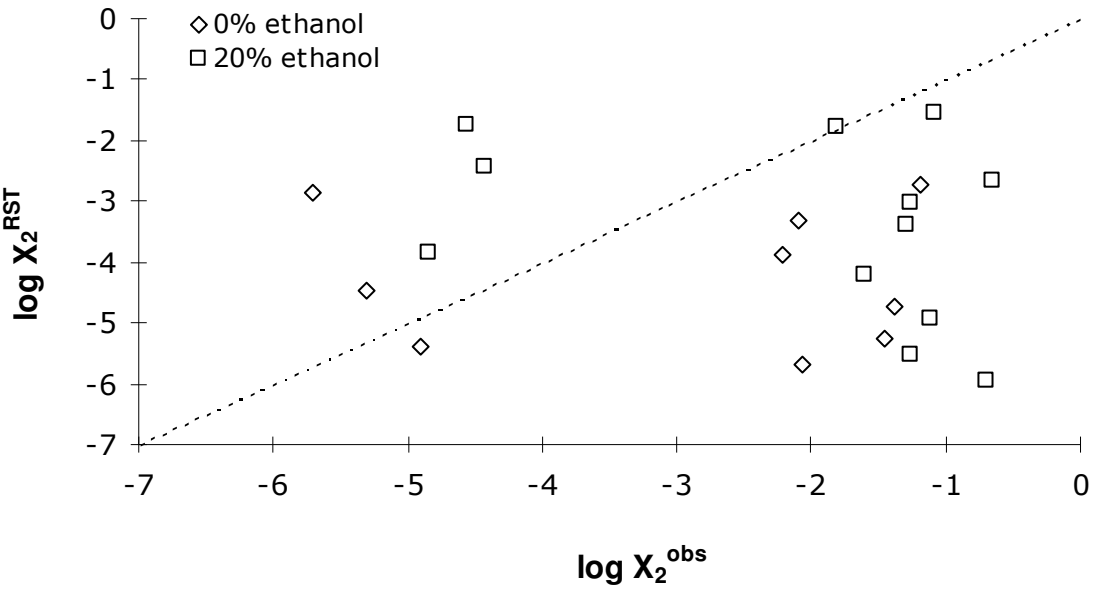

Figure 4.17. Calculated log X_2^{RST}, (Equation 4.4) plotted against the experimental log mole fraction solubility, log X_2^{obs}, in HFA-227 with 0 and 20% ethanol. The broken line illustrates the line of unity.

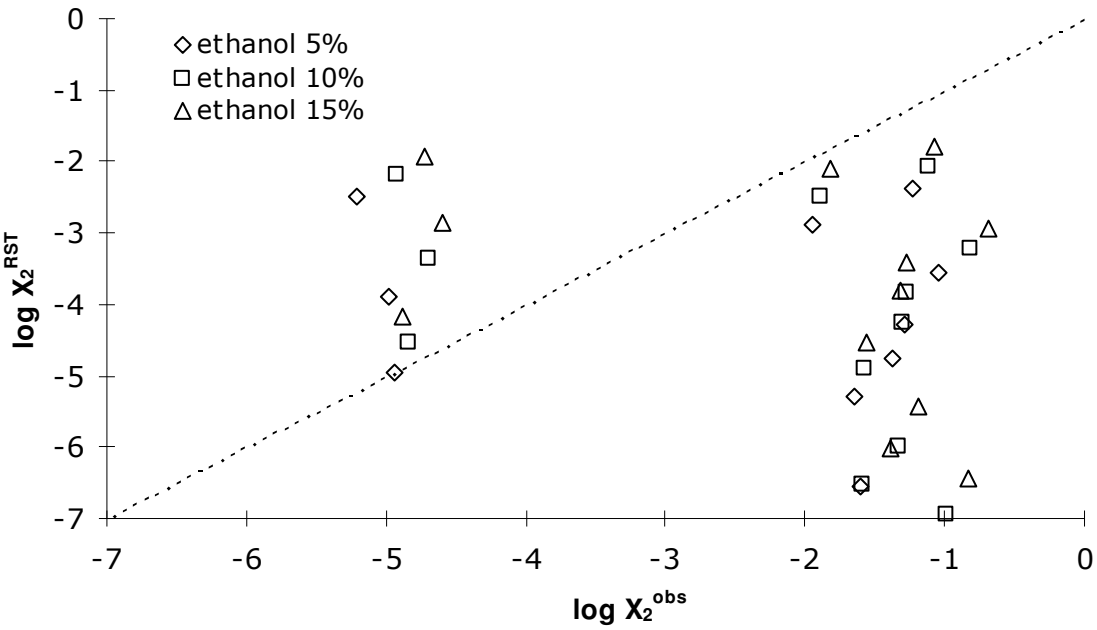

Figure 4.18. Calculated log X_2^{RST}, (Equation 4.4) plotted against the experimental log mole fraction solubility, log X_2^{obs}, in HFA-227 with 5, 10 and 15% ethanol. The broken line illustrates the line of unity.

VI. Deviation from Ideality in HFA-227

Previous work indicated that theoretical solubility values moved toward ideality when ethanol was added to HFA-134a as a cosolvent. Figure 4.17 shows that the solubility in HFA-227 was over-predicted for 2 of the 13 compounds at 0% ethanol. As the ethanol concentration increases, the values shift up and to the right, where some log X_2^{obs} values become over-predicted to varying degrees according to the ideal solubility model (Figure 4.18).

The opposite trend was seen for activity coefficient, where as the ethanol concentration increased, the activity coefficients shift to the left, towards the line of unity. Many calculated values became less over-predicted with the addition of ethanol. Those compounds that behaved most ideally in HFA-227 have activity coefficient values closest to zero, and line up along the line of unity. Table 4.1 shows the log γ_2^{obs} values at 0 and 20% ethanol for 13 compounds.

Caffeine and naphthalene appear to behave most ideally in HFA-227 at 0% ethanol, where the log γ_2^{obs} are 0.659 and 0.603. Benzoic acid and naphthoic acid appear to behave the most ideally in HFA-227 at 20% ethanol, where the log γ_2^{obs} are -0.059 and -0.105. Dehydrocholesterol, cholesterol and albuterol had activity coefficient values furthest away from zero at 0% ethanol, indicating that they are the least ideally behaved compounds. Therefore, it appears that the most ideal compounds are not related to the hydrogen bond potential, as seen with HFA-134a.

The average log γ_2^{obs} also represents the AAE value between the ideal solubility model and the experimental solubility at each cosolvent concentration. Therefore, Table 4.1 also shows that the AAE improves with the addition of ethanol for each compound. The deviation from ideality decreased the most for compounds such as naphthylacetic acid, naphthoic acid and naphthol. No direct relationship was found between a solute's physical properties and the ability to behave ideally in HFA-227. In general, HFA-227 is not an ideal solvent, yet some compounds can behave close to ideal.

Compound	Activity Coefficient (log γ_2^{obs})	
	0% ethanol	*20% ethanol*
Dehydrocholesterol	4.404	3.521
Cholesterol	4.210	3.057
Albuterol	3.201	1.331
Naphthoic acid	2.633	-0.059
Naphthylacetic acid	2.577	0.308
Anthracene	2.426	2.367
Naphthol	1.864	-0.202
Phenanthrene	1.598	1.310
Benzoic acid	1.455	-0.105
Nitronaphthalene	1.167	1.003
Methoxynaphthalene	0.780	0.658
Naphthalene	0.659	0.559
Caffeine	0.603	0.143

Table 4.1. Log activity coefficient, log γ_2^{obs}, values for 0 and 20% ethanol in HFA-227.

VII. Physical Property Correlation in HFA-227

The theoretical models proposed in this work represent poor approximations for the selected compounds in HFA-227, resulting in fairly large predictive errors. Therefore, a correlation to physical properties was investigated in order to better predict the solubility in HFA-227. Table 4.2 displays the solutes investigated along with nine solutes from Dickinson *et al*.,[9] where the solubilities were also determined in HFA-227. Five of the nine compounds obtained from Dickinson *et al*. were phenol groups with a different substituent group in the para position. All nine compounds from Dickinson *et al.* contained hydrogen-bonding groups. The 22 compounds were regressed against 12 different physical properties using a MLR computer program (MedCalc Statistical Software). Only one significant one parameter equation was determined. The crystal term used in ideal solubility resulted in a significant p-value of 0.001, and was regressed against the solubilities resulting in Equation 4.6:

$$\log X_2 = -0.017(\text{MP}-25) - 1.60 \qquad (4.6)$$

$$\text{AAE} = 0.89$$

The plot of Equation 4.6 can be seen in Figure 4.19, where the AAE is 0.89, or a factor error of 7.76.

Additional physical properties were investigated as second and third parameters in order to decrease the error of the predicted equation. For all two and three parameter equations, the crystal term was always significant according to the p-value (< 0.05). The addition of a second parameter to the crystal term showed a decrease in error for equations utilizing the number of OH groups for each compound, or the number of hydrogen donating groups for each compound, as seen in Table 4.2. Equation 4.15 shows an improved correlation to the solubility in HFA-227 with the incorporation of the number of OH groups (Figure 4.20).

$$\log X_2 = -0.016(\mathrm{MP} - 25) - 0.983(\mathrm{OH}) - 1.10 \qquad (4.15)$$

$$\mathrm{AAE} = 0.65$$

Table 4.2 also provides the coefficient of each parameter, where the coefficient of the crystal term for the majority of the equations is -0.02, slightly more negative then the coefficient of the crystal term for HFA-134a, -0.01. This difference points to the possibility that the crystal term may have a greater impact on solubility in HFA-277 than in HFA-134a. The addition of a third parameter further decreased the predictive error for HFA-227. Physical properties such as the number of COOH and OH groups, or the number of OH groups and the molar volume, in addition the crystal term showed an improved predictive equation. The lowest error was found when the number of OH groups and the logP of each compound were utilized along side the crystal term, according to Equation 4.20 (Figure 4.21).

$$\log X_2 = -0.018(\text{MP} - 25) - 1.117(\text{OH}) - 0.172(\text{logP}) - 0.272 \qquad (4.20)$$

$$\text{AAE} = 0.58$$

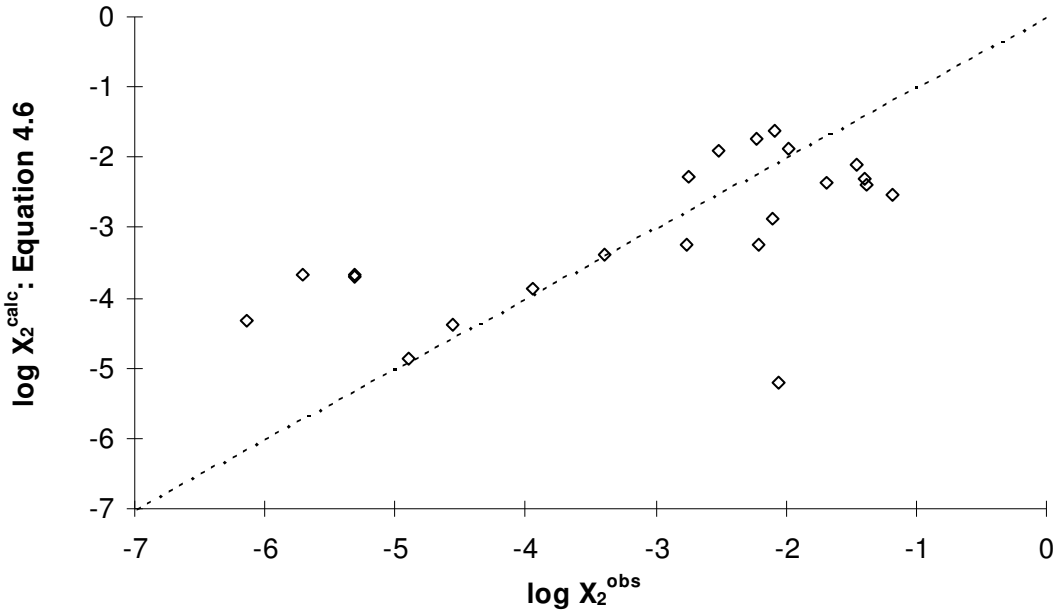

Figure 4.19. Calculated solubility in HFA-227, log X_2^{calc}, according to Equation 4.6 plotted against the experimental solubility, log X_2^{obs}. The broken line illustrates the line of unity.

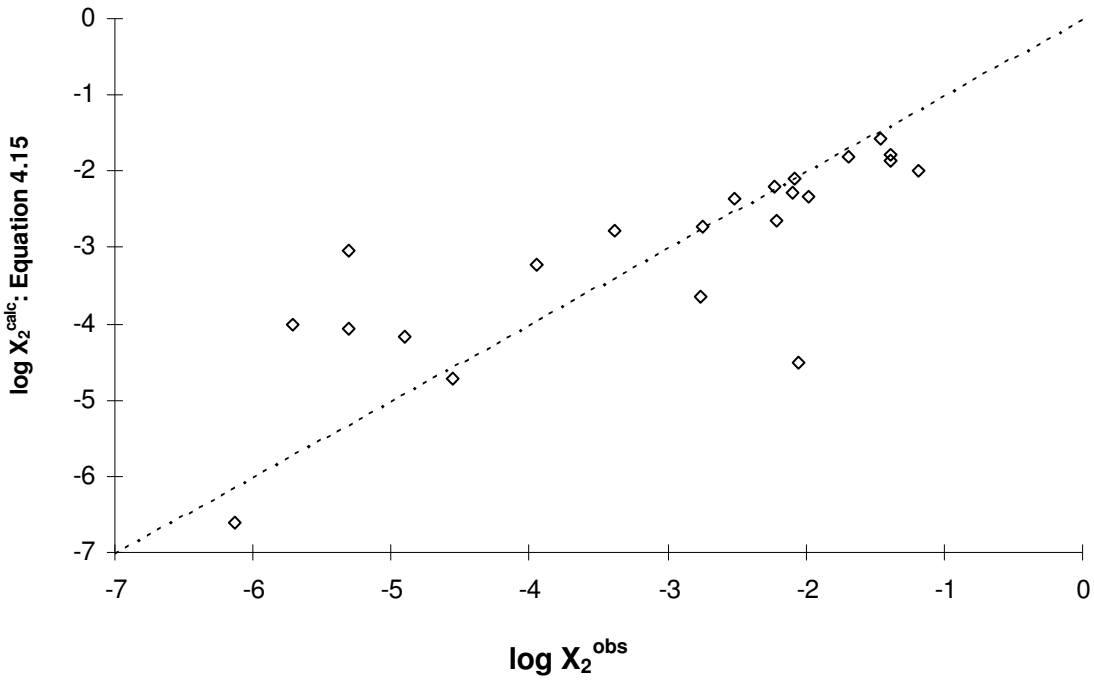

Figure 4.20. Calculated solubility in HFA-227, log X_2^{calc}, according to Equation 4.15 plotted against the experimental solubility, log X_2^{obs}. The broken line illustrates the line of unity.

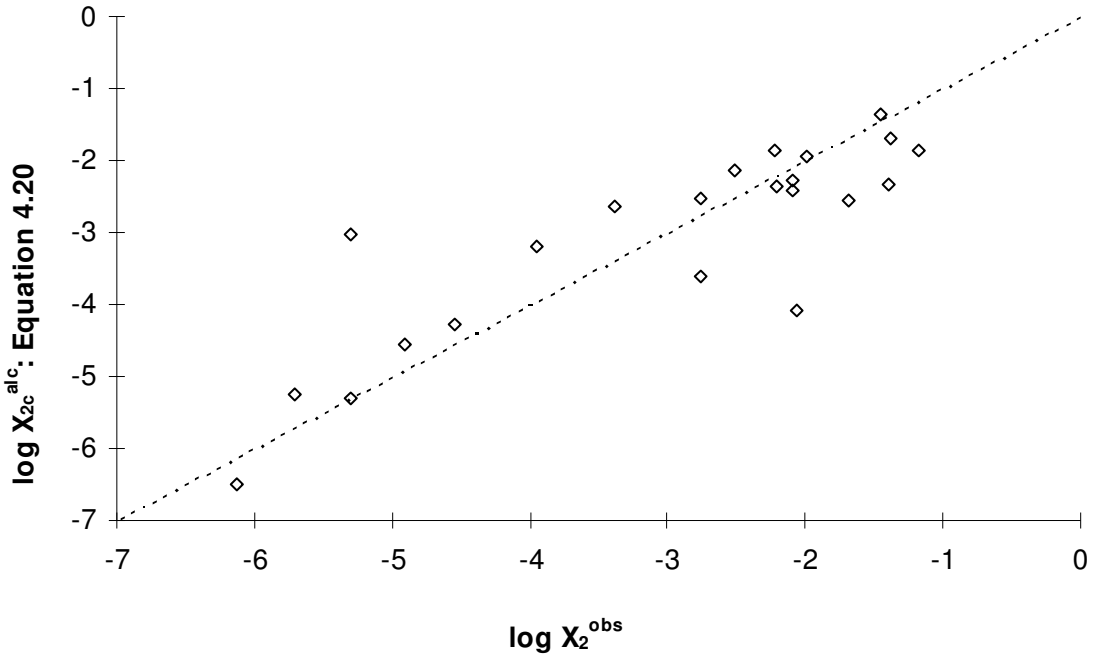

Figure 4.21. Calculated solubility in HFA-227, log X_2^{calc}, according to Equation 4.20 plotted against the experimental solubility, log X_2^{obs}. The broken line illustrates the line of unity.

Equation #	Parameter #1	Parameter #2	Parameter #3	Intercept	AAE
1 Parameter					
4.6	(-0.017)(MP – 25)			-1.60	0.89
2 Parameter					
4.7	(-0.018)(MP – 25)	(-0.115)logP		-1.10	0.92
4.8	(-0.016)(MP – 25)	(-0.006)MV		-0.67	0.92
4.9	(-0.017)(MP – 25)	(-0.002)MW		-1.25	0.91
4.10	(-0.017)(MP – 25)	(+0.176)COOH		-1.647	0.89
4.11	(-0.017)(MP – 25)	(+0.382)HA		-2.020	0.89
4.12	(-0.017)(MP – 25)	(-0.016)SP		-1.423	0.88
4.13	(-0.017)(MP – 25)	(-0.539)HD		-1.181	0.86
4.14	(-0.018)(MP – 25)	(-123.032)HBN		-0.975	0.81
4.15	(-0.016)(MP – 25)	(-0.983)OH		-1.10	0.65
3 Parameter					
4.16	(-0.011)(MP – 25)	(-0.736)OH	(-0.010)MW	+0.455	0.89
4.17	(-0.018)(MP – 25)	(+0.428)HA	(-0.600)HD	-1.60	0.83
4.18	(-0.016)(MP – 25)	(-0.990)OH	(-0.007)MV	-0.102	0.65
4.19	(-0.016)(MP – 25)	(-1.189)OH	(-0.720)COOH	-0.816	0.65
4.20	(-0.018)(MP – 25)	(-1.117)OH	(-0.172)logP	-0.272	0.58

Table 4.2. Regression equations for 22 compounds in HFA-227.

Compound	**MP (ºC)**	**logP**	**MW**	**MV**	**log X_2**
4-Aminophenol	189	-0.29	109.13	81.6	-4.552
Biphenylacetic acid	147	3.25	212.25	159.8	-5.304
4-Bromophenol	65	2.5	173.01	92.4	-2.753
4-Chlorophenol	43	2.43	173.01	86.4	-2.518
Dodecan-1-ol	26	5.13	186.34	220.6	-2.089
9H-Hexadecafluorononanoic acid	67	7.6	446.09	224.5	-1.390
4-Methylphenol	33	1.94	108.14	95.9	-2.226
Perfluorononanoic acid	70	8.64	464.08	247	-1.686
Phenol	41	1.48	94.11	81.4	-1.984

Table 4.3. Compounds obtained from Dickinson *et al*.,[9] and their physical properties.

VIII. Physical Property Correlation: HFA-227 with Ethanol

A correlation to physical properties was investigated in HFA-227 with ethanol (0 – 20% w/w). The 13 solutes were regressed against 12 physical properties using a MLR computer program. A correlation was determined using the crystal term from ideal solubility to predict the solubility in HFA-227 with 0 – 20% w/w ethanol, resulting equations 4.21 and 4.25:

$$\log X_2^{0\%\ ethanol} = -0.02(MP - 25) - 1.20 \qquad (4.21)$$

$$AAE = 1.02$$

$$\log X_2^{20\%\ ethanol} = -0.02(MP - 25) - 0.51 \qquad (4.25)$$

$$AAE = 1.18$$

The AAE for the 13 solutes in HFA-227 with 0 and 20% ethanol is 1.02 and 1.18, indicating the predicted solubility is off by a factor of 10.47 and 15.14, respectively, from the experimental solubility (Figure 4.22). The intercept values for Equations 4.21 and 4.25 decreased from -1.20 to -0.51, as observed earlier in the decrease for activity coefficient, γ_2, with an increase in ethanol. Table 4.4 shows the regression equations for HFA-227 with 0 – 20% w/w ethanol, where the AAE is seen to decrease for two and three parameter equations.

Figure 4.23 shows the solubility in HFA-227 with 5, 10 and 15% ethanol plotted against the calculated solubility from Equations 4.22, 4.23, and 4.24 found in Table 4.4. The data points appeared to be in two separate clusters, where the solutes with low solubilities, such as cholesterol, albuterol, anthracene and dehydrocholesterol, are all over predicted. Those solutes with higher solubilities, on average, are under predicted according the regression equations utilizing the crystal term.

Table 4.4 presents some of the significant two and three parameter regression equations determined by MLR for all five ethanol concentrations in HFA-227. Equations 4.26 and 4.30 show the regression equations utilizing two parameters in HFA-227 with 0 and 20% ethanol, the crystal term (MP – 25) and molar volume (MV). On average, the AAE is improved by a factor of three compared to the prediction of solubility with just the crystal term, as shown by Figures 4.24 and 4.25. The predictive error was found to decrease at 20% ethanol, similar to that in HFA-134a.

$$\log X_2^{0\%\ ethanol} = -0.01(02(MP - 25) - 0.02(MV) + 1.63 \qquad (4.26)$$

$$AAE = 0.79$$

$$\log X_2^{20\%\ ethanol} = -0.01(02(MP - 25) - 0.02(MV) + 2.68 \qquad (4.30)$$

$$AAE = 0.51$$

Figures 4.24 and 4.25 illustrate the improved relationship, where more of the solutes appear to move closer to the line of unity (broken line), especially for the solutes with higher solubilities in HFA-227, indicating an improved predictive equation. Interestingly, the crystal term coefficient decreased to -0.01 and the molar volume coefficient remained constant at -0.02 for all five ethanol concentrations.

When a third parameter was utilized in order to better predict the solubility in HFA-227, the error slightly decreased compared to that of a two parameter equation, as shown by Equation 4.36 and 4.40, where OH is the number of OH groups for each compound:

$$\log X_2^{0\% \text{ ethanol}} = -0.016(\text{MP} - 25) - 1.106(\text{OH}) - 0.278(\log\text{P}) + 0.078 \qquad (4.36)$$

$$\text{AAE} = 0.52$$

$$\log X_2^{20\% \text{ ethanol}} = -0.015(\text{MP} - 25) - 0.764(\text{OH}) - 0.326(\log\text{P}) + 0.994 \qquad (4.40)$$

$$\text{AAE} = 0.59$$

The intercept values for three parameter equations increased with increasing ethanol concentration, unlike the intercept values for a two parameter equation, indicating that the activity coefficient, γ_2, may be more significant with an increase in cosolvent in HFA-227. The intercept values in HFA-134a decrease with increasing ethanol concentration, revealing dissimilarity in solubility trends between the two propellants. For the 13 compounds investigated, 54% were predicted within 0.5 log units of observed values at both 0 and 20% w/w ethanol in HFA-227, according to Equations 4.36 and 4.40.

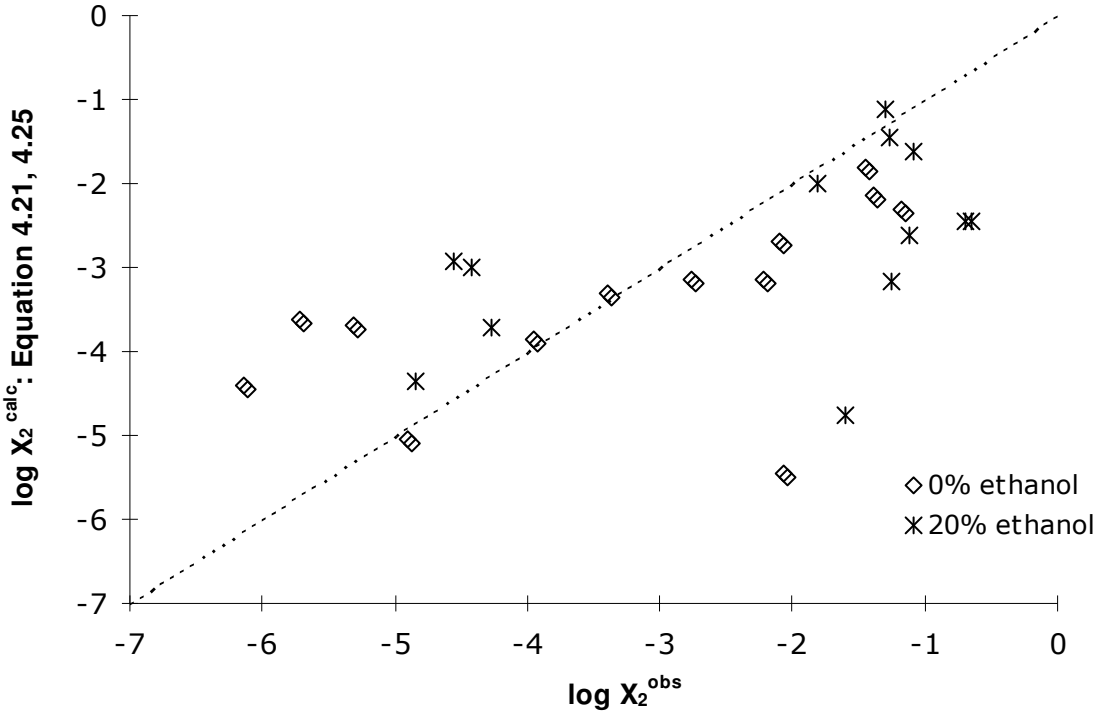

Figure 4.22. Calculated solubility according to Equation 4.21 and 4.25 plotted against experimental solubility in HFA-227 with 0 and 20% ethanol. The broken line illustrates the line of unity.

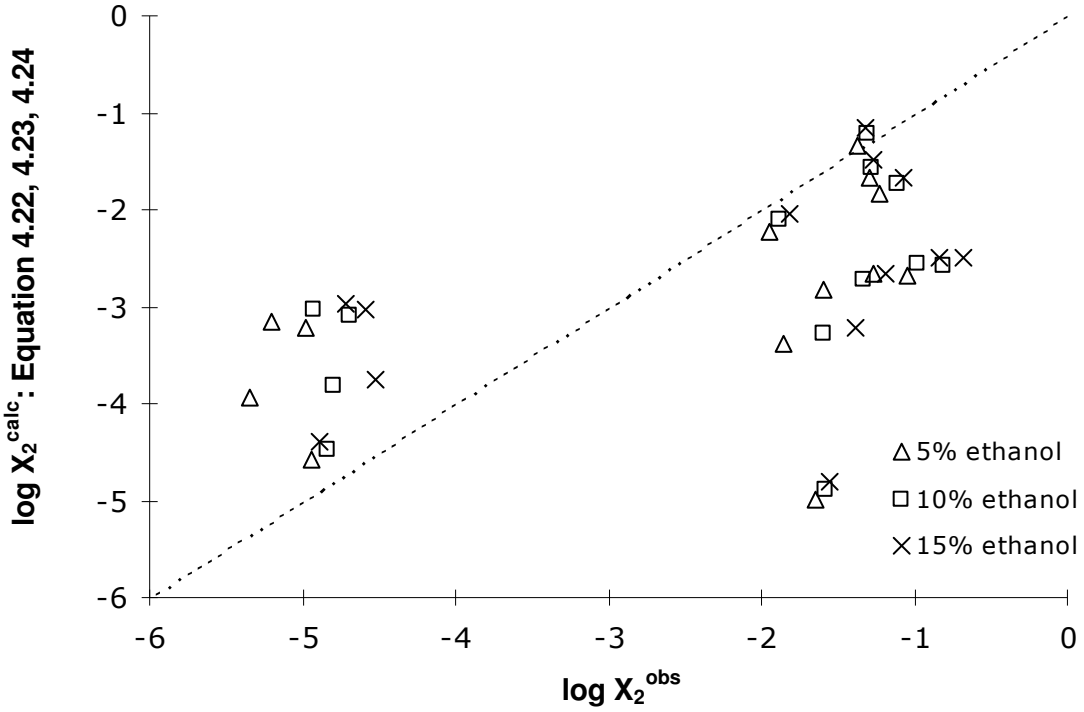

Figure 4.23. Calculated solubility according to Equations 4.22, 4.23, 4.24 plotted against experimental solubility in HFA-227 with 5, 10 and 15% ethanol. The broken line illustrates the line of unity.

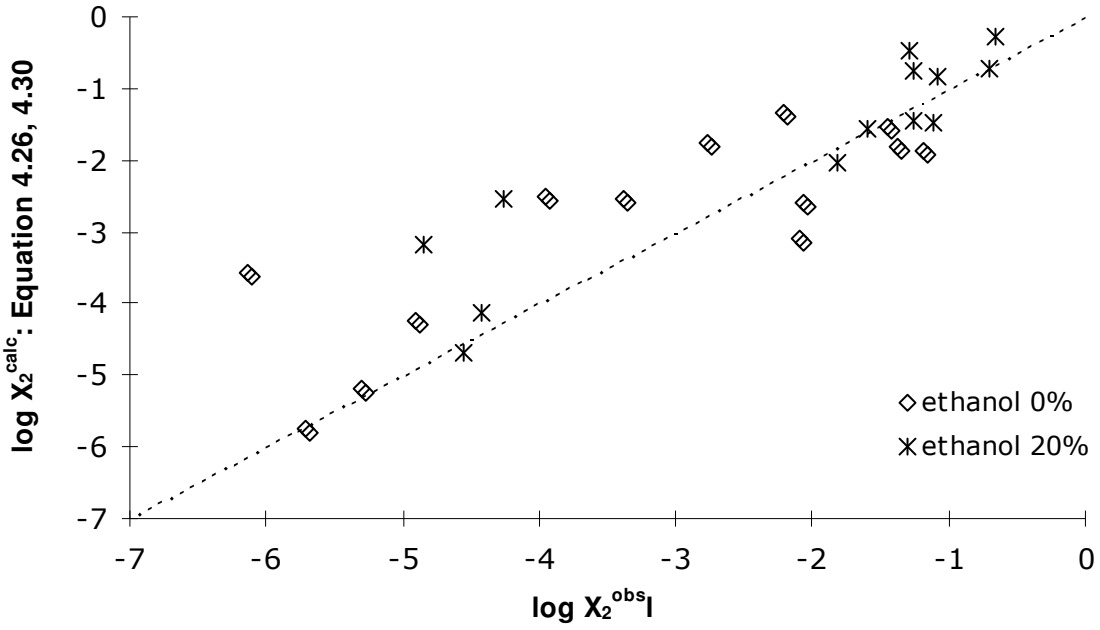

Figure 4.24. Calculated solubility according to Equations 4.26 and 4.30 plotted against experimental solubility in HFA-227 with 0 and 20% ethanol. The broken line illustrates the line of unity.

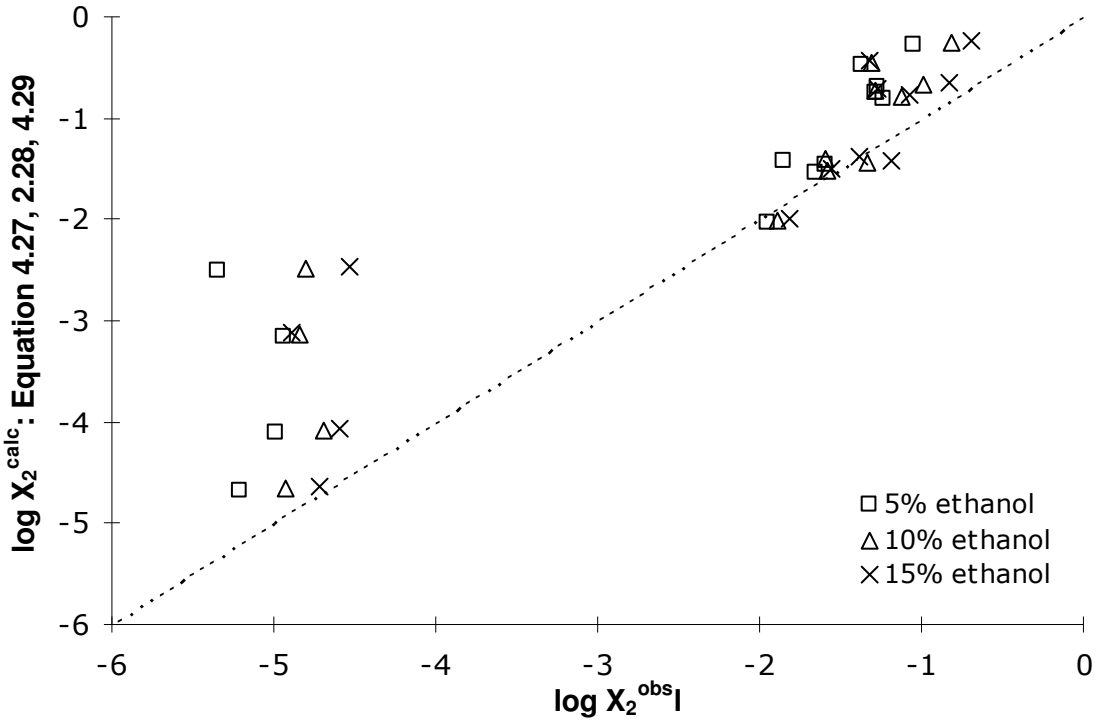

Figure 4.25. Calculated solubility according to Equations 4.27, 4.28, 4.29 plotted against experimental solubility in HFA-227 with 5, 10 and 15% ethanol. The broken line illustrates the line of unity.

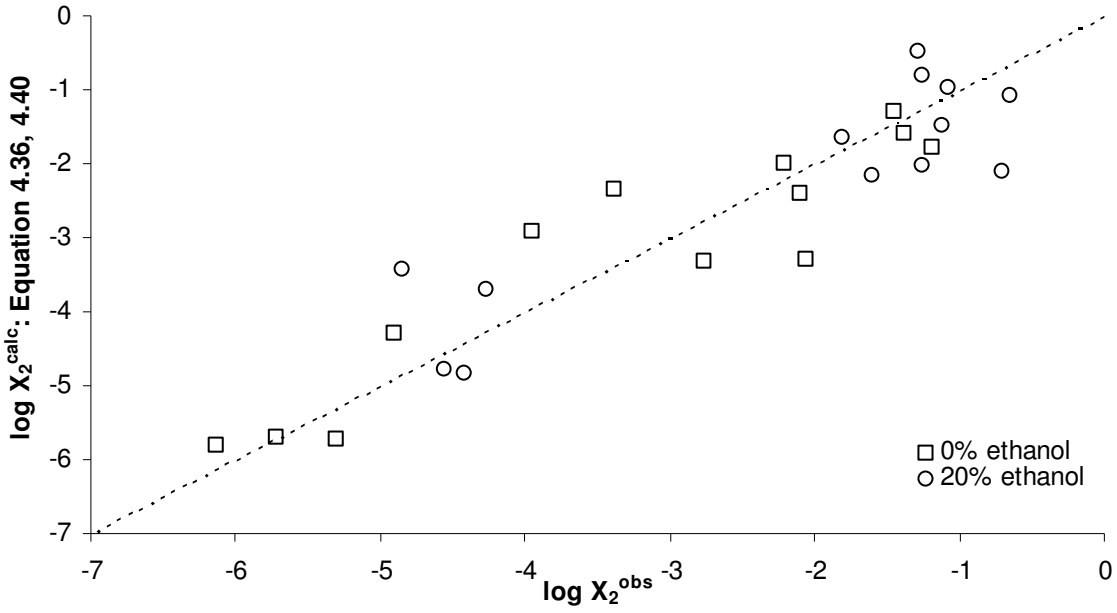

Figure 4.26. Calculated solubility according to Equations 4.36 and 4.40 plotted against experimental solubility in HFA-227 with 0 and 20% ethanol. The broken line illustrates the line of unity.

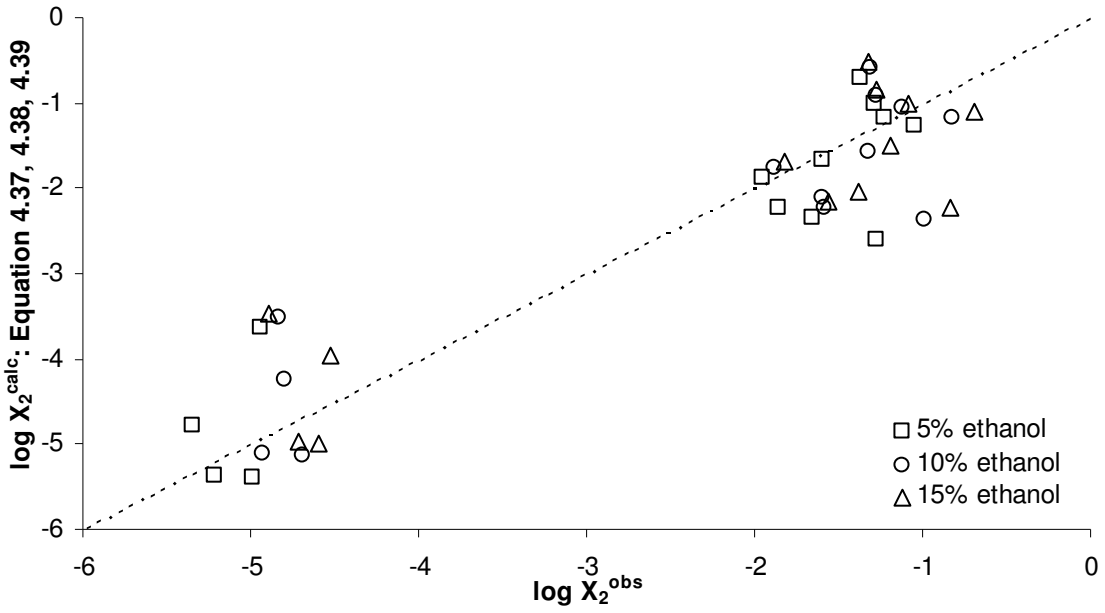

Figure 4.27. Calculated solubility according to Equations 4.37, 4.38, 4.39 plotted against experimental solubility in HFA-227 with 5, 10 and 15% ethanol. The broken line illustrates the line of unity.

Equation #	% Ethanol	Parameter #1	Parameter #2	Parameter #3	Intercept	AAE
1 parameter						
4.21	0	(-0.02)(MP-25)			-1.20	1.02
4.22	5	(-0.02)(MP-25)			-0.73	1.23
4.23	10	(-0.02)(MP-25)			-0.62	1.21
4.24	15	(-0.02)(MP-25)			-0.55	1.21
4.25	20	(-0.02)(MP-25)			-0.51	1.18
2 parameters						
4.26	0	(-0.02)(MP-25)	(-0.29)logP		0.13	0.71
4.27	5	(-0.02)(MP-25)	(-0.34)logP		0.87	0.73
4.28	10	(-0.02)(MP-25)	(-0.34)logP		0.97	0.74
4.29	15	(-0.02)(MP-25)	(-0.34)logP		1.03	0.77
4.30	20	(-0.02)(MP-25)	(-0.33)logP		1.03	0.77
2 parameters						
4.31	0	(-0.01)(MP-25)	(-0.02)MV		1.63	0.79
4.32	5	(-0.01)(MP-25)	(-0.02)MV		2.70	0.77
4.33	10	(-0.01)(MP-25)	(-0.02)MV		2.72	0.61
4.34	15	(-0.01)(MP-25)	(-0.02)MV		2.74	0.56
4.35	20	(-0.01)(MP-25)	(-0.02)MV		2.68	0.51
3 parameters						
4.36	0	(-0.016)(MP-25)	(-2.206(OH)	(-0.278)logP	+0.078	0.52
4.37	5	(-0.015)(MP-25)	(-1.061)OH	(-0.335)logP	+0.818	0.48
4.38	10	(-0.015)(MP-25)	(-0.923)OH	(-0.334)logP	+0.924	0.53
4.39	15	(-0.015)(MP-25)	(-0.849)OH	(-0.334)logP	+0.990	0.57
4.40	20	(-0.015)(MP-25)	(-0.764)OH	(-0.326)logP	+0.994	0.59

Table 4.4. Regression equations correlated to the log mole fraction solubility in HFA-227 with 0 – 20% w/w ethanol utilizing physical property combinations.

IX. Physical Property Correlation for Activity Coefficient in HFA-227

The regular solution theory (RST) model did not adequately account for the deviation from ideality, also knows as the activity coefficient, in HFA-227. Another tool for examining the activity coefficient is multiple linear regression (MLR) against the compounds physical properties. Using this method, an improved prediction may possibly be obtained. Table 4.5 illustrates a few of the physical properties examined, with corresponding AAE values, for the activity in HFA-227. The calculated activity coefficients were regressed against the experimental values obtained from Equation 2.6 for the 22 compounds investigated.

According to Table 4.5, the combined use of the molar volume and HBN results in a significant ($p<0.05$) predictive equation for the log activity coefficient. Figure 4.28 shows the resulting relationship, where the AAE is 0.60, according to Equation 4.54:

$$\log \gamma_2 = 0.012(\text{MV}) + 204.446(\text{HBN}) - 0.660 \qquad (4.54)$$

$$\text{AAE} = 0.60$$

Although the relationship in Equation 4.54 is off by an error factor of 3.98, a regression equation represents an improved method of predicting the activity coefficient in HFA-227.

Equation #	Parameter #1	Parameter #2	Intercept	AAE
1 Parameter				
4.41	(0.006)MV		1.226	0.86
4.42	(0.096)logP		1.792	0.86
4.43	(0.002)MW		1.832	0.86
4.44	(-0.073)COOH		2.172	0.85
4.45	(-0.294)HA		2.526	0.84
4.46	(0.025)SP		1.861	0.84
4.47	(0.628)HD		1.666	0.78
4.48	(99.551)HBN		1.702	0.77
4.49	(0.707)OH		1.766	0.76
2 Parameter				
4.50	(0.194)logP	(167.336)HBN	0.673	0.73
4.51	(0.006)MV	(0.712)OH	0.826	0.73
5.52	(0.007)MV	(0.743)HD	0.442	0.71
4.53	(0.138)logP	(0.817)OH	1.192	0.69
4.54	(0.012)MV	(204.446)HBN	-0.660	0.60
Molecular Weight (MW) Hydrogen Bond Number (HBN) Solubility Parameter (SP)				

Table 4.5. Physical property correlations to log activity coefficient in pure HFA-227 according to multiple linear regression (MLR).

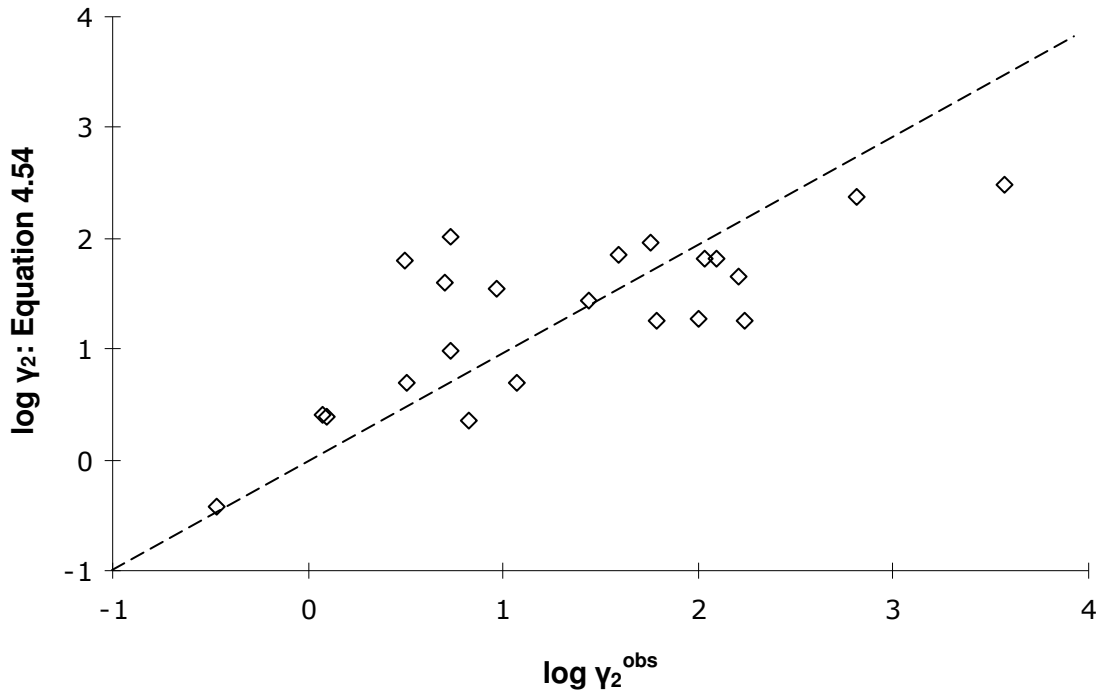

Figure 4.28. Calculated log activity coefficient, log γ_2^{calc}, (Equation 4.54) plotted against the experimental log activity coefficient, log γ_2^{obs}, in HFA-227. The broken line illustrates the line of unity.

X. Physical Property Correlation for Activity Coefficient in HFA-227 with Ethanol

The log activity coefficient, log γ_2^{obs}, for 13 solutes in HFA-227 with 0 – 20% w/w ethanol were regressed against 12 different physical properties. Table 4.6 shows the results of the one and two parameter regression equations, and the corresponding AAE values.

Both polarity (logP) and a compound's molar volume were each found to be significant single parameters to predict the log activity coefficient in all five ethanol concentrations. However, adding a second parameter, a solute's hydrogen bond number (HBN) (Equation 3.2), to the molar volume, improved the predictive equations, as seen from the AAE values in Table 4.6. Equations 4.70 and 4.74 in HFA-227 with 0 and 20% ethanol show that a two parameter equation utilizing the parameters molar volume and HBN result in AAE values ranging from 0.32 to 0.36, or factor error values ranging from 2.09 to 2.29.

$$\log \gamma_2^{0\%\ ethanol} = 206.720(HBN) + 0.018(MV) - 1.624 \qquad (4.70)$$

$$AAE = 0.32$$

$$\log \gamma_2^{20\%\ ethanol} = -51.123(HBN) + 0.018(MV) - 1.832 \qquad (4.74)$$

$$AAE = 0.35$$

Figures 4.29 and 4.30 show the relationship between the calculated log activity coefficient, log γ_2^{calc}, and the experimental log activity coefficient, log γ_2^{obs}. The same error values were found for the log mole fraction solubility, log X_2^{calc}, when the predictive equations for log activity coefficient, log γ_2^{calc}, were added to the ideal solubility model, log X_2^{ideal} (Figures 4.31, 4.32). A reasonable approach to predicting solubility in HFA-227 with 0 – 20% ethanol is described in Equations 4.75 to 4.79:

$$\log X_2^{0\%\ ethanol} = \log X_2^{ideal} - 206.720(\text{HBN}) + 0.018(\text{MV}) - 1.624 \quad (4.75)$$

$$\text{AAE} = 0.32$$

$$\log X_2^{5\%\ ethanol} = \log X_2^{ideal} - 32.949(\text{HBN}) + 0.020(\text{MV}) - 2.111 \quad (4.76)$$

$$\text{AAE} = 0.35$$

$$\log X_2^{10\%\ ethanol} = \log X_2^{ideal} + 6.370(\text{HBN}) + 0.019(\text{MV}) - 2.031 \quad (4.77)$$

$$\text{AAE} = 0.33$$

$$\log X_2^{15\%\ ethanol} = \log X_2^{ideal} + 31.443(\text{HBN}) + 0.019(\text{MV}) - 1.961 \quad (4.78)$$

$$\text{AAE} = 0.36$$

$$\log X_2^{20\%\ ethanol} = \log X_2^{ideal} + 51.123(\text{HBN}) + 0.018(\text{MV}) \text{ -1.832} \quad (4.79)$$

$$\text{AAE} = 0.35$$

Equation #	% Ethanol	Parameter #1	Parameter #2	Intercept	AAE*
1 Parameter					
4.55	0	(0.274)logP		1.080	0.73
4.56	5	(0.335)logP		0.172	0.60
4.57	10	(0.335)logP		-0.029	0.55
4.58	15	(0.335)logP		-0.126	0.56
4.59	20	(0.327)logP		-0.175	0.54
1 Parameter					
4.60	0	(0.016)MV		-0.673	0.65
4.61	5	(0.020)MV		-1.960	0.36
4.62	10	(0.019)MV		-2.060	0.33
4.63	15	(0.019)MV		-2.106	0.36
4.64	20	(0.018)MV		-2.067	0.35
2 Parameter					
4.65	0	(-0.092)logP	(0.020)MV	-1.000	0.64
4.66	5	(-0.109)logP	(0.025)MV	-2.348	0.34
4.67	10	(-0.061)logP	(0.022)MV	-2.277	0.32
4.68	15	(-0.038)logP	(0.021)MV	-2.239	0.35
4.69	20	(-0.016)logP	(0.019)MV	-2.124	0.34
2 Parameter					
4.70	0	(206.72)HBN	(0.018)MV	-1.624	0.32
4.71	5	(32.949)HBN	(0.020)MV	-2.111	0.35
4.72	10	(-6.370)HBN	(0.019)MV	-2.031	0.33
4.73	15	(-31.443)HBN	(0.019)MV	-1.961	0.36
4.74	20	(-51.123)HBN	(0.018)MV	-1.832	0.35

*Average Absolute Error
#Molar Volume (MV)
**Hydrogen Donating (HD)
Hydrogen Bond Number (HBN)

Table 4.6. Physical property combinations correlated to the log activity coefficient, γ_2, in HFA-227/ethanol according to multiple linear regression (MLR), where all parameters were found to be significant.

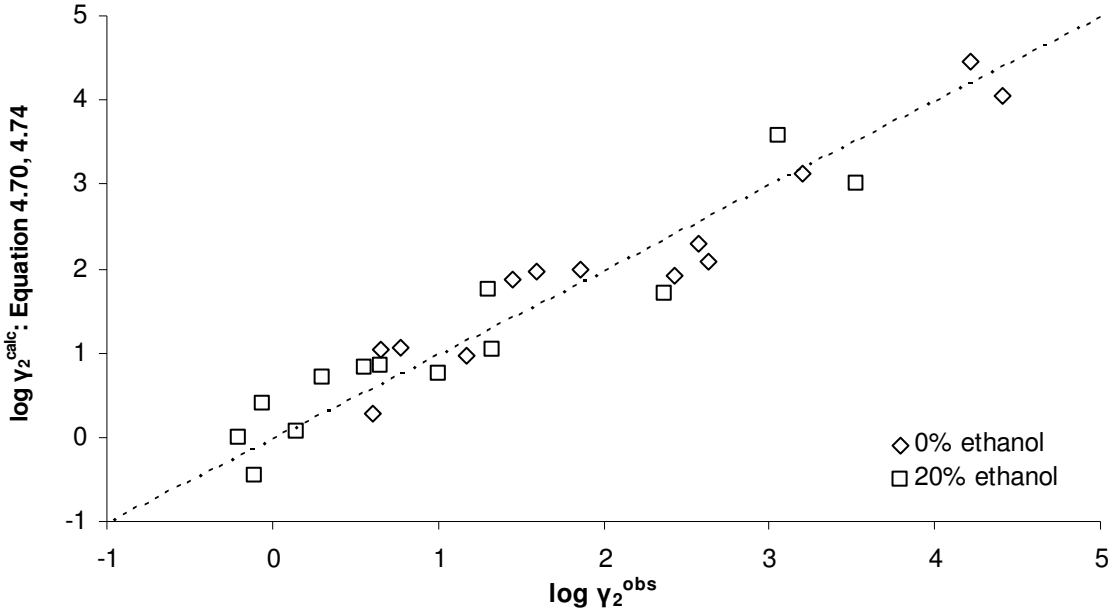

Figure 4.29. Calculated log activity coefficient, log γ_2^{calc}, (Equations 4.70, 4.74) plotted against the experimental log activity coefficient, log γ_2^{obs}, in HFA-227 with 0 and 20% ethanol. The broken line illustrates the line of unity.

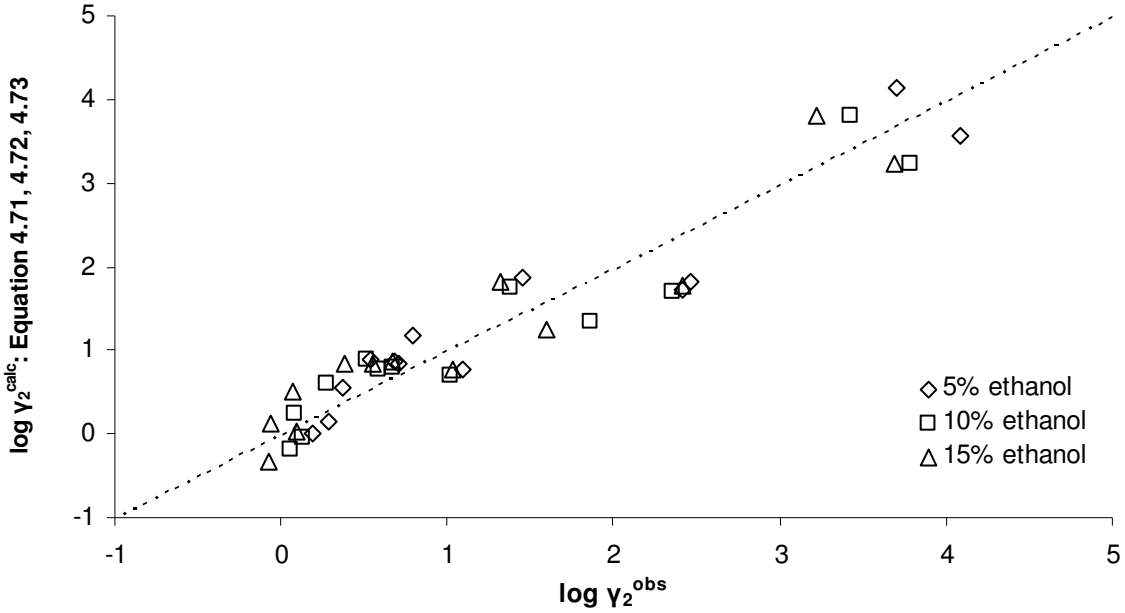

Figure 4.30. Calculated log activity coefficient, log γ_2^{calc}, (Equations 4.71, 4.72, 4.73) plotted against the experimental log activity coefficient, log γ_2^{obs}, in HFA-227 with 5, 10 and 15% ethanol. The broken line illustrates the line of unity.

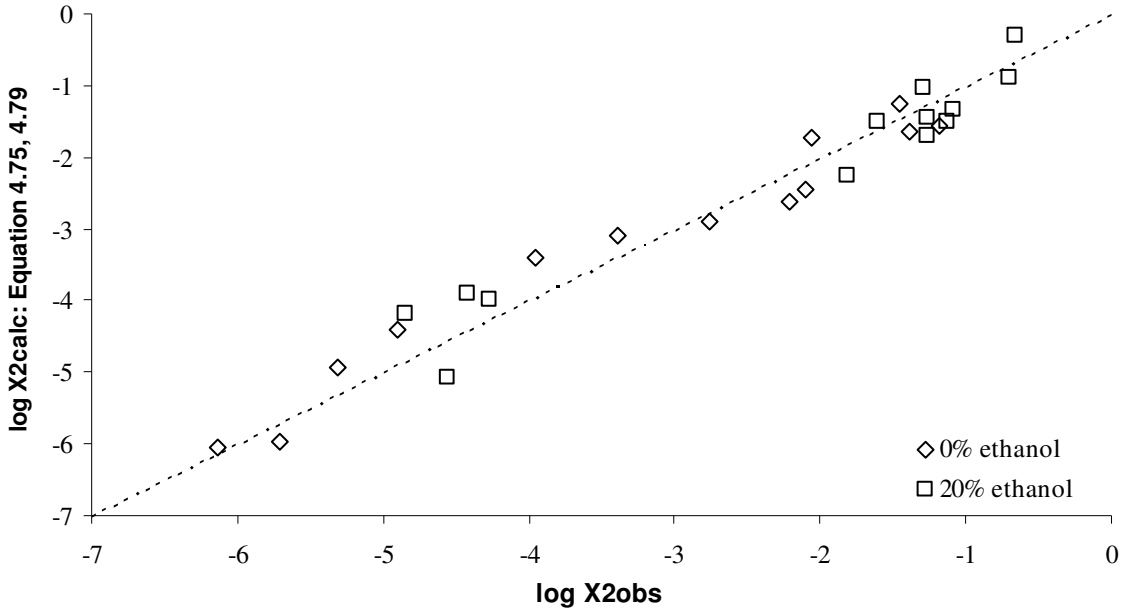

Figure 4.31. Calculated solubility, log X_2^{calc}, (Equations 4.75, 4.79) plotted against the experimental log mole fraction solubility, log X_2^{obs}, in HFA-227 with 0 and 20% ethanol. The broken line illustrates the line of unity.

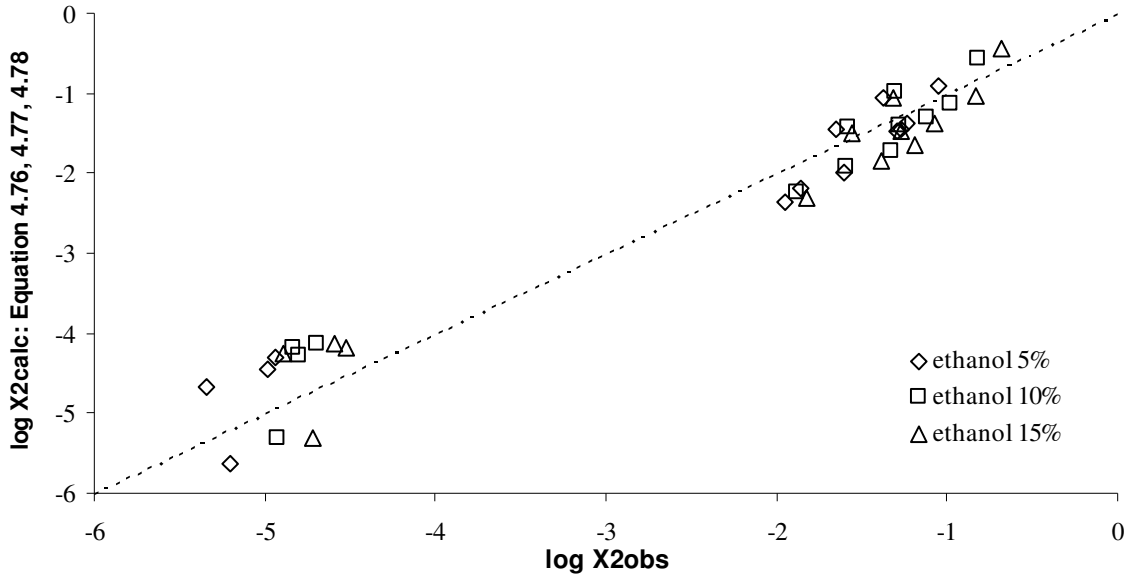

Figure 4.32. Calculated solubility, log X_2^{calc}, (Equations 4.76, 4.77, 4.78) plotted against the experimental log mole fraction solubility, log X_2^{obs}, in HFA-227 with 5, 10 and 15% ethanol. The broken line illustrates the line of unity.

# Parameters	Variables	AAE				
		0% ethanol	*5% ethanol*	*10% ethanol*	*15% ethanol*	*20% ethanol*
1	$\log X_2^{ideal}$	2.12	1.44	1.24	1.17	1.12
2	$\log X_2^{ideal} - \log \gamma_2^{RST}$	3.06	3.27	3.09	2.89	2.66
2	-0.02(MP – 25) – X	1.02	1.23	1.21	1.21	1.18
3	-0.01(MP – 25) – X(MV) + X	0.79	0.77	0.61	0.56	0.51
4	-X(MP – 25) – X(OH) – X(logP) + X	0.52	0.48	0.53	0.57	0.59
4	$\log X_2^{ideal}$ – X(HBN) + X(MV) – X	0.32	0.35	0.33	0.36	0.35

Table 4.7. Summary of the key equations evaluated and the associated average absolute errors (AAE).

XI. Factor Increase in HFA-227 with Ethanol

The solubility enhancement, as a result of the introduced polar cosolvent, can be illustrated in terms of factor increase, which is customarily defined as the ratio of the solubility obtained with a cosolvent to that without, i.e.,

$$\text{Factor Increase} = \frac{X_2^{ternary}}{X_2^{binary}} \tag{4.80}$$

Here, X_2^{binary} and $X_2^{ternary}$ refer to the mole fraction solubility of the solute in pure HFA-227 and HFA-227 with 20% w/w ethanol, respectively. The factor increase for HFA-HFA-227 can be seen in Table 4.8, where the values range from 1.15 to 492.15. All the compounds investigated were seen to increase in solubility when ethanol was added. This increase in solubility was seen for solutes with logP values both higher and lower than HFA-227. These results suggest that a factor increase in solubility due to ethanol in HFA-227 is not based on a solutes polarity, as seen in aqueous systems.

HFA-227 has a logP of 2.0, and ethanol has a logP of -0.187, therefore, added ethanol increases the polarity of the HFA-227a solvent. Although a slight correlation has been shown to exist between polarity and factor increase in HFA-134a, no such relationship exists in HFA-227, as seen by the logP values in Table 4.8.

However, those compounds with both hydrogen accepting and donating groups appeared to have a higher factor increase value in HFA-227 compared to those with little or no hydrogen bonding groups.

Hydrogen bonding between the solutes with capable functional groups may have taken place, thus resulting in an appreciable solubility enhancement. The solutes with no hydrogen bonding functional groups were found to have the lowest factor increase values.

Compound	Factor Increase	logP
1-Naphthoic acid[1]	492.15	3.13
1-Naphthylacetic acid[1]	185.43	2.74
2-Naphthol[1]	116.30	2.71
Albuterol[2]	74.15	0.11
Benzoic acid[1]	36.26	1.88
Dehydrocholesterol[1]	7.63	4.04
Cholesterol[1]	2.89	9.85
Caffeine[1]	2.89	-0.13
Phenanthrene[1]	1.94	4.49
1-Nitronaphthalene[1]	1.46	3.18
2-Methoxynaphthalene[1]	1.32	3.36
Naphthalene[1]	1.26	3.32
Anthracene[1]	1.15	4.49
[1]Sigma-Aldrich (St. Louis, MO) [2]Byron Chemical Co. (Long Island, NY)		

Table 4.8. Factor increase of 13 crystalline compounds in HFA-227 from 0 to 20% w/w ethanol and corresponding logP values.

XII. Linear Relationship

A solubility curve for each solute investigated in this study was found to be fairly linear from 0 – 20% ethanol with positive slopes. A log-linear model was applied to the solubility values in HFA-227, as described by Millard *et al.,*[23] which describes an exponential increase in a non-polar drugs solubility with a linear increase in cosolvent concentration according to Equation 4.81:

$$\log S_{mix} = \log S_w + \sigma f_c \qquad (4.81)$$

Where S_{mix} and S_w are the total solute solubilities in the cosolvent-water mixture and in water, respectively, σ is the cosolvent solubilization power for the particular cosolvent-solute system, and f_c is the volume fraction of the cosolvent in the aqueous mixture. Values of S are either molarity or grams per liter. The log-linear model assumes that the solvent mixture is ideal and that no degradation or solvation occurs. The log-linear model was applied to the solubilities in HFA-227. However, the log-linear model did not show the same relationship as that seen in aqueous systems. Therefore, a linear approach was evaluated to fit the solubility data in HFA-227. The linear approach was found to be more applicable, where the average R^2 value of the linear plot for all 13 solutes is 0.84 (RSD: 37%) compared to an R^2 of -5.15 (RSD: 144%) for a log-linear model (Table 4.9). The normalized % w/w solubility values ($C^{tot}/C^{HFA\text{-}227}$) for all 13 compounds were plotted as a function of fraction ethanol. Figures 4.33 and 4.44 are grouped by high and low slope

values. The normalized % w/w solubility reflects the extent of solubilization in HFA-227, where C^{tot} is the % w/w solubility with ethanol, and $C^{HFA\text{-}227}$ is the %w/w solubility in pure HFA-227 with no ethanol. The solutes in Figures 4.33 and 4.34 cannot be grouped by polarity, as done so by Millard *et al.,*[23] where the slope of the line was found to correlate to a solute's logP. However, the linear approach to solubility in HFA-227 with cosolvent may be a useful predictive tool.

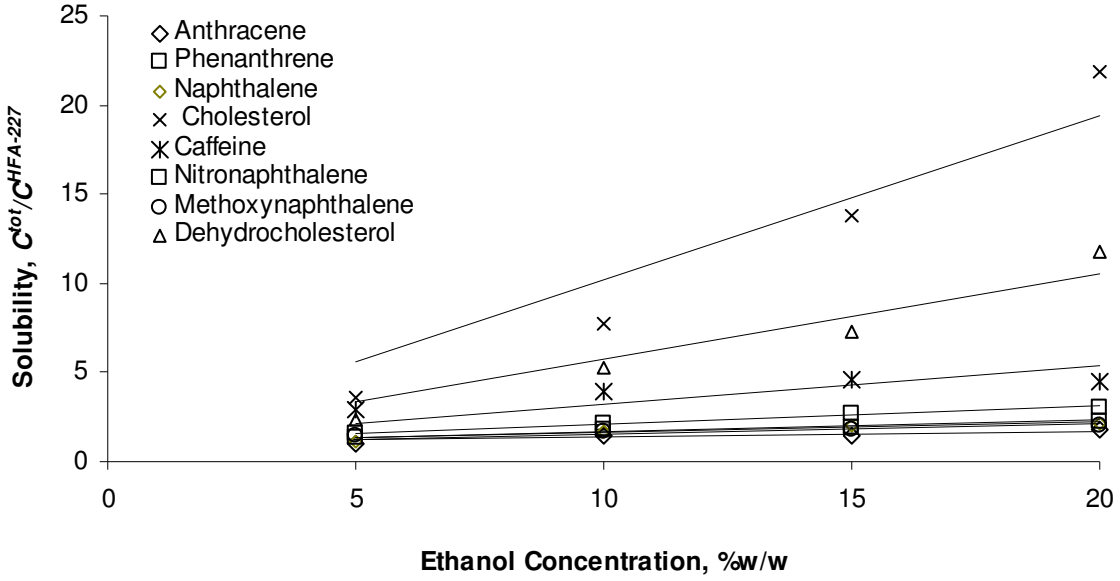

Figure 4.33. Normalized solubility ($C^{tot}/C^{HFA-227}$) in HFA-227 plotted against the fraction ethanol for low slope values.

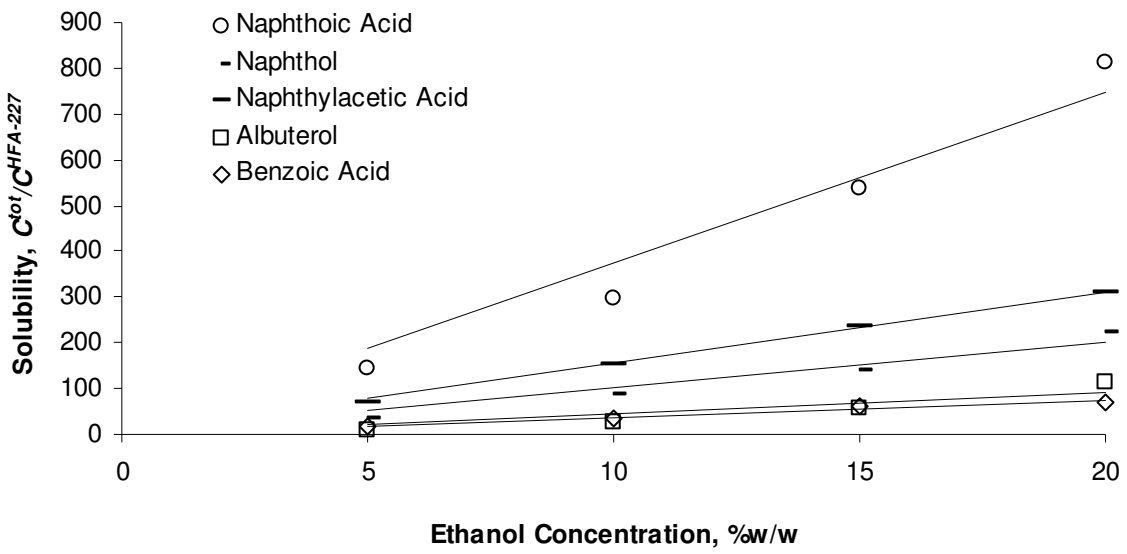

Figure 4.34. Normalized solubility ($C^{tot} / C^{HFA-227}$) in HFA-227 plotted against the fraction ethanol for high slope values.

Compound	R^2	
	log-linear model	***linear model****
Anthracene	0.31	0.84
Phenanthrene	0.30	0.98
Naphthalene	0.58	0.92
Cholesterol	0.70	0.91
Caffeine	-22.90	-0.17
Naphthoic acid	-11.20	0.95
Nitronaphthalene	-0.11	0.94
Naphthol	-5.69	0.94
Naphthylacetic acid	-13.20	1.00
Methoxynaphthalene	-9.93	0.88
Albuterol	0.68	0.80
Dehydrocholesterol	0.81	0.92
Benzoic Acid	-7.40	0.99
*best describes increase in solubility in HFA-227 due to ethanol		

Table 4.9. R^2 of line using the log-linear model and the linear model for 13 solutes in HFA-227 with 0 – 20% ethanol, where the linear model best describes the increase in solubility due to ethanol.

XIII. 2H-3H, Decafluoropentane (DFP) Correlation

Detailed investigations on solute behavior in HFA and HFA/cosolvent systems are limited due to the lack of a low volatility model propellant that is liquid at room temperature and atmospheric pressure. Therefore 2H,3H-decafluoropentane (DFP) was investigated as a potential liquid model for hydrofluoroalkane propellants.

The log mole fraction solubilities of 13 crystalline compounds in HFA-134a (log $X_2^{HFA\text{-}134a}$) and HFA-227 (log $X_2^{HFA\text{-}227}$) with 0, 5, 10, 15 and 20% w/w ethanol were compared to those in DFP (log X_2^{DFP}) with 0, 5, 10, 15 and 20% w/w ethanol. In order to assess the suitability of DFP as a liquid model propellant, solubility data in HFA-134a/ethanol and were plotted against those in DFP/ethanol as seen in Figures 4.35 and 4.36.

The solubility in HFA-134a ranged from -1.24 to -5.34 log mole fraction solubility, log $X_2^{HFA\text{-}134a}$. Compounds such as phenanthrene, naphthalene and naphthylacetic acid in HFA-134a/ethanol had the largest deviation from the solubility in DFP/ethanol. However, anthracene, nitronaphthalene and cholesterol had the most similar solubilities in HFA-134a/ethanol to that in DFP/ethanol. Table 4.10 describes the correlation between solubility in HFA-134a and DFP according to the R^2 of the line, slope and AAE values.

The solubility in HFA-227 ranged from -0.65 to -6.14. Compounds such as albuterol, methoxynaphthalene and naphthyl acetate had the greatest deviation in HFA-227 from the solubility in DFP. On the other hand, cholesterol, dehydrocholesterol and anthracene has similar solubilities in both HFA-227 and DFP.

The correlation between log mole fraction solubility in DFP/ethanol, log X_2^{DFP}, and the log mole fraction solubility in HFA-227/ethanol, log $X_2^{HFA\text{-}227}$ are shown Figures 4.37 and 4.38. Table 4.10 describes the correlation between HFA-227/ethanol and DFP/ethanol according to R^2, slope and AAE. The AAE for the relationship between HFA-227 and DFP solubility was slightly higher in HFA-227 compared to that in HFA-134a. Although the structure of HFA-227 may be more similar to that of DFP, a direct comparison of solubilities revealed that DFP is a better liquid model for HFA-134a compared to HFA-227.

% Ethanol	R^2	Slope	AAE
HFA-134a			
0	0.12	1.02	0.70
5	0.23	0.99	0.68
10	0.37	0.94	0.66
15	0.46	0.95	0.69
20	0.27	0.99	0.71
HFA-227			
0	-0.50	0.99	1.00
5	-1.99	0.99	1.08
10	-1.12	0.96	1.07
15	-1.23	0.97	1.14
20	-1.83	0.99	1.13

Table 4.10. R^2, slope and AAE of relationship between solubility in HFA-134/ethanol and HFA-227/ethanol with the solubility in DFP/ethanol.

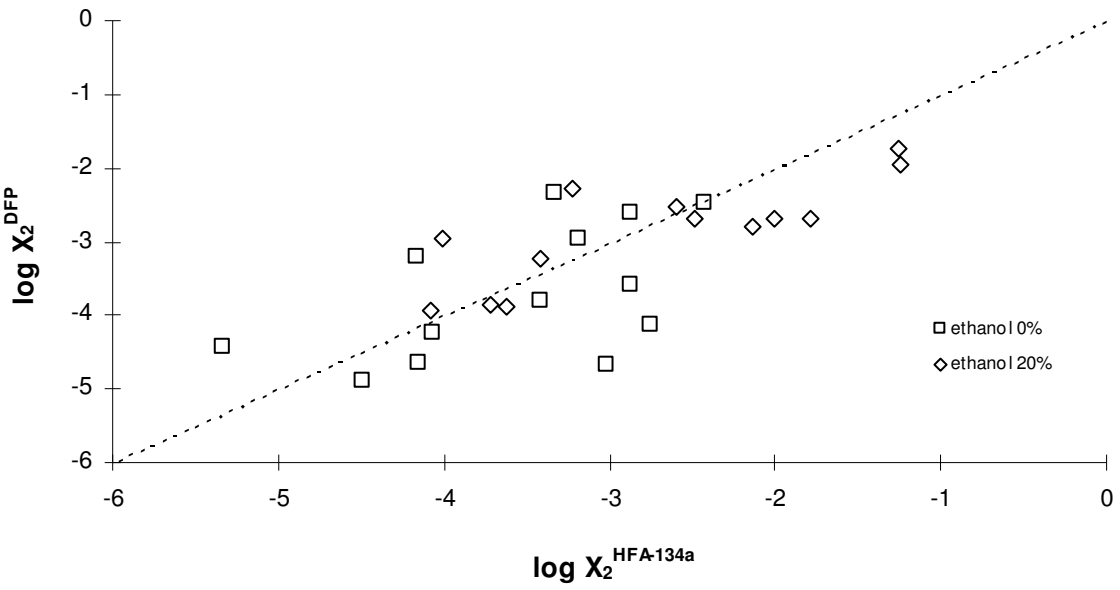

Figure 4.35. Log mole fraction solubility, log $X_2^{HFA\text{-}134a}$ plotted against the log mole fraction solubility in DFP, log X_2^{DFP} with 0 and 20% ethanol. The broken line illustrates the line of unity.

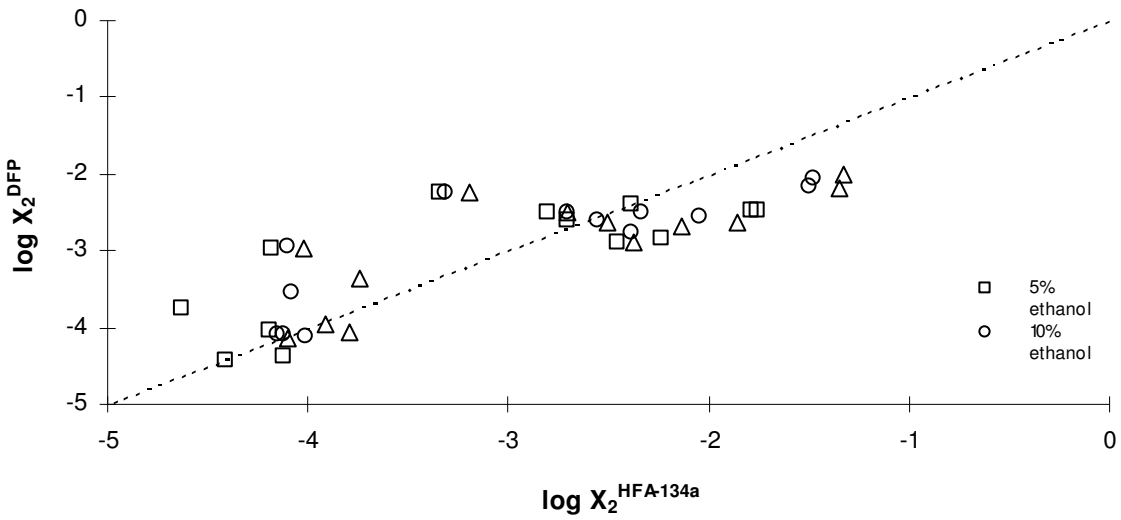

Figure 4.36. Log mole fraction solubility, log $X_2^{HFA\text{-}134a}$ plotted against the log mole fraction solubility in DFP, log X_2^{DFP} with 5, 10 and 15% w/w ethanol. The broken line illustrates the line of unity.

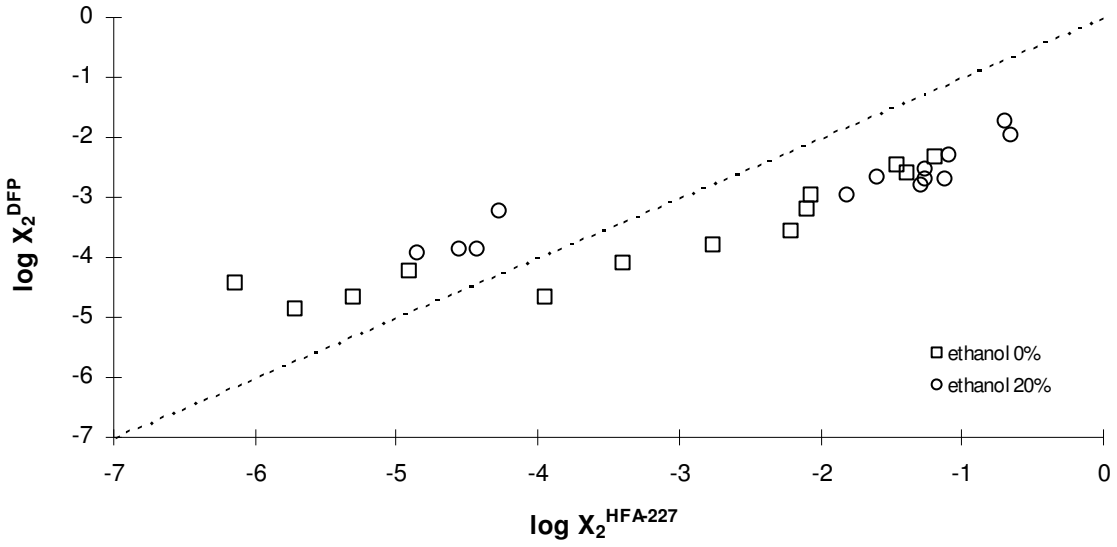

Figure 4.37. Log mole fraction solubility in HFA-227, log $X_2^{HFA\text{-}227}$ plotted against the log mole fraction solubility in DFP, log X_2^{DFP} with 0 and 20% w/w ethanol. The broken line illustrates the line of unity.

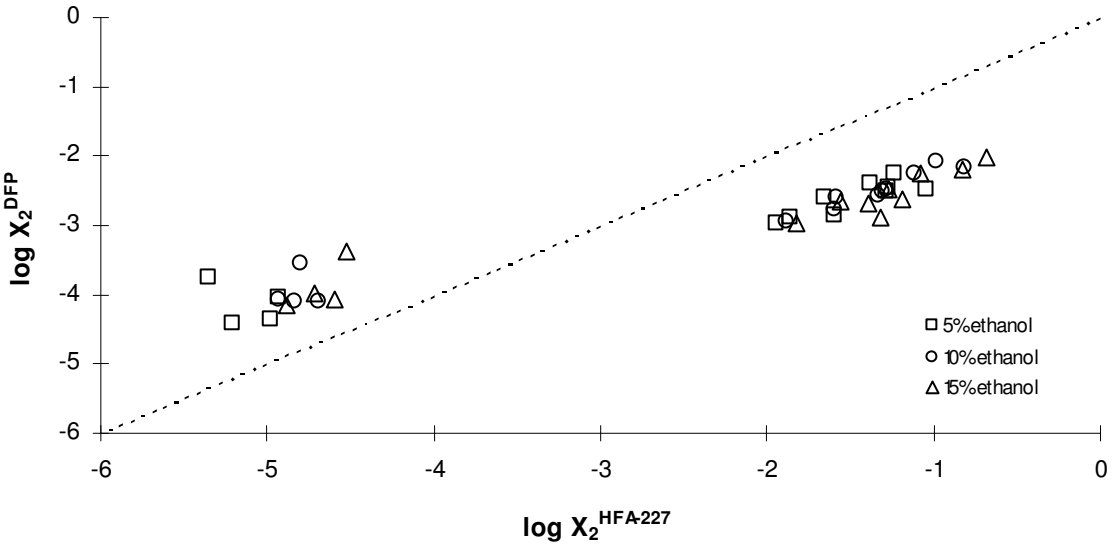

Figure 4.38. Log mole fraction solubility in HFA-227, log $X_2^{HFA\text{-}227}$ plotted against the log mole fraction solubility in DFP, log X_2^{DFP} with 5, 10 and 15% w/w ethanol. The broken line illustrates the line of unity.

XIV. Modeling Studies in DFP compared to HFA-134a and HFA-227

In order to improve the applicability of DFP as a liquid model for hydrofluoroalkane propellants, linear regression was applied. The log mole fraction solubility in DFP/ethanol was regressed against those in HFA-134a/ethanol and HFA-227/ethanol. Equations 4.82 and 4.86 describe the regression relationship between HFA-134 and DFP for 0 and 20% w/w ethanol, where a DFP coefficient and intercept term are used (Figures 4.39). Figure 4.40 illustrates the regression relationship between HFA-134a and DFP with 5, 10, and 15% w/w ethanol, where the error is decreased compared to a direct correlation (Table 4.11).

$$\log X_2^{0\%\ ethanol} = 0.51(\log X_2^{DFP}) - 1.68 \qquad (4.82)$$

$$AAE = 0.53$$

$$\log X_2^{20\%\ ethanol} = 1.16(\log X_2^{DFP}) + 0.58 \qquad (4.86)$$

$$AAE = 0.45$$

A correlation exists between log mole fraction solubility in HFA-134/ethanol and DFP/ethanol as seen by the AAE as described in Table 4.11. The coefficient and intercept terms are both seen to increase with an increase in ethanol, resulting in a lower AAE.

Linear regression was also applied to the log mole fraction solubility data in DFP/ethanol compared to that in HFA-227/ethanol, where Equations 4.87 and 4.91 describe the regression relationship with 0 and 20% ethanol (Figure 4.41). Figure 4.42 describes the regression relationship between HFA-227 and DFP with 5, 10, and 15% ethanol, according to the equations shown in Table 4.12.

$$\log X_2^{0\%\ ethanol} = 1.79(\log X_2^{DFP}) + 3.33 \qquad (4.87)$$

$$AAE = 0.56$$

$$\log X_2^{20\%\ ethanol} = 2.14(\log X_2^{DFP}) + 3.90 \qquad (4.91)$$

$$AAE = 0.49$$

A correlation also exists between log mole fraction solubility in HFA-227/ethanol and DFP/ethanol according to the AAE shown in Table 4.12.

The application of a regression equation improves the correlation between DFP/ethanol and both HFA-134a/ethanol and HFA-227/ethanol. DFP appears to be a good liquid model for both HFA-134a and HFA-227. A slightly better model was seen for HFA-227 compared to HFA-134a when the regression equation was utilized, as seen by the overall lower AAE values presented in Table 4.12. The use of DFP can be useful tool for solubility analysis in hydrofluoroalkane propellants with ethanol.

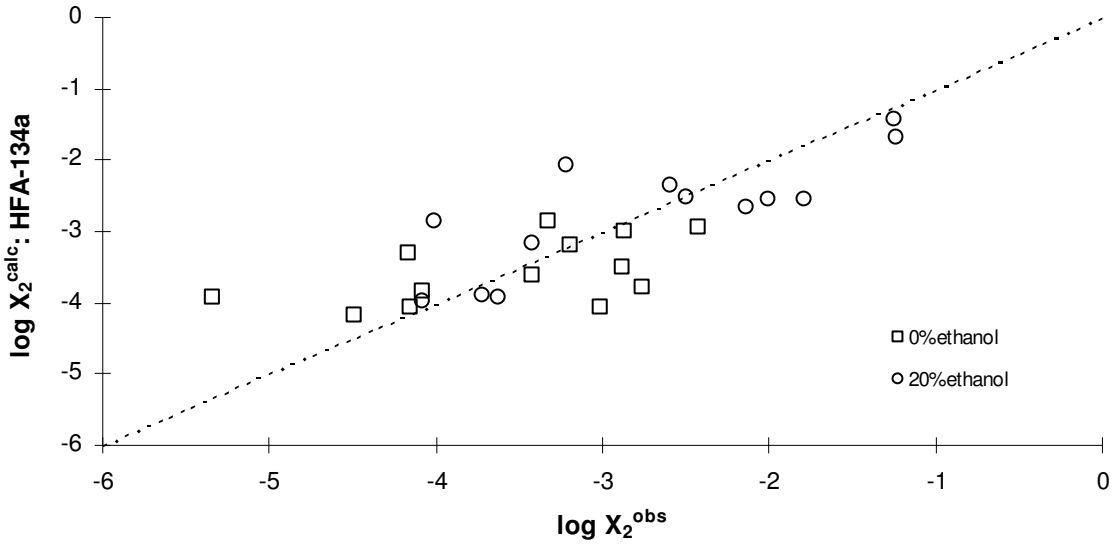

Figure 4.39. MLR model (Equations 4.82) for log mole fraction solubility, log X_2^{HFA}, in HFA-134a with 0 and 20% w/w ethanol. The broken line illustrates the line of unity.

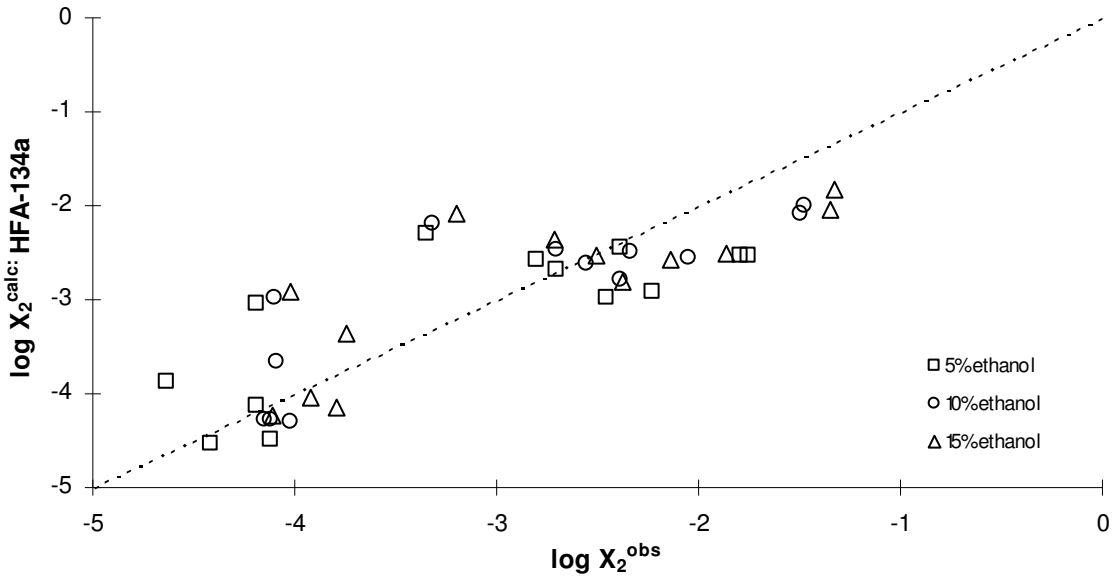

Figure 4.40. MLR model (Equation 4.86) for log mole fraction solubility, log X_2^{HFA}, in HFA-134a with 5, 10, and 15% ethanol. The broken line illustrates the line of unity.

Equation #	Prediction of:	% DFP	Intercept	AAE
4.82	$HFA^{0\%ethanol}$	$(0.51)DFP^{0\%\ ethanol}$	-1.68	0.53
4.83	$HFA^{5\%ethanol}$	$(1.03)DFP^{5\%ethanol}$	+0.01	0.50
4.84	$HFA^{10\%ethanol}$	$(1.13)DFP^{10\%ethanol}$	+0.34	0.44
4.85	$HFA^{15\%ethanol}$	$(1.12)DFP^{15\%ethanol}$	+0.45	0.48
4.86	$HFA^{20\%ethanol}$	$(1.16)DFP^{20\%ethanol}$	+0.58	0.45

Table 4.11. Regression equations for calculation of HFA-134a solubility/cosolvent mixtures using the liquid model DFP.

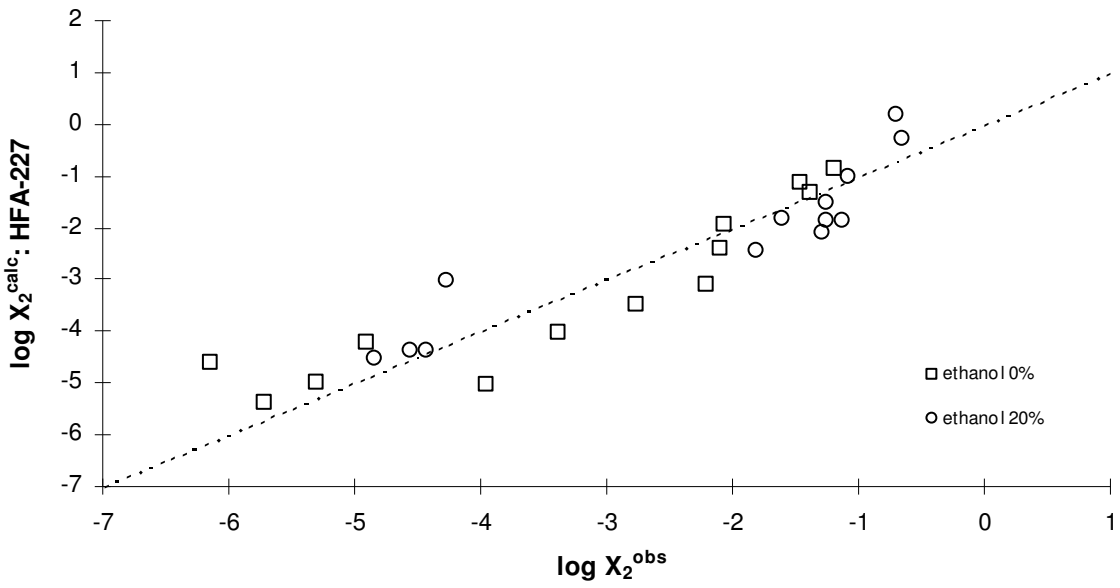

Figure 4.41. MLR model (Equation 4.87) for log mole fraction solubility, log X_2^{HFA}, in HFA-227 with 0 and 20% ethanol. The broken line illustrates the line of unity.

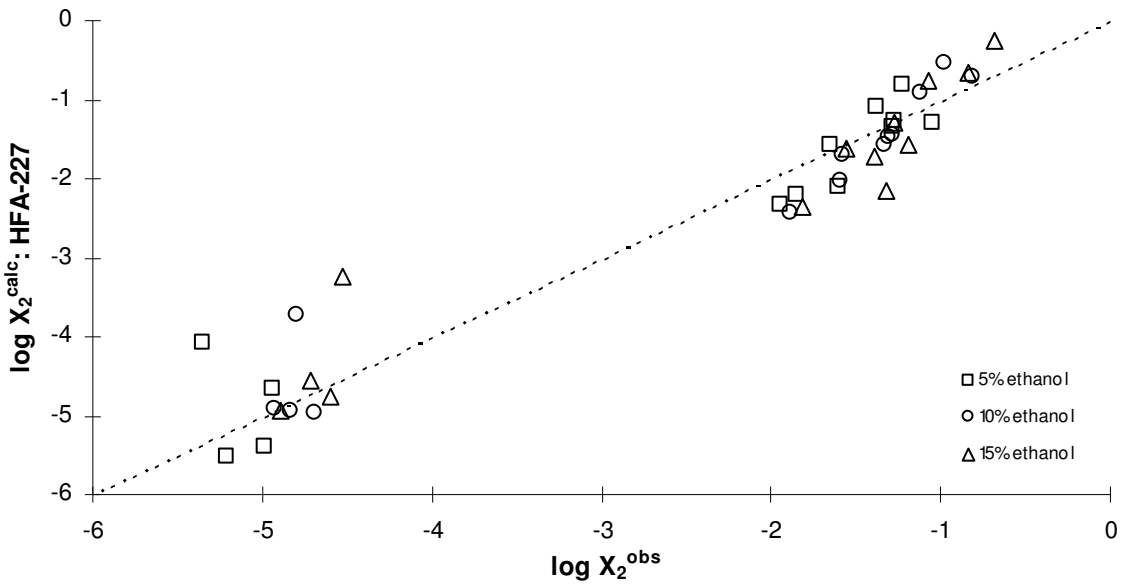

Figure 4.42. MLR model (Equation 4.91) for log mole fraction solubility, log X_2^{HFA}, in HFA-227 with 5, 10 and 15% ethanol. The broken line illustrates the line of unity.

Equation #	Prediction of:	% DFP	Intercept	AAE
4.87	$HFA^{0\%ethanol}$	$(1.79)DFP^{0\%\ ethanol}$	3.33	0.56
4.88	$HFA^{5\%ethanol}$	$(2.17)DFP^{5\%ethanol}$	4.08	0.35
4.89	$HFA^{10\%ethanol}$	$(2.18)DFP^{10\%ethanol}$	3.99	0.30
4.90	$HFA^{15\%ethanol}$	$(2.20)DFP^{15\%ethanol}$	4.18	0.37
4.91	$HFA^{20\%ethanol}$	$(2.14)DFP^{20\%ethanol}$	3.90	0.49

Table 4.12. Regression equations for calculation of HFA-227 solubility/cosolvent mixtures using the liquid model DFP.

XV. Factor Increase in DFP compared to HFA-134a and HFA-227

The solubility enhancement, as a result of the introduced polar cosolvent, can be illustrated in terms of factor increase, which is customarily defined as the ratio of the solubility obtained with a cosolvent to that without. The factor increase for HFA-134a, HFA-227 and DFP can be seen in Table 4.13, where the compounds are in decreasing order of DFP factor increase.

Naphthol, naphthoic acid and naphthylacetic acid had the largest factor increase values in all solvents, possibly due to their increase hydrogen-bonding potential compared to some compounds such as anthracene, naphthalene and phenanthrene.

The HFA-134a factor increase of albuterol, naphthalene and benzoic acid had the most similar trends in DFP. Compounds such as naphthol, dehydrocholesterol and methoxynaphthalene had similar factor increase values in HFA-227 as compared to those in DFP. The difference in factor increase values between HFA-134a and HFA-227 compared to DFP may be due to size or hydrogen bonding potential of the compounds investigated.

Compound	Factor Increase HFA-134a	Factor Increase HFA-227	Factor Increase DFP
Naphthol[1]	69.00	116.30	117.48
Naphthoic Acid[1]	10.55	492.15	92.82
Benzoic Acid[1]	43.74	36.26	42.64
Naphthylacetic Acid[1]	9.27	185.43	26.31
Albuterol[2]	16.82	74.15	15.69
Cholesterol[1]	5.96	2.89	10.14
Dehydrocholesterol[1]	3.42	7.63	6.02
Caffeine[1]	4.99	2.89	1.89
Phenanthrene[1]	1.18	1.94	1.67
Naphthalene[1]	1.28	1.26	1.23
Methoxynaphthalene[1]	1.93	1.32	1.15
Anthracene	1.11	1.15	0.85
Nitronaphthalene[1]	1.34	1.46	0.49

[1]Sigma-Aldrich (St. Louis, MO)
[2]Byron Chemical Co. (Long Island, NY)

Table 4.13. Solubility of 13 crystalline compounds in HFA-134a and DFP; factor increase from 0 to 20% w/w ethanol in HFA-134a and DFP.

XVI. Temperature-Dependent Solubilities for a Series of Chlorobenzene Compounds in HFA-134a

The solubilities of 5 congeners, 1,2,3-trichlorobenzene, 1,3,5-trichlorobenzene, 1,2,4,5-tetrachlorobenzene, pentachlorobenzene, and hexachlorobenzene, were measured experimentally at three temperatures. The log mole fraction solubilities of the compounds at 11, 25, and 48˚C, as well as their ideal solubility at 25˚C, can be found in Table 4.14. The melting point, molecular weight and logP for the compounds are found in Table 4.15. The solubility of all the compounds increased with increasing temperature, however, the miscibility of the series seems to decrease with the addition of each chlorine to the benzene ring. A possible explanation for the reduced solubility is that each chlorine group increases the logP of the compound, moving it farther away from that of the solvent. Another explanation is that as chlorines are added to the series the melting point typically rises, increasing the crystal terms contribution to solubility. The exception to this is pentachlorobenzene, which, despite its high molecular weight, possesses a melting point over 50º C less than 1,2,4,5-tetrachlorobenzene. This discrepancy in melting points can be attributed to the molecules symmetry or, in the case of pentachlorobenzene, lack there of. The rotational symmetry values for 1,2,4,5-tetrachlorobenzene and pentachlorobenzene are 4 and 2, respectively. The melting properties of these compounds, when used to determine ideal solubility, allow a good estimation of the order of solubility. They do not, however, shed light on the magnitude of deviation from these ideal values. In an attempt to describe the activity associated with the mixing of this

series of chlorobenzene compounds with HFA-134a, a thermodynamic analysis was performed.

Compound	log X_2			log X_i
	11ºC	**25ºC**	**48ºC**	**25ºC**
1,2,3-trichlorobenzene	-2.09	-1.78	-1.58	-0.25
1,3,5-trichlorobenzene	-2.40	-2.08	-1.78	-0.33
1,2,4,5-tetrachlorobenzene	-3.50	-3.23	-2.76	-1.01
Pentachlorobenzene	-3.38	-3.03	-2.76	-0.61
Hexachlorobenzene	-4.68	-4.40	-3.91	-1.25

Table 4.14. Solubility values in log mole fraction for the compounds at three temperatures as well as the ideal solubility at 25˚C.

Compound	MP (˚C)	MW	logP
1,2,3-trichlorobenzene	53	181	3.77
1,3,5-trichlorobenzene	65	181	4.04
1,2,4,5-tetrachlorobenzene	139	215	4.23
Pentachlorobenzene	86	250	4.60
Hexachlorobenzene	230	284	4.89

Table 4.15. The melting point, molecular weight, and logP values for the series of chlorobenzene compounds.

XVII. Thermodynamic Analysis of a Series of Chlorobenzene Compounds in HFA-227

The first thermodynamic property calculated and examined was the enthalpy of solution (ΔH_s). When the log natural mole fraction solubilities for the series of chlorobenzene compounds were graphed over the inverse of temperature, a linear relationship was observed (Figure 4.43) The slope of the regressed line allowed for determination of the enthalpy of solution for that compound. The assumption that the enthalpy of solution is constant over the range of 11 to 38˚ C for the compounds selected appears to be valid based on R^2 values ranging from 0.95 to 1.00. The ΔH_s ranged from 23.1 to 36.5 kJ/mol and can be seen in Table 4.16. The enthalpy values increased with the addition of each chlorine, the opposite of solubility, which decreased with each addition. The lone exception to this was pentachlorobenzene, whose value was nearly equal to 1,2,3-trichlorobenzene. Since greater enthalpy values oppose solubility, a good correlation with the order of observed solubility and melting point was seen. The free energy of solution (ΔG_s) was calculated by Equation 2.12 and can be seen in Table 4.16. In the interest of brevity only the 25º C data will be presented for all the thermodynamic values throughout this work. The mole fraction solubility of each compound was the only variable when calculating ΔG_S, as a result of this, the values correspond with the solubility. The less soluble the compound the higher the ΔG_s values it possesses. The positive values for ΔG_s mean the process is endothermic and requires energy. The entropic contribution to the dissolution process, ΔS_s, was calculated by substituting the

previously determined ΔG_s and ΔH_s values in Equation 2.10. As expected, the $-T\Delta S_s$ component appears to aid in the solubilization, with values ranging from -11.07 to -16.72 kJ/mol. The negative values observed represent an increase in the disorder of the system that is energetically favorable. In order to further elucidate the factors aiding and hindering the solubility of this series of chlorobenzenes in HFA-134a the three thermodynamic properties were broken into their melting and mixing components.

The thermodynamics of melting, the breaking down of the crystal structure and forming a supercooled liquid, was analyzed for each compound. The DSC was used to identify the enthalpy (ΔH_{melt}) and entropy of melting (ΔS_{melt}). The enthalpies of melting ranged from 16.8 to 20.78 kJ/mol (Table 4.17) These values increased with the addition of chlorines to the benzene ring with the exception of hexachlorobenzene. The ΔS_{melt} values, also seen in Table 4.17, are between 50.18 and 58.05 J/molK for the trichlorobenzenes through pentachlorobenzene. These values are in good agreement with Walden's rule which assumes the entropy of melting for rigid organic nonelectrolytes to be 56.5 J/mol. Hexachlorobenzene, however, has an entropy of melting that is just 34.83 J/mol. This means that less disorder is gained when the solid is transformed to a supercooled liquid compared to the other compounds. A possible reason for this would the rigidity of the molecule as well as the rotational symmetry it possesses. The change in Gibbs free energy for the melting of the compounds (ΔG_{melt}) was determined by Equation 2.16. The ΔG_{melt} values ranged from 1.41 to 7.12 kJ/mol and can be seen in Table 4.17. The values

possessed a correlation to the solubility of the compounds with higher ΔG_{melt} values resulting in lower solubility.

The thermodynamics of mixing the supercooled liquid solutes with the solvent were determined for the series of chlorobenzene compounds. The ΔG_{mix} values ranged from 8.79 to 18.08 kJ/mol and were found to increased with the addition of chlorine groups. This increase is also in agreement with the increasing logP values for the series. The ΔH_{mix} of the chlorobenzenes range from 6.28 to 19.06 kJ/mol and are less than the ΔH_{melt} for each respective compound with the exception of hexachlorobenzene. It should also be noted that 1,2,3-trichlorobenzene and pentachlorobenzene have ΔH_{mix} values substantially less than the others. Lower ΔH_{mix} values imply that the compound behaves more similarly to the solvent, with regards to interactions, than those with higher values. The ΔS_{mix} for the compounds were determined to fall between -20.91 and 5.91 J/mol. Two of the compounds, 1,2,3-trichlorobenzene and pentachlorobenzene, possessed negative ΔS_{mix} values when mixed with HFA-134a, meaning there is a reduction in the randomness of the molecules when mixed and some level of structuring is taking place.

In an attempt to facilitate comparisons, a table summarizing all the thermodynamic parameters is displayed below (Table 4.19) The change in free energy ultimately determines solubility and is thus a logical starting point for analysis. Looking at the melting and mixing components of ΔG_s it is easy to see that the main contributor, or barrier to solubility, is the mixing process. While the average change in the enthalpy of melting is much larger than that of the $\Delta H_{mix,}$ it is offset by the large gain in entropy

experienced when going from a solid to a super-cooled liquid. Conversely, despite comparatively small changes in enthalpy with mixing, the entropic contribution for this process is much less favorable, with two of the compounds possessing negative entropy values. These unfavorable mixing parameters suggest some level of structuring is taking place when the solute is placed in HFA-134a. While solute-solvent or solvent-solvent interactions could account for the low ΔS_{mix} values observed , the data does not allow for this determination. The low and in some cases unfavorable ΔS_{mix} values play a large role in limiting solubility of this series of chlorobenzenes. While solubility is not typically thought to be limited by the entropy of mixing, the idea is not unheard of. Friesen and Webster[24] determined that for the aqueous solubility of a series of highly chlorinated dibenzo-p-dioxins the entropy changes may be more important than enthalpy.

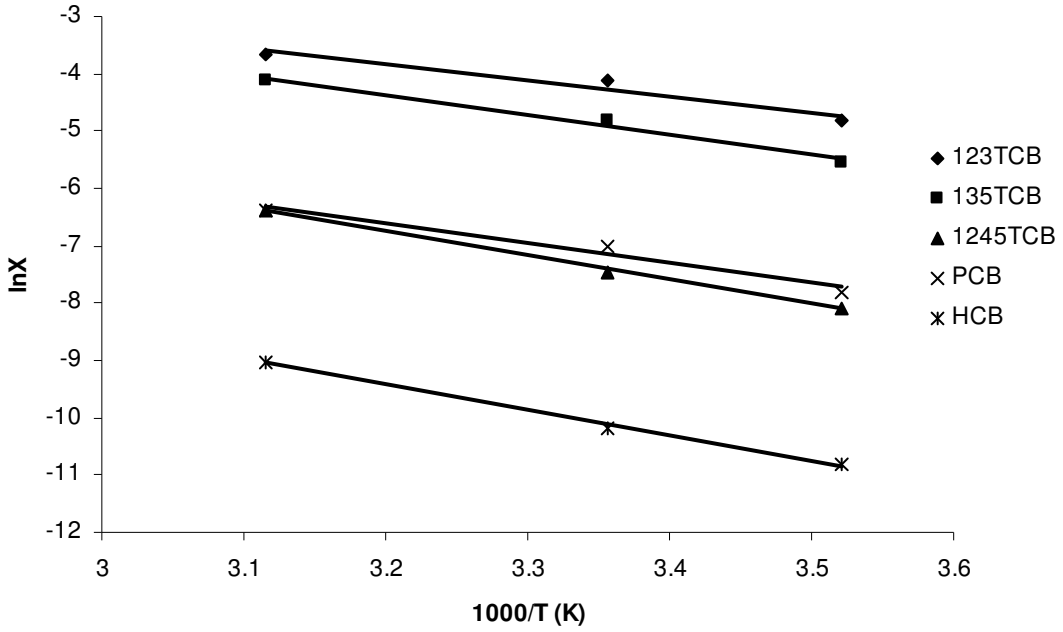

Figure 4.43. Mole fraction solubility plotted against the inverse of temperature.

Compound	ΔG_s	ΔH_s	$T\Delta S_s$	ΔS_s (J/molK)
1,2,3-Trichlorobenzene	10.20	23.14	12.94	43.42
1,3,5-Trichlorobenzene	11.91	28.74	16.83	56.46
1,2,4,5-Tetrachlorobenzene	18.48	35.21	16.72	56.09
Pentachlorobenzene	17.35	28.43	11.07	37.14
Hexachlorobenzene	25.21	36.56	11.36	38.09

Table 4.16. Free energy, enthalpy, and entropy changes of solution for the series of chlorobenzene compounds at 25˚C (All values are in kJ/mol unless noted otherwise).

Compound	ΔG_{melt}	ΔH_{melt}	$T\Delta S_{melt}$	ΔS_{melt} (J/molK)
1,2,3-Trichlorobenzene	1.41	16.86	15.45	51.83
1,3,5-Trichlorobenzene	1.89	17.06	15.18	50.90
1,2,4,5-Tetrachlorobenzene	5.78	20.74	14.96	50.18
Pentachlorobenzene	3.47	20.78	17.31	58.05
Hexachlorobenzene	7.12	17.51	10.38	34.83

Table 4.17. Free energy, enthalpy, and entropy changes of melting for the series of chlorobenzene compounds at 25˚C (All values are in kJ/mol unless noted otherwise).

Compound	ΔG_{mix}	ΔH_{mix}	$-T\Delta S_{mix}$	ΔS_{mix} (J/molK)
1,2,3-Trichlorobenzene	8.79	6.28	2.51	-8.41
1,3,5-Trichlorobenzene	10.02	11.68	-1.66	5.56
1,2,4,5-Tetrachlorobenzene	12.71	14.47	-1.76	5.91
Pentachlorobenzene	13.88	7.65	6.23	-20.91
Hexachlorobenzene	18.08	19.06	-0.97	3.26

Table 4.18. Free energy, enthalpy, and entropy changes of mixing for the series of chlorobenzene compounds in HFA-134a at 25˚C (All values are in kJ/mol unless noted otherwise).

Compound	ΔG_s	ΔG_{melt}	ΔG_{mix}	ΔH_s	ΔH_{melt}	ΔH_{mix}	$-T\Delta S_s$	$-T\Delta S_{melt}$	$-T\Delta S_{mix}$
1,2,3-Trichlorobenzene	10.20	1.41	8.79	23.14	16.86	6.28	-12.94	-15.45	2.51
1,3,5-Trichlorobenzene	11.91	1.89	10.02	28.74	17.06	11.68	-16.83	-15.18	-1.66
1,2,4,5-Tetrachlorobenzene	18.48	5.78	12.71	35.21	20.74	14.47	-16.72	-14.96	-1.76
Pentachlorobenzene	17.35	3.47	13.88	28.43	20.78	7.65	-11.07	-17.31	6.23
Hexachlorobenzene	25.21	7.12	18.08	36.56	17.51	19.06	-11.36	-10.38	-0.97

Table 4.19. Free energy, enthalpy, and entropy changes for the series of chlorobenzene compounds in HFA-134a at 25˚C (All values are in kJ/mol).

XVIII. A Comparison of the Thermodynamics of Trichlorobenzene Solubility in HFA-134a and Water

In order to better understand the interactions occurring between the two trichlorobenzene compounds and HFA-134a it is essential to have a point of reference. Comparing the thermodynamics of solubility for the selected compounds in the propellant with those of a solvent with known interactions would be of great utility. Water was selected as the comparator of choice due to is well known ability to interact with itself as well as other compounds through hydrogen bonding, resulting in a highly structured liquid phase. Much less is known about the behavior of the HFA-134a system due to its volatility, which makes many tests extremely difficult or impossible. It has been proposed that HFA-134a has the ability to hydrogen bond, due to its highly electronegative fluorines and lone hydrogen, and can interact with itself through this mechanism. If this were true, similar thermodynamic values or trends may be expected for the trichlorobenzenes when compared to the aqueous system.

The solubility of 1,2,3-trichlorobenzene and 1,3,5-trichlorobenzene were determined at three temperatures in water and HFA-134a. The solubility values in water can be seen in Table 4.20. Both compounds displayed greater solubility as the temperature was increased. As with HFA-134a, 1,2,3-trichlorobenzene has a greater aqueous solubility than 1,3,5-trichlorobenzene at all temperatures considered. When the solubilities were graphed over the inverse of temperature a linear relationship was observed. The van't

Hoff plots for 1,2,3-trichlorobenzene and 1,3,5-trichlorobenzene displaying solubilities in water, HFA-134a as well as the ideal solubility can be seen in Figure 4.44 and Figure 4.45 respectively. The lines of the van't Hoff plots for each compound exhibit similar slopes for water, HFA-134a and ideal solubility. This suggests that compounds deviate from ideality by a constant over the temperature range examined. Since deviation from ideality is attributed to the activity coefficient, the fact that the aqueous solubilities are lower than those in HFA-134a imply that the activity coeffient is more pronounced in the aqueous system for these compounds. This is logical when comparing the polarity of water with those of HFA-134 and the trichlorobenzenes.

The thermodynamic parameters for the aqueous solubility of the trichlorobenzenes were determined and compared to their HFA-134a counterparts. The parameters for the overall solution process, in both water and HFA-134a, can be seen in Table 4.21. The change in free energy is greater in the aqueous solution, as expected with lower solubility values. The heat or enthalpy change is fairly similar between the two systems with the most significant difference being a 12% decrease, 3.5 kJ/mol, for 1,3,5-trichlorobenzene in the aqueous system opposed to that in HFA-134a. The change in entropy for the solutes in the aqueous solutions was about half of the change present in HFA-134a. This considerably less favorable entropy of solution in the aqueous system is responsible for the decreased solubility and can most likely be attributed to the highly organized structure of water. The main difference seen between the two systems is the less

energetically favorable change in entropy in water, resulting in elevated ΔG_s compared to those of HFA-134a.

When comparing the contributions made by the melting and mixing parameters to the overall thermodynamic properties of the solution for water and HFA-134a, the melting parameters can be disregarded. While they still play an important role in the energetics of the overall process, the melting parameters are derived from solute alone and are therefore solvent independent. Because of this, these parameters are constant for each compound considered and can be seen in Table 4.15 previously accompanied with a discussion. The mixing process is responsible for the differences observed in the solution parameters, and ultimately solubility, for HFA-134a and water. Table 4.22 displays the mixing parameters for the trichlorobenzenes in the solvents. The change in free energy of mixing is significantly higher for the compounds in water, reflecting the lower solubility in this system. The enthalpy of mixing for 1,2,3-trichlorobenzene is comparable in both mediums but, 1,3,5-trichlorobenzene displays a 43% greater change in enthalpy in HFA-134a than it does in water, implying that the differences in the interactions of the solute and solvent are less pronounced in the aqueous system. While entropy is always thought to aid solubility, in this case it appears to be inhibiting it, with three of the compounds possessing negative ΔS_{mix} values. The only solute that possessed a positive change in entropy of mixing was 1,3,5-trichlorobenzene in HFA-134a a value of 5.56 J/molK. When considering the two systems, the mixing of the solutes is more entropically favorable in HFA-134a, perhaps due to water's higher affinity for structuring via self-

association and/or hydrate formation. Despite this, similarities in the system do seem to exist with three of the four compounds possessing negative entropy values and the lone positive value being small. While no definitive conclusions can be made, the data suggest the possibility of structuring of the solvent limiting the solubility of these non-polar solutes in HFA-134a, although to a lesser extent than water.

	log X_2			log X_i
Compound	**4ºC**	**25ºC**	**48ºC**	**25ºC**
1,2,3-Trichlorobenzene	-3.12	-2.84	-2.51	-0.25
1,3,5-Trichlorobenzene	-3.42	-3.19	-2.77	-0.33

Table 4.20. Solubility values in log mole fraction for 1,2,3-trichlorobenzene and 1,3,5-trichlorobenzene at 4, 25, and 48˚C as well as the ideal solubility at 25˚C.

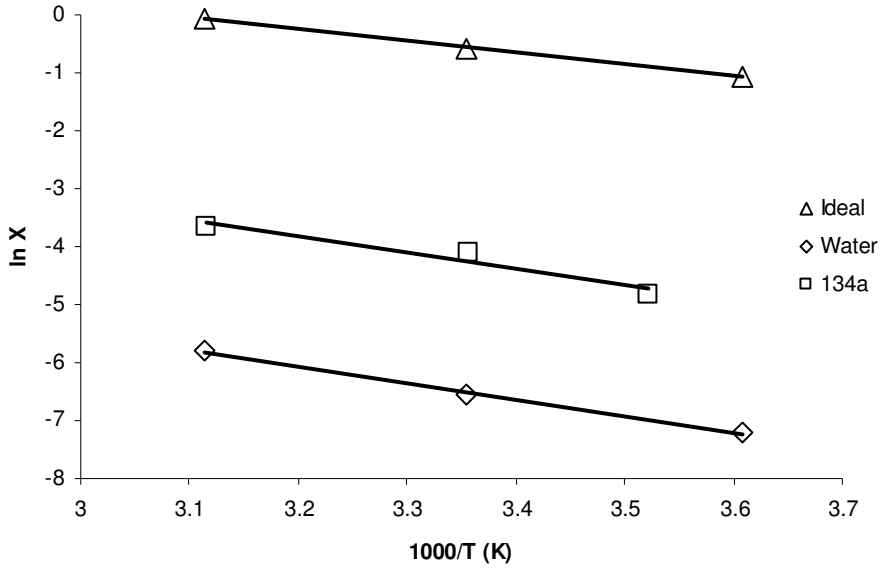

Figure 4.44. van't Hoff plots for 1,2,3-trichlorobenzene in water, HFA-134a and the ideal solubility.

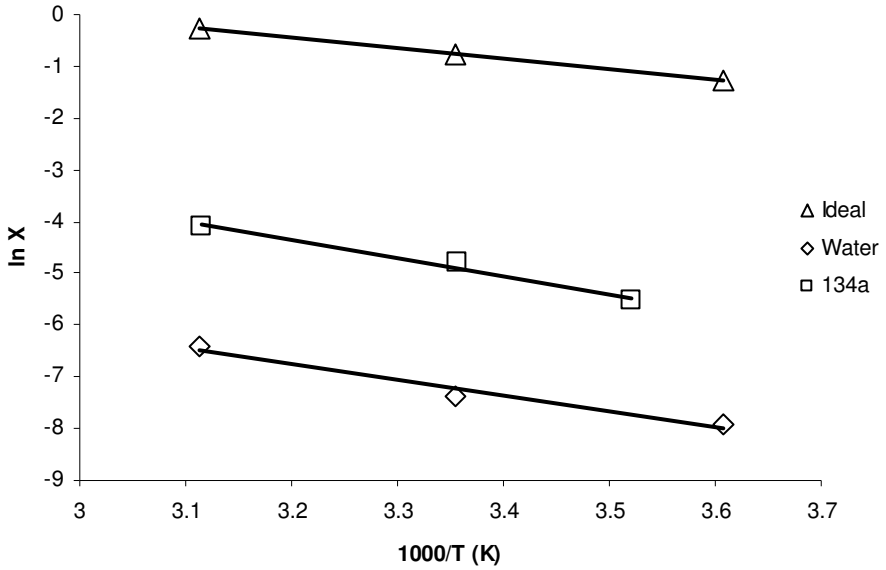

Figure 4.45. van't Hoff plots for 1,3,5-trichlorobenzene in water, HFA-134a and the ideal solubility.

Compound	ΔG_s	ΔH_s	$-T\Delta S_s$	ΔS_s (J/molK)
1,2,3-Trichlorobenzene	10.20	23.14	-12.94	43.42
1,3,5-Trichlorobenzene	11.91	28.74	-16.83	56.46
1,2,3-Trichlorobenzene	16.27	23.95	-7.68	25.76
1,3,5-Trichlorobenzene	18.28	25.22	-5.67	19.03

Table 4.21. Changes in free energy, enthalpy, and entropy of solution for 1,2,3-trichlorobenzene and 1,3,5-trichlorobenzene in HFA-134a and in water (italicized) at 25˚C (All values are in kJ/mol unless noted otherwise).

Compound	**ΔG_{mix}**	**ΔH_{mix}**	**$-T\Delta S_{mix}$**	**ΔS_{mix} (J/molK)**
1,2,3-Trichlorobenzene	8.79	6.28	2.51	-8.41
1,3,5-Trichlorobenzene	10.02	11.68	-1.66	5.56
1,2,3-Trichlorobenzene	14.73	7.09	7.77	-26.07
1,3,5-Trichlorobenzene	16.18	8.16	9.50	-31.87

Table 4.22. Changes in free energy, enthalpy, and entropy of mixing for 1,2,3-trichlorobenzene and 1,3,5-trichlorobenzene in HFA-134a and in water (italicized) at 25˚C (All values are in kJ/mol unless noted otherwise).

XIX. Thermodynamics of Compounds Capable of Hydrogen Bond Donating and Accepting in HFA-134a

The step wise progression of the series of chlorobenzene compounds was helpful in understanding what aids and inhibits solubility in HFA-134a for relatively non-polar molecules with no traditional hydrogen bond donating or accepting groups. To further understand the interactions and thermodynamics of solutes in HFA-134a, compounds capable of hydrogen bond donating and/or accepting were examined. The 11 compounds chosen, along with their melting points, molecular weights, and logP, can be seen in Table 4.23. The solubility of these compounds at 4, 25, and 37˚C can be seen in Table 4.24. As expected, the solubility increased for all compounds as the temperature increased. The order of solubility, from least to greatest, was predicted perfectly for the series of chlorobenzene compounds by ideal solubility. While this was not the case for these compounds, a strong correlation was still observed with the highest and lowest melting compounds possessing the lowest and highest solubilities, respectively.

The thermodynamics of the dissolution process were determined for all 11 compounds. The change in free energy, enthalpy, and entropy for each solution can be seen in Table 4.25. The change in free energy was positive for all compounds, with values ranging from 30.78 kJ/mol for the least soluble compound, 5,5-diphenyl hydantoin, to 8.81 kJ/mol for the most soluble compound, 4-bromo-2-fluoro aniline. The change in enthalpy of solution was also positive for all compounds but values were typically lower than

observed for the series of chlorobenzenes. The change in entropy of solution produced the most interesting results with only four of the compounds possessing positive entropy values. This suggests that for the majority of compounds the dissolution process is actually causing a gain in order and hindering solubility. This offers a possible explanation for the typically low solubility of compounds in HFA-134a.

The thermodynamics of the dissolution process were determined for all 11 compounds. The change in free energy, enthalpy, and entropy for each solution can be seen in Table 4.25. The change in free energy was positive for all compounds, with values ranging from 30.78 kJ/mol for the least soluble compound, 5,5-diphenyl hydantoin, to 8.81 kJ/mol for the most soluble compound, 4-bromo-2-fluoro aniline. The change in enthalpy of solution was also positive for all compounds but values were typically lower than observed for the series of chlorobenzenes. The change in entropy of solution produced the most interesting results with only four of the compounds possessing positive entropy values. This suggests that for the majority of compounds the dissolution process is actually causing a gain in order and hindering solubility. This offers a possible explanation for the typically low solubility of compounds in HFA-134a.

The melting process is typically composed of a large increase in enthalpy and a similarly large increase in entropy. The free energy of melting was positive for all compounds, ranging from 0.85 to 20.18 kJ/mol for the 11 compounds examined. The change in enthalpy of melting was also positive for all compounds, as expected, due to the energy

required to breakdown the crystalline structure of the solute. The entropy of melting values also behaved as expected, with positive values for all compounds. These positive changes in entropy represent the disorder gained when transitioning from a highly ordered crystal and forming a super-cooled liquid. The values of the thermodynamic parameters for the melting process can be seen in Table 4.26.

The thermodynamic mixing parameters are of great importance for predicting and understanding solubility. These parameters dictate the deviation from ideality for the solutes in the solvent and provide insight into interactions. The change in free energy for the mixing process was positive for all compounds. The change in enthalpy of mixing returned interesting results, with seven of the 11 compounds exhibiting negative values. In order to obtain a negative enthalpy of mixing value the solute and solvent must have a greater affinity for each other than themselves. An explanation for this would be that a solvated solution is formed. The entropy of mixing was negative for all compounds but 3-chloro 4-fluoro aniline. It is possible that if solvated solutions are formed the entropy of their mixing is negative.

Unlike the previous set of chlorobenzene compounds, the free energy change of mixing was not always the greatest contributor to that of the solution with four of the 11 compounds possessing larger ΔG_{melt} values than ΔG_{mix} values. This was primarily due to negative enthalpy of mixing values. While the enthalpy of mixing usually opposes solubility, in this case it actually promotes it for the majority of the solutes. Entropy is

normally thought of as the driving force of the solubility or dissolution process but in this case it actually opposes it for all but four compounds. These thermodynamic parameters allow important insight into the interactions taking place and lend credence to the theory that HFA-134a is able to strongly interact with solutes. It also reinforces the theory developed from the series of chlorobenzenes that entropy is not a large contributor to solubility in HFA-134a.

Compound	MP (°C)	MW	logP
2,4-Difluorobenzoic acid	461.15	158.10	2.04
2,6-Difluorobenzoic acid	430.65	158.10	1.82
3,5-Difluorobenzoic acid	394.15	158.10	2.44
3,5-Dinitro benzoic acid	477.15	212.12	1.69
2-Methyl-4-nitro aniline	404.15	240.26	1.55
4-Methyl-3-nitro aniline	350.15	152.15	1.83
3-Chloro-4-fluoro aniline	317.15	145.56	1.94
4-Bromo-2-fluoro aniline	311.15	190.01	2.39
5,5-Diphenyl hydantoin	568.15	252.27	2.52
3-(Trifluoromethyl) benzoic acid	379.15	190.12	2.95
[3-(Trifluoromethyl) phenyl]acetic acid	348.15	204.15	2.08

Table 4.23. The melting point, molecular weight, and logP values for the 11 compounds examined.

Compound	log X_2			log X_i
	4°C	**25°C**	**37°C**	**25°C**
2,4-Difluorobenzoic acid	-4.00	-3.74	-3.59	-3.53
2,6-Difluorobenzoic acid	-3.24	-3.15	-2.98	-1.58
3,5-Difluorobenzoic acid	-2.78	-2.65	-2.54	-0.42
3,5-Dinitro benzoic acid	-4.81	-4.64	-4.45	-1.50
2-Methyl-4-nitro aniline	-3.75	-3.59	-3.35	-1.83
4-Methyl-3-nitro aniline	-2.62	-2.59	-2.57	-0.44
3-Chloro-4-fluoro aniline	-2.25	-1.93	-1.44	-0.20
4-Bromo-2-fluoro aniline	-1.92	-1.54	-1.36	-0.15
5,5-Diphenyl hydantoin	-5.69	-5.39	-5.39	-3.02
3-(Trifluoromethyl)benzoic acid	-2.37	-2.18	-1.99	-0.64
[3-(Trifluoromethyl) phenyl]acetic acid	-1.86	-1.69	-1.46	-0.48

Table 4.24. The log mole fraction solubility at 4, 25, and 37˚C of the 11 compounds as well as their ideal solubility at 25˚C.

Compound	ΔG_s	ΔH_s	$-T\Delta S_s$	ΔS_s (J/molK)
2,4-Difluorobenzoic acid	21.34	20.61	0.72	-2.43
2,6-Difluorobenzoic acid	17.98	12.35	5.63	-18.87
3,5-Difluorobenzoic acid	15.10	11.32	3.78	-12.68
3,5-Dinitro benzoic acid	26.47	17.48	8.99	-30.14
2-Methyl-4-nitro aniline	20.51	18.93	1.58	-5.28
4-Methyl-3-nitro aniline	14.79	2.43	12.35	-41.43
3-Chloro-4-fluoro aniline	10.99	38.06	-27.07	90.80
4-Bromo-2-fluoro aniline	8.81	27.57	-18.77	62.95
5,5-Diphenyl hydantoin	30.78	16.07	14.71	-49.35
3-(Trifluoromethyl)benzoic acid	12.44	18.16	-5.72	19.20
[3-(Trifluoromethyl) phenyl]acetic acid	9.66	18.81	-9.14	30.66

Table 4.25. The change in free energy, enthalpy, and entropy of solution for the 11 compounds in HFA-134a at 25˚C (All values are in kJ/mol unless noted otherwise).

Compound	ΔG_{melt}	ΔH_{melt}	$-T\Delta S_{melt}$	ΔS_{melt} (J/molK)
2,4-Difluorobenzoic acid	20.18	57.09	-36.91	123.79
2,6-Difluorobenzoic acid	9.01	29.30	-20.28	68.03
3,5-Difluorobenzoic acid	2.37	9.74	-7.37	24.71
3,5-Dinitro benzoic acid	8.56	22.81	-14.25	47.80
2-Methyl-4-nitro aniline	10.43	39.78	-29.35	98.43
4-Methyl-3-nitro aniline	2.51	16.88	-14.37	48.21
3-Chloro-4-fluoro aniline	1.13	18.84	-17.71	59.41
4-Bromo-2-fluoro aniline	0.85	20.36	-19.51	65.45
5,5-Diphenyl hydantoin	17.26	36.31	-19.05	63.91
3-(Trifluoromethyl)benzoic acid	3.68	17.23	-13.55	45.44
[3-(Trifluoromethyl) phenyl]acetic acid	2.76	19.24	-16.48	55.27

Table 4.26. The change in free energy, enthalpy, and entropy of melting for the 11 compounds in HFA-134a at 25˚C (All values are in kJ/mol unless noted otherwise).

Compound	ΔG_{mix}	ΔH_{mix}	$-T\Delta S_{mix}$	ΔS_{mix} (J/molK)
2,4-Difluorobenzoic acid	1.16	-36.47	37.63	-126.22
2,6-Difluorobenzoic acid	8.96	-16.95	25.91	-86.90
3,5-Difluorobenzoic acid	12.73	1.58	11.15	-37.39
3,5-Dinitro benzoic acid	17.91	-5.33	23.24	-77.94
2-Methyl-4-nitro aniline	10.08	-20.85	30.92	-103.71
4-Methyl-3-nitro aniline	12.28	-14.45	26.73	-89.64
3-Chloro-4-fluoro aniline	9.86	19.22	-9.36	31.39
4-Bromo-2-fluoro aniline	7.95	7.21	0.75	-2.50
5,5-Diphenyl hydantoin	13.53	-20.24	33.77	-113.26
3-(Trifluoromethyl) benzoic acid	8.76	0.94	7.82	-26.24
[3-(Trifluoromethyl) phenyl]acetic acid	6.90	-0.44	7.34	-24.61

Table 4.27. The change in free energy, enthalpy, and entropy of mixing for the 11 compounds in HFA-134a at 25˚C (All values are in kJ/mol unless noted otherwise).

CHAPTER 5

CONCLUSION

In this work, the solubilities of 22 solutes were investigated in HFA-134a, and 13 solutes in HFA-227 with 0 – 20% w/w ethanol. The solubilities in HFA-227 with ethanol ranged from 0.001 to 3.282% w/w, where the solubilities always increase when ethanol was added. The extent of solubilization data was plotted against the fraction ethanol where the relationship was found to be linear and always positive.

Predictive models such as the ideal solubility and regular solution theory (RST) were applied. No clear predictive trend was observed for the theoretical models in HFA-227, where the AAE values were all over 1.0, or an error factor of at least 10. However, the predictive ability of ideal solubility improved with an increase in ethanol concentration, as the deviation from ideal, log γ_2, decreased. The addition of an intercept to the crystal term (MP – 25) yielded a significant two parameter regression equation at all five ethanol concentrations. However, adding a third and fourth parameter to the regression, such as the number of OH groups on a solute and the logP of a solute, resulted in an improved equation to the solubility in pure HFA-227 and HFA-227 with ethanol.

A regression approach was also used to predict the activity coefficient. Parameters such as molar volume and hydrogen bond number (HBN) were applied to a regression equation resulting in a significant correlation to the activity coefficient of 13 compounds

in HFA-227 with 0 – 20% ethanol. These equations were combined with the ideal solubility equation, creating a useful predictive equation with AAE values ranging from 0.32 to 0.36, or factor errors of 2.09 to 2.29.

These correlations can be used to estimate the solubility of a solute in HFA-227/ethanol mixtures from the knowledge of its chemical structure alone, without experimental measurements. Thus, the regression equations serve as helpful pre-formulation tools for solubility studies in the propellant HFA-227. Further studies are necessary to improve the correlation and broaden its applicability.

A liquid model for the HFA propellants was identified and used to predict HFA solubilities. Correlation studies show that DFP is a useful liquid model to study the propellants HFA-134a and HFA-227 with ethanol for the 13 compounds investigated. Regression analysis shows that DFP/cosolvent system can be used to adequately describe the solubility in HFA-134a/cosolvent and HFA-227/cosolvent systems, where the AAE values ranged from 0.3 to 0.56, or factor errors of 2.0 to 3.6. DFP has similar physico-chemical properties to both HFA-227 and HFA-134a, yet remains a liquid at room temperature and standard atmospheric pressure, making it a potentially good liquid model for both propellants.

In an attempt to understand the interactions helping and hindering solubility in HFA-134a a thermodynamic analysis of a series of chlorobenzene compounds as well as a group of

hydrogen donating and/or accepting compounds was performed. When considering the series of chlorobenzene compounds, ideal solubility was able to accurately predict the order of solubility for the compounds. The low and in some cases unfavorable ΔS_{mix} that was found limits the solubility of this series of compounds and suggest that entropy, not enthalpy, may play the larger role in solubility in HFA-134a. When compared to the thermodynamic parameters of water for like compounds the data suggested the possibility of a similar structuring of the solvent limiting the solubility of these non-polar solutes, although to a lesser extent than in water. The compounds capable of hydrogen accepting and donating exhibited negative enthalpy of mixing values when placed in HFA-134a, a stark contrast to the values obtained for the chlorobenzenes. This suggests HFA-134a is able to strongly interact with solutes capable of donating or accepting hydrogen. While these results are interesting, follow up studies with a greater number of temperature points and compounds should be performed in order to systematically delineate intermolecular interactions within HFA systems.

REFERENCES

1. Gandevia B. 1975. Historical Review of the Use of Parasympathicolytic Agents in the Treatment of Respiratory Disorders. Postgrad Med J 51:13-20.
2. Smyth HDC. 2003. The influence of formulation variables on the performance of alternative propellant-driven metered dose inhalers. Adv Drug Deliv Rev. 55:807-828.
3. Hoye J, Gupta A, Myrdal P. 2008. Solubility of Solid Solutes in HFA-134a With a Correlation to Physico-Chemical Properties. J Pharm Sci. 97:198-208.
4. Hendeles L, Colice GL, Meyer RJ. 2007. Withdrawal of Albuterol Inhalers Containing Chlorofluorocarbon Propellants. N Engl J Med. 356:1344-1351.
5. Hoye J, Gupta A, Myrdal P. 2008. Solubility of Solid Solutes in HFA-134a With a Correlation to Physico-Chemical Properties. J Pharm Sci. 97:198-208.
6. Scatchard G. 1931. Equilibria in nonelectrolyte solutions in relation to the vapor pressures and densities of the components. Chem Rev. 8: 321-333.
7. Hildebrand JH. 1919. Solubility. III. Relative values of internal pressures and their practical application. J Am Chem Soc. 41: 1067-1080.
8. Ran Y, Yalkowsky SH. 2001. Prediction of Drug Solubility by the General Solubility Equation. J Chem Inf Comput Sci. 41:354-357.
9. Dickinson PA, Seville PC, McHale H, Perkins NC, Taylor G. 2000. An investigation of the solubility of various compounds in the hydrofluoroalkane propellants and possible model liquid propellants. J Aerosol Med. 13: 179-186.

10. Gupta A, Stein SW, Myrdal PB. 2003. Balancing Ethanol Cosolvent Concentration with Product Performance in 134a Based Pressurized Metered Dose Inhalers. J Aerosol Med. 16:167-174.
11. Rogueda PC. 2003. HPFP, a model propellant for pMDIs. Drug Dev Ind Pharm. 29:39-49.
12. Ridder KB, Davies-Cutting CJ, Kellaway IW. 2005. Surfactant Solubility and Aggregate Orientation in Hydrofluoroalkanes. Int J Pharm. 295:57-65.
13. Walden P. 1908. Melting heat, specific cohesion and molecular size at melting temperature. Zeitschrift fuer Elektrochemie. 14:713-724.
14. Fedors R. 1974. A method for estimating both the solubility parameters and molar volumes of liquid. Polym Eng Sci. 14:147-154.
15. Howlett DJ. 1998. MDI technology: can it meet the challenges of CFC replacement and increasing regulatory demand? Resp Drug Deliv. VI:123-131.
16. Li Q, Zhang Z, Zhong C, Liu Y, Zhoe Q. 2003. Solubility of solid solutes in supercritical carbon dioxide with and without cosolvents. Fluid Phase Equilib. 207:183-192.
17. Li Q, Zhong C, Zhang Z, Zhou Q. 2003. An equilibrium model for the correlation of the solubility of solids in supercritical fluids with cosolvent. Sep Sci Tech. 38:1705-1719.
18. Dalby RN, Philips EM, Byron PR. 1991. Determination of drug solubility in aerosol propellants. Pharm Res. 8:1206-1209.

19. Gupta A, Myrdal PB. 2004. Novel method for the determination of aerosol in propellants. J Pharm Sci. 93:2411-2419.
20. Gupta A, Myrdal PB. 2004. On-line high-performance liquid chromatography method for analyte quantitation from pressurized metered dose inhalers. J Chromatogr A. 1033:101-106.
21. Gupta A, Myrdal PB. 2005. A comparison of two methods to determine the solubility of compounds in aerosol propellants. Int J Pharm. 292:201-209.
22. Myrdal PB, Krzyzaniak JF, Yalkowsky SH. 1996. Modified Trouton's Rule for Predicting the Entropy of Boiling. Ind Eng Chem Res. 35:1788-1792.
23. Millard J, Alvarex-Nunez F, Yalkowsky S. 2002. Solubilization by cosolvents. Establishing useful constants for the log-linear model. Int J Pharm. 245:153-166.
24. Friesen K, Webster GRB. 1990. Temperature Dependence of the Aqueous Solubilities of Highly Chlorinated Dibenzo-p-Dioxins. Environ Sci Technol. 24:97-101.